สารออกฤทธิ์ทางชีวภาพจากรากและใบของต้นสำมะงา

นางสาวสิริกร ก่ออานันต์

วิทยานิพนธ์นี้เป็นส่วนหนึ่งของการศึกษาตามหลักสูตรปริญญาวิทยาศาสตรดุษฎีบัณฑิต
สาขาวิชาเทคโนโลยีชีวภาพ
คณะวิทยาศาสตร์ จุฬาลงกรณ์มหาวิทยาลัย
ปีการศึกษา 2557

BIOACTIVE COMPOUNDS FROM ROOTS AND LEAVES OF *Clerodendrum inerme*

Miss Sirikorn Kor-arnan

A Dissertation Submitted in Partial Fulfillment of the Requirements
for the Degree of Doctor of Philosophy Program in Biotechnology
Faculty of Science
Chulalongkorn University
Academic Year 2014

Thesis Title	BIOACTIVE COMPOUNDS FROM ROOTS AND LEAVES OF *Clerodendrum inerme*
By	Miss Sirikorn Kor-arnan
Field of Study	Biotechnology
Thesis Advisor	Assistant Professor Pattara Thiraphibundet, Ph.D.

Accepted by the Faculty of Science, Chulalongkorn University in Partial Fulfillment of the Requirements for the Doctoral Degree

.....Dean of the Faculty of Science
(Professor Supot Hannongbua, Dr.rer.nat.)

THESIS COMMITTEE

.....Chairman
(Associate Professor Vudhichai Parasuk, Ph.D.)

.....Thesis Advisor
(Assistant Professor Pattara Thiraphibundet, Ph.D.)

.....Examiner
(Associate Professor Santi Tip-pyang, Ph.D.)

.....Examiner
(Associate Professor Chanpen Chanchao, Ph.D.)

.....External Examiner
(Assistant Professor Jongkolnee Jongaramruong, Ph.D.)

สิริกร ก่ออานันต์ : สารออกฤทธิ์ทางชีวภาพจากรากและใบของต้นสำมะงา (BIOACTIVE COMPOUNDS FROM ROOTS AND LEAVES OF *Clerodendrum inerme*) อ.ที่ปรึกษาวิทยานิพนธ์หลัก: ผศ. ดร.พัฒทรา ธีรพิบูลย์เดช, 107 หน้า.

การศึกษานี้ได้ประเมินสารออกฤทธิ์ทางชีวภาพจากรากและใบของต้นสำมะงา การแยกสิ่งสกัดไดคลอโรมีเทนด้วยเทคนิคทางโครมาโตกราฟี ได้สารบริสุทธิ์จำนวน 15 สาร (สารบริสุทธิ์จากใบจำนวน 8 สารและสารบริสุทธิ์จากรากจำนวน 7 สาร) คือ (3β, 22*E*, 24*S*)-stigmasta-5,22,25-trien-3-ol (1), pectolinarigenin (2), acacetin (3), 5,8-dihydroxy-7,4'-dimethoxyflavone (4), scutellarein-4'-methyl ether (5), ladanein (6), 5-hydroxy-4′,7-dimethoxyflavone (7) และ (3β,*22E*,24*S*)-stigmasterol-5,22,25-triene-3-yl-glucopyranoside (8) ร่วมกับสารบริสุทธิ์จากราก, stigmasterol (9), *n*-hexadecyl propionate (10), lupeol laurate (11), β-amyrin decosanoate (12), betulinic acid (13), 6,11,12,16-tetrahydroxy-5,8,11,13-abitetetraen-7-one (14) and 3-*O*-acetyl-betulinic acid (15) การทดสอบฤทธิ์ยับยั้งจุลชีพ ฤทธิ์ยับยั้งเอนไซม์โคลีนเอสเทอเรส และฤทธิ์ยับยั้งการเกิด amyloid plaque ของสารบริสุทธิ์ จากสิ่งสกัดไดคลอโรมีเทน พบว่าสาร 1 มีฤทธิ์ยับยั้งการเจริญของ *S. aureus* ได้มากที่สุด สาร 7 ฤทธิ์ยับยั้งการเจริญของ *P. aeruginosa* ได้มากที่สุดและสาร 3 มีฤทธิ์ยับยั้งการเจริญของ *C. albicans* ได้มากที่สุด และสาร 3 มีฤทธิ์ยับยั้งการเกิด amyloid aggregation ดีที่สุด นอกจากนี้สาร 7 มีฤทธิ์ยับยั้งเอนไซม์อะเซติลโคลีนเอสเทอเรส ได้มากที่สุด ขณะที่สาร 2 ยับยั้งเอนไซม์บิวเทอริลโคลีนเอสเทอเรส ได้มากที่สุด การศึกษานี้สนับสนุนว่าสำมะงาเป็นแหล่งของสารออกฤทธิ์ทางชีวภาพได้ โดยเฉพาะอย่างยิ่ง ฤทธิ์ยับยั้งจุลชีพ ฤทธิ์ยับยั้งเอนไซม์โคลีนเอสเทอเรส และฤทธิ์ยับยั้งการเกิด amyloid aggregation และยังพบความสัมพันธ์ของโครงสร้างสารและหมู่แทนที่ต่อการออกฤทธิ์ของสารบริสุทธิ์ที่ได้จากการศึกษานี้ด้วย

สาขาวิชา เทคโนโลยีชีวภาพ ลายมือชื่อนิสิต .....

ปีการศึกษา 2557 ลายมือชื่อ อ.ที่ปรึกษาหลัก .....

5273809023 : MAJOR BIOTECHNOLOGY
KEYWORDS: CLERODENDRUM INERME / ANTIAMYLOID AGGREGATION / ANTICHOLINESTERASE ACTIVITY / ANTIMICROBIAL ACTIVITY

SIRIKORN KOR-ARNAN: BIOACTIVE COMPOUNDS FROM ROOTS AND LEAVES OF *Clerodendrum inerme*. ADVISOR: ASST. PROF. PATTARA THIRAPHIBUNDET, Ph.D., 107 pp.

This study has evaluated bioactive compounds from roots and leaves of *Clerodendrum inerme*. CH_2Cl_2 extracts of plant materials were separated with various chromatography techniques. There were obtained 15 isolates compounds (8 isolates from leaves and 7 isolated from roots), (3β, *22E 24S*)-stigmasta-5,22,25-trien-3-ol (1), pectolinarigenin (2), acacetin (3), 5,8-dihydroxy-7,4'-dimethoxyflavone (4), scutellarein-4'-methyl ether (5), ladanein (6), 5-hydroxy-4′,7-dimethoxyflavone (7) and (3β,22*E*,24*S*)-stigmasterol-5,22,25-triene-3-yl-glucopyranoside (8) including isolated compounds from roots, stigmasterol (9), *n*-hexadecyl propionate (10), lupeol laurate (11), β-amyrin decosanoate (12), betulinic acid (13), 6,11,12,16-tetrahydroxy-5,8,11,13-abitetetraen-7-one (14) and 3-*O*-acetyl-betulinic acid (15). Selected compounds were evaluated biological activity (antimicrobial activity, anti-cholinesterase activity and anti-Aβ disaggregation activity). It was found bioactive compounds from CH_2Cl_2 extract of *C. inerme.* Among selected compounds, compound 1 has more active against *S. aureus* growth, compound 7 has more active against *P. aeruginosa* growth and compound 3 has more active against *C. albicans*. Compound 3 has more active against Aβ-aggregation. Furthermore, compound 7 has more active on AChE activity and compound 2 has more active on BChE activity. This study supports that *C. inerme* is possible source of bioactive compounds especially antimicrobial activity, anti-cholinesterase activity and anti-Aβ digaggregation activity. The structure relation activity of phytochemicals from this study depended on type of its skeleton and the substituents were also observed.

Field of Study: Biotechnology Student's Signature .....

Academic Year: 2014 Advisor's Signature .....

ACKNOWLEDGEMENTS

I would like to deepest gratitude to my advisor, Assistant Professor Dr. Pattara Thiraphibundet for her given opportunity, guidance and valuable suggestion throughout the course of thesis.

I also gratefully acknowledge the member of thesis committee, Associate Professor Dr. Vudhichai Parasuk, Associate Professor Dr. Santi Tip-pyang, Associate Professor Dr. Chanpen Chanchao and Assistant Professor Dr. Jonkolnee Jongaramruang for their discussion and guidance.

I would like to faithful gratitude to Dr. Jirapast Sichaem for his helpful and suggestion.

Finally, I would like to thank National Science and Technology Development Agency (NSTDA) and the 90th anniversary of Chulalongkorn University fund (Ratchadaphiseksomphot Endowment Fund) for the financial support.

CONTENTS

Page

Page

LISTS OF TABLES

Table Page

LIST OF FIGURES

LISTS OF ABBREVIATIONS

δ	chemical shift
δ_C	chemical shift of carbon
δ_H	chemical shift of carbon
CC	column chromatography
^{13}C-NMR	carbon-13 nuclear magnetic resonance
COSY	correlated spectroscopy
IC_{50}	concentration that required for 50% inhibition *in vitro*
J	coupling constant
Acetone-*d6*	deuterated acetone
$CDCl_3$	deuterated chloroform
CD_3OD	deuterated methanol
CH_2Cl_2	dichloromethane
DMSO	dimethyl sulfoxide
d	doublet (NMR)
dd	doublet of doublet (NMR)
ESIMS	electrospray ionization mass
HMBC	heteronuclear multiple bond correlation experiment
HSQC	heteronuclear single quantum correlatin
HRESIMS	high resolution electrospray inonization mass spectrometry

Hz	hertz
Kg	kilogram
L	liter
MeOH	methanol
µg	microgram
µl	microliter
M	molar (mole per liter)
µM	micromolar
MW	molecular weight
mg	milligram
ml	milliliter
mM	millimolar
m/Z	mass per charge
NMR	nuclear magnetic resonance
NOESY	nuclear overhauser enhancement spectroscopy
S	singlet
TLC	thin layer chromatography
UV	ultraviolet
2D NMR	two dimensional nuclear magnetic resonance

CHAPTER I
INTRODUCTION

Traditional herbs have a long history to combine knowledge, skills, practices, believes and experiences in different cultures. These herbs contain the active ingredients with a variety therapeutic activities and use to treat many diseases. The definition of bioactive compounds are essential and nonessential compounds that occur in nature, are part of the food chain, and can be shown to have an effect on human health [1]. Bioactive compounds are commonly found in herbs and medicinal plants. *Clerodendrum inerme* is one of medicinal plant in Thailand. It widely distributes along seaside. Although, this plant has the medicinal information, it is not widely used in Thai community. This study then interests to evaluate the bioactive compounds and support some medicinal properties. It may encourage the use of *C. inerme* to treat Alzheimer's disease and as the antimicrobial agents.

1.1 Botanical of *Clerodendrum inerme* L. Gaertn.

Clerodendrum inerme L. Gaertn. is one of medicinal plant in Verbenaceae family. Its common name is Clerodendrum and scrambling, and harmless clerodendron. This plant usually grows along beach forest and distributes proximity to the sea around Western Australia, Northern Territory, Cape York Peninsula, North East Queensland, New South Wales and Asia, Malaysia and the Pacific Islands. Plant characteristics of *C. inerme* are shown in Fig 1.1.

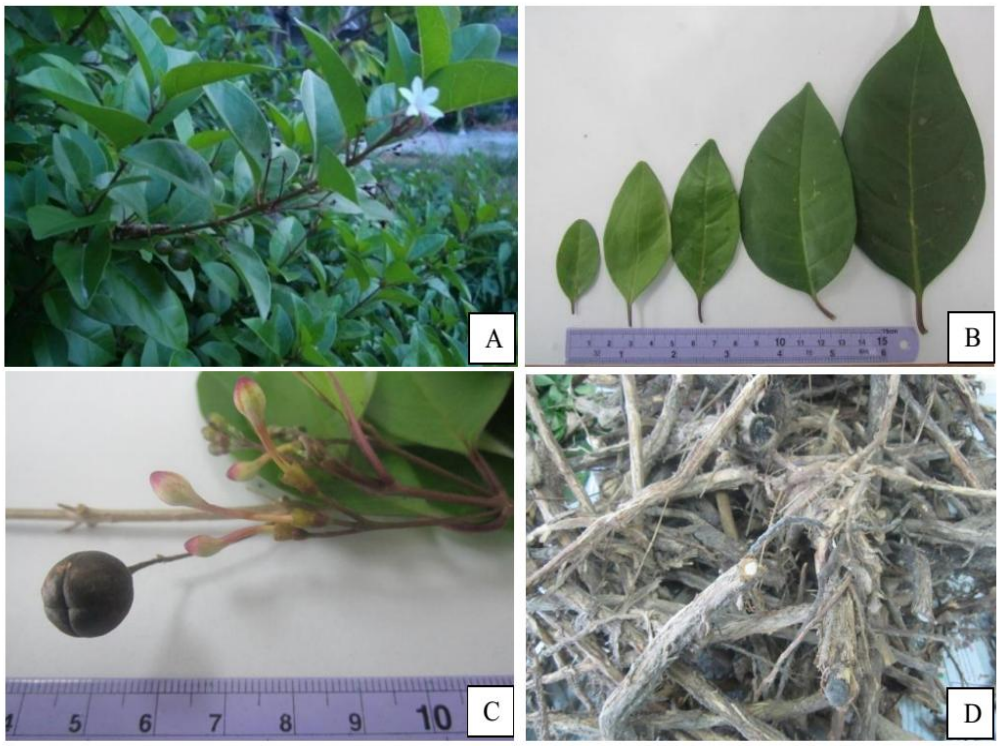

Figure 1.1 *C. inerme* collected from Rayong province in Thailand (a) whole plant, (b) leaves, (c) fruit and flower and (d) roots

1.2 Tradition Use and Biological Activities of *C. inerme*

C. inerme is a traditional herb to cure many diseases [2]. Leaves are used for relieve skin inflammation and itching. Roots are used to relieve flu, hepatitis and rhumatiods. Moreover, this plant have been studied its biological activities. The MeOH extract of leaves had anti-oxidation activity in almost the same level as α-tocopherol in the DPPH assay [3]. Gurudeeban *et al* [4] reported that the MeOH extract of *C. inerme* contained 0.74% of phenolics and 0.13% flavonoids so it exhibited high anti-oxidation activity against DPPH, hydroxyl and nitric oxide radicals [4]. Additional, the

IC_{50} value of DPPH inhibition of the stem extract was 24.1 μg/mL and this extract showed the inhibition of linoleic acid oxidation (53.0%) [5].

The leaf extracts have reported to possess hepatoprotective activity [6], hypertension effect in rabbits [7], diuretic activity [8] including cytotoxicity on Human Caucasian gastric adenocarcinoma (AGS), human colon cancer (HT-29) and breast cancer cell line (MDA-MB-435S) [9].

Furthermore, *C. inerme* also had the antifungal property. The alcoholic extract can control the growth of *Botrytis cinerea* [10]. Moreover, the EtOAc and hexane extracts of leaves at 1 mg/mL showed higher activity against human pathogen fungi than ketoconazole by the poison plate technique testing. These extracts inhibited the growth of *Trichophyton rubrum* and *E. floccosum* with the same potency [11].

The antimicrobial activity of EtOH, benzene, MeOH and aqueous extracts of *C. inerme* leaves were evaluated by disc diffusion method on gram positive bacteria (*Bacillus subtilis* ATCC 6633 and *Staphylococcus aureus* ATCC 25923), gram negative bacteria (*Escherichia coli* ATCC 25922 and *Psedomaonas aeruginosa* ATCC 27853) and fungal strains (*Aspergillus niger* ATCC 16404, *Aspergillus flavus* ATCC 9807, *Candida albicans* ATCC5027 and *Candida glabrata* ATCC 66032). Among all extracts, MeOH extract at 1 mg/mL had the highest inhibition on *S. aureus* and *A. niger* (16.67 ± 0.47 and 15.0 ± 0.0 mm, respectively) with the same MIC values (0.78 mg/ml) [12].

Isolated compounds from *C. inerme,* (5*S*,6R,8αR)-5,6,8α-trimethyl-5-(2-(3-oxo-cyclobutyl)-ethyl)-3,4,4α,5,6,7,8,8α-octahydro-naphthalene-1-carboxylic acid methyl ester, 17-(1, 2-dimethyl-propenyl)-10, 13-dimethyl-2,3,4,7,8,10,12,13,14, 15,16,17-dodecahydro-1H-cyclopenta[α]phenanthren-3-ol, and (3*R*, 4α*R*, 5*S*, 6*R*, 8α*R*)-5-(2-furan-3-yl-ethyl-3,4α,5,6,8α-pentamethyl-3,4,4α,5,6,7,8,8α-octahydro-naphthalen-1-ol were determined for their antibacterial properties. They were tested against *Bacillus pumillis*, *Micrococcus luteus*, *Klebsiella pneumonia* and *Escherichia coli*. *E. coli* had more susceptible to these compounds. Furthermore, antifungal activity of these compound against *Aspergillus flavus*, *Cladosporium herbarum*, *Lasiodiplodia theobromae* and *Physoderma maydis* were evaluated. The susceptibility of *P. maydis* had more than another microorganisms. Structures of these isolated compounds were shown in Fig. 1.2

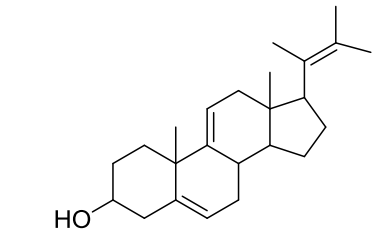

17-(1, 2-dimethyl-propenyl)-10, 13-dimethyl-2,3,4,7,8,10,12,13,14,15,16,17-dodecahydro-1H-cyclopenta[α]phenanthren-3-ol

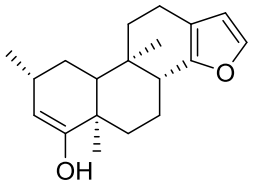

(3R,4αR,5S,6R,8αR)-5-(2-furan-3-yl-ethyl)-3,4α,5,6,8α-pentamethyl-3,4,4α,5,6,7,8,8α-octahydro-naphthalen-1-ol

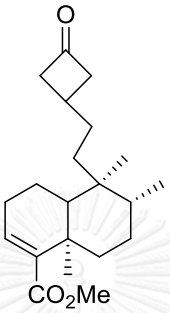

(5S,6R,8αR)-5,6,8α-trimethyl-5-(2-(3-oxo-cyclobutyl)-ethyl)-3,4,4α,5,6,7,8,8α-octahydro-naphthalene-1-carboxylic acid methyl ester

Figure 1.2 Isolated compounds from *C. inerme* [13]

C. inerme also had the insecticide property. The protection of stored-wheat from infestations of *Sitophilus oryzae* showed the effect on mortality and progeny production of rice weevil. Adult insects were exposed to 2.5 and 5% of EtOH extract with treated-wheat. It was found that the beetles mortality was increased in dose dependent manner and the progeny production was completely suppressed at lowest dose [14]. This plant used to control three species of mosquito vectors as insecticide property on *Anopheles stephensi, Aedes aegypti* and *Culex quinquefasciatus.* MeOH extract was treated at a concentration range of 20-100 ppm at difference larval from I-stage to pupa-stage. The lethal concentrations (LC_{50}) of *A. stephensi*, *A. aegypti* and

C. quinquefasciatus were 55.04-80.17%, 45.75-68.17% and 34.77-55.10% respectively [15].

There was only one studied about Alzheimer Disease on glutamate releasing inhibition and prevent of kainic acid inducing [16]. An excess of glutamate releasing associated with several neurological diseases. This study found that acacetin from *C. ienrme* showed a potency to treat the neurological diseases. It can inhibit glutamate release from hippocampal synaptosomes by attenuating voltage-dependent Ca^{2+} entry and effectively prevents KA-induced excitotoxicity.

1.3 Phytochemicals from *C. inerme*

Genus *Clerodendrum* is found the first since 1753. It has more than 500 species, for example, *C. indicum*, *C. phlomidis*, *C. serratum*, *C. trichotomum*, *C. chinense* and *C. pelasites*. Plants in this species consist of different phytochemicals, such as, alkaloids, flavonoids, glycosides, terpenoids and steroids [17]. Difference of phytochemicals depends on species and a variety. Although *C. inerm*e is one of clerodendrum plant, it has a diversification of phytochemicals difference from another clerodendrum. The structures of phytochemicals of *C. inerme* are shown in Fig. 1.3

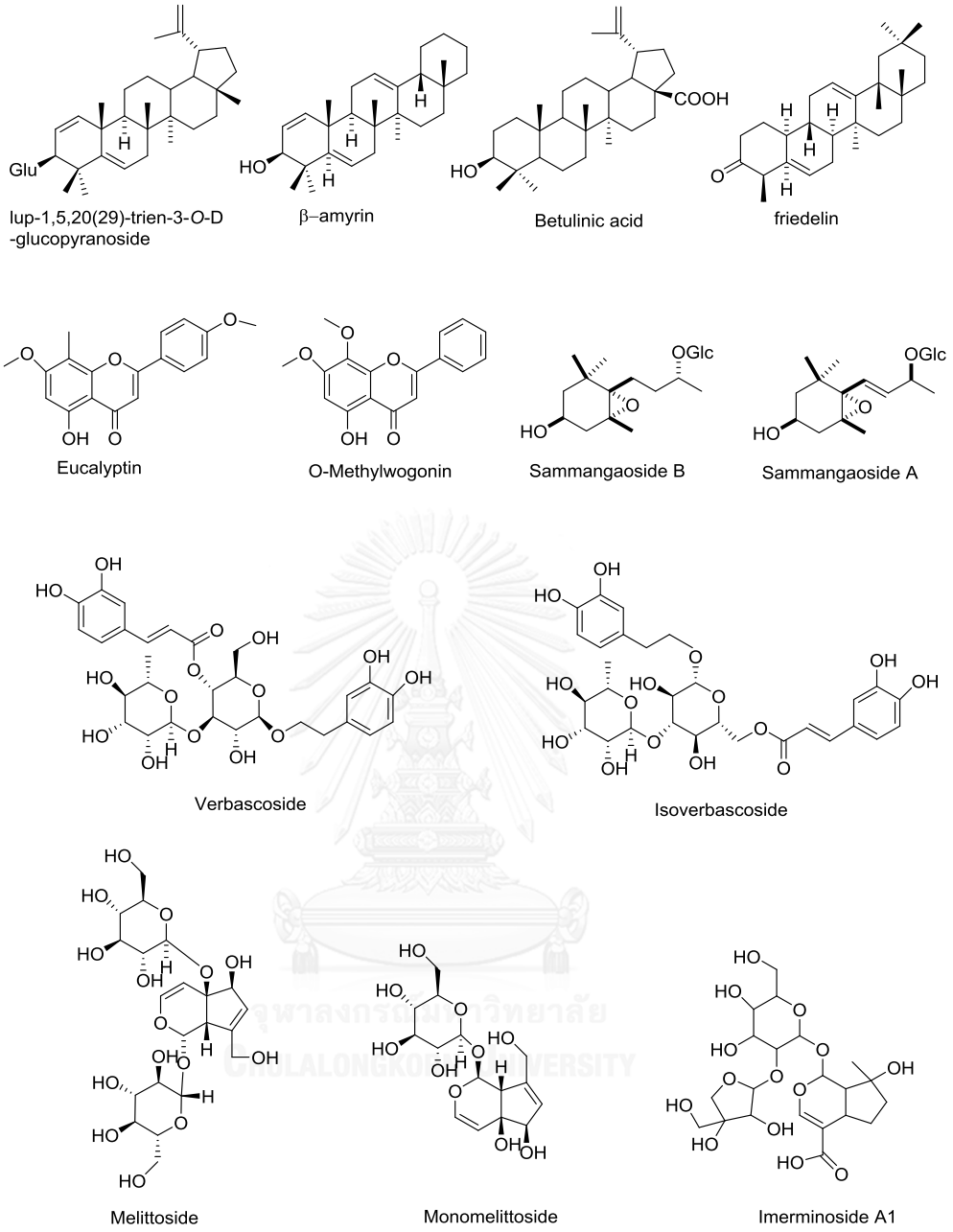

Figure 1.3 Phytochemicals from flowers, leaves and aerial parts of *C. inerme*

1.4 Alzheimer Disease

Alzheimer's Disease (AD) is one of dementia symptom. Dementia is approximately 50-75% of AD disorder [18]. AD behavior exhibits memory impairment, behavior disturbance, language deterioration, visuospatial deficits, abnormal sensory,

gait disturbances and seizures. In present, although, there are many postulations the causes of AD, such as, neurotransmitter dysfunction, β-amyloids (Aβ) plaques accummulation, tau hyperphosphorylation, genetic disorder of GSK3 and neurofibrillary tangles, the precise cause of AD are unclear. Then, the exactly treats of this disease is interesting to investigate.

Aβ plaque and cholinesterase dysfunction are found to be related each other. Cholinergic dysfunction is responsible by Aβ accumulation which affects the synaptic activity [19, 20]. Aβ peptide accumulation can reduce pyruvate dehydrogenase activity, generate acetyl CoA from pyruvate, reduce choline acetyltransferase (ChAT) activity, reduce acetylcholine (ACh) and reduce ACh releasing from synaptic vesicles (Fig. 1.4)

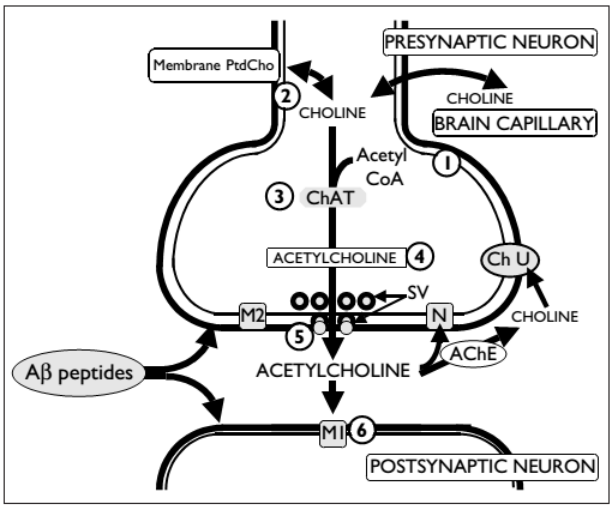

Figure 1.4 Aβ modulate cholinergic transmission [21]

The accummulation of Aβ fibrils in brain is one of AD disorder. Aβ-fibrils consist Aβ monomer and each monomer has 40 amino acid [22, 23]. Aβ is the proteolytic product of β-secretases and γ-secretases enzymes from β-APP precursor [24]. Proteolytic activity products are Aβ40, Aβ42 and its shorter and longer chain [25]. Aβ42 is approximately 5–15% [26]. When soluble Aβ changes the conformation to form β-sheet and this β-sheet is oligomerized of β-sheet to form insoluble fibrils [27, 28]. The Aβ fibril may cause neurotransmission dysfunction. Conformation of Aβ monomer is shown in Fig. 1.5

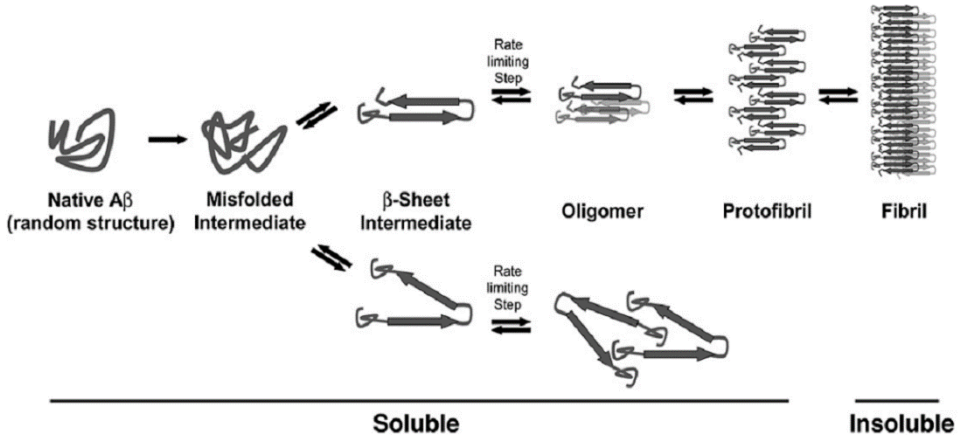

Figure 1.5 Conformation change of Aβ monomer to Aβ fibrils [29]

Aβ fibrils are neurotoxicity and change the neuron morphology. They affect neuron morphology by change axonal trafficking, activation the microglia, change neuritic and increasing dysmorphic-neurites [30]. Moreover, camera lucida drawing is shown the apical dendrite of pyramidal cell from cerebral cortex of 4 disorder. The

indication of the different apical dendrite of different neurobehavior are shown in Fig. 1.6

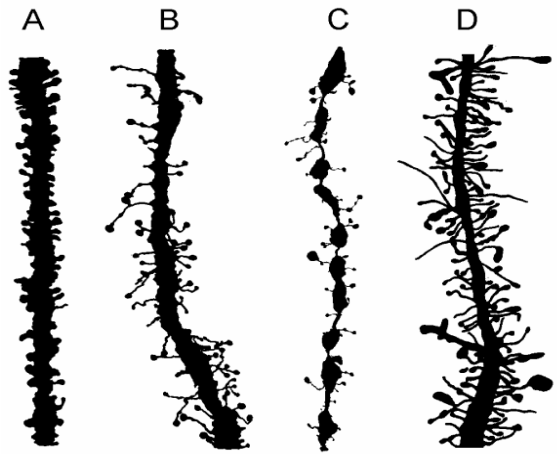

Figure 1.6 Camera drawing of apical dendrite of human cerebral cortex: 6-month old infant (A), 10-month old infant (B), 5.5 month-old child (severe neurobehavioral failure) (C), adult (fragile X syndrome) (D) [31]

Clinical drugs, e.g, donepezil, rivastigmine, galantamine and memantine (Fig. 1.7) are used for treatment AD disease. Although AD disease is commonly treated with clinical drugs, they may have some disadvantages and they can only improve disease-progression.

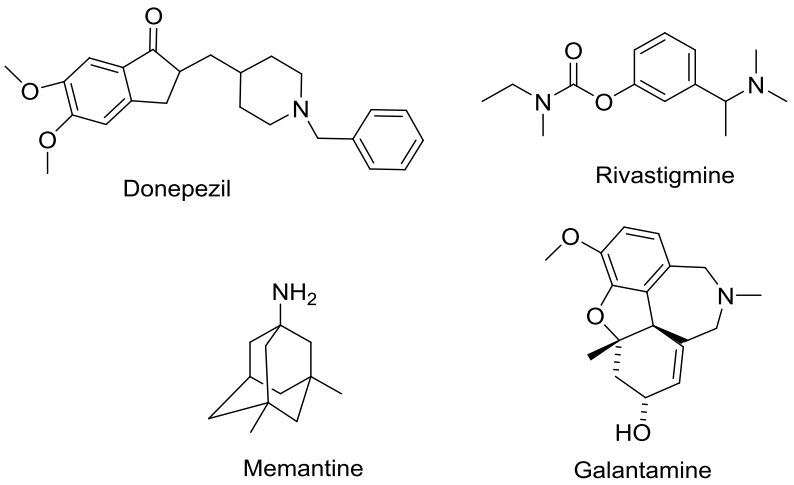

Figure 1.7 Commercial AD drug

To solve the disadvantages of clinical drugs, medicinal plant is an alternative treatment. They have no side effects and have bioavailability. Moreover, medicinal plants have been observed the potency of activity against the most common of AD causes (amyloid aggregation and cholinesterase activity), such as,

Flavonoids, 5,7,4'-trimethoxyflavone and 5,7-dimethoxyflavone, from *Kaempferia parviflora* had a potency of AChE and BChE inhibitions. 5,7,4'-Trimethoxyflavone showed 47.1% of AChE inhibition and 46.2% of BChE inhibition and 5,7-dimethoxyflavone showed 42.6% of AChE inhibition and 84.6% of BChE inhibition [32]. Flavonoids glycosides (tiliroside and quercitin) and flavonoids (3-methoxy quercetin and quercetin) from *Agrimonia pilosa* had AChE inhibition activity [34]. Isorahmnetin-3-*O*-glucuronid from the whole plant of *Persicaria thungergii* had AChE inhibition activity with IC_{50} of 8.2 μM [35]. Steroidal saponin (Longipetalosides A) from *Tribulus longipetalus* had the AChE inhibitory effect (31.3 %) and BChE inhibitory effect (32.2 %) [33].

Among Thai plants, *Cymbopogon citratus*, *Citrus hystrix* and *Zingiber cassumunar* were compared for AChE and BChE inhibitory activities using Ellman's colorimetric method [36]. *C. citratus* oil exhibited the highest activity (IC_{50} of AChE was 0.34 ± 0.07 µL/mL and IC_{50} of BChE was 2.14 ± 0.18 µL/mL) [37]. The aqueous extract of *Ganoderma lucidum* can preserve synaptophysin from Aβ-induced synaptotoxicity. *G. lucidum* aqueous extract also antagonized Aβ-triggered DEVD cleavage activities in a dose-dependent manner. Moreover, phosphorylation of c-Jun N-terminal kinase, c-Jun, and p38 MAP kinase was attenuated by this plant extract.

Medicinal plants were also observed the anti- Aβ aggregation activity *in vitro* and *in vivo* studies, such as

Twenty-seven herbs were selected to extract with methanol (90%) and chloroform, and all extracts were evaluated their ability to protect PC12 rat pheochromocytoma and primary neuronal cells from Aβ (1-42) toxicity by 3-(4,5-dimethylthiazol-2-yl)-2,5-diphenyltetrazolium bromide reduction assay and lactate dehydrogenase efflux assay. Efficacy of herbal extracts on neuronal cells protectivity from amyloid is determined by MTT reduction assay. The results showed that *Curcuma aromatia* and *Zingiber officinale* extracts effectively protected cells from Aβ (1-42) toxicity. Several extracts showed cytotoxicity at high concentration (150 µg/mL) and included protect cells from Aβ (1-42) toxicity [38]. Moreover, it was found that EGb761 was able to block Aβ (1–42)-induced cell apoptosis, reactive oxygen species (ROS) accumulation, mitochondrial dysfunction and activation of c-jun N-terminal kinase

(JNK), extracellular signal-regulated kinase 1/2 (ERK1/2) and Akt signaling pathways [39]. Hesperidin (a flavanone glycoside) showed Aβ-disaggregation activity *in vivo* study. Three-month-old APPswe/PS1dE9 transgenic mice were treated with hesperidin at 50 mg/kg - 100 mg/kg per day. There was no Aβ deposition after 16 weeks of treatment. Hesperidin amount 100 mg/kg per day can reduce the learning and memory deficits and improve locomotor activity. Moreover, it can inhibit glycogen synthase kinase-3β phosphorylation activity by hesperidin treatment at 100 mg/kg per day [40].

Resveratrol and catechin were treated on PC12 cells at 10^{-6} M of Aβ (1–41) for 16 h. It can decrease 24% of cell viability and the IC_{50} value was $1.1\pm0.14\times10^{-8}$ M. Moreover, synergistic activity of 25 μM of resveratrol and 50 μM of catechin can protect PC12 cells from Aβ toxicity [41]. Quercetin from whole plant of *Elsholtzia rugulosa* Hemsl had anti- amnesic effects. Aβ25-35 (10 nmol) was feed to mice orally for 8 days after injection. Learning and memory behaviors were evaluated by spontaneous alternation in Morris Water Maze testing and the step-through positive avoidance test. It was found that, quercetin improved the learning, improved memory capabilities, conferred robust neurovascular coupling protection, involved the maintenance of the NVU integrity, reduced the neurovascular oxidation, modulated the microvascular function, improved of cholinergic system, and regulated the neurovascular RAGE signaling pathway and regulated ERK/CREB/BDNF pathway [42].

Quercetin and rutin had anti-amyloidogenic property. Rutin inhibited β-secretase activity. Moreover, quercetin and rutin decreased ROS generation in H_2O_2-

treated APPswe cells, increased intracellular GSH content and increased the redox status [43]. Flavonoid glycosides (24%) and terpene trilactones (6%) were the two main components in *Ginkgo biloba* leaves. The inhibitory activities of flavonoids, *e.g.*, ginkgolides A, B, and C and bilobalide were evaluated towards Aβ42 fibril formation. It was found that flavonoids showed weak to moderate inhibitory activities [44].

Curcumin, a small dietary polyphenolic molecule showed high the Aβ-disaggregation activity. Curcumin showed effective on Aβ40-induced toxicity in human neuroblastoma SH-SY5Y cells. It was found that curcumin can reduce Aβ-membrane interactions and attenuate Aβ-induced membrane disruptions. Concomitantly, membrane morphology and lipid packing were disrupted. Curcumin dose-dependently ameliorated Aβ neurotoxicity and reduced either the rate or extents of Aβ insertion into anionic lipid monolayers [45]. The characteristics of high potent of medicinal plants were shown in Fig. 1.8

Figure 1.8 Important of medicinal plants have the anti-Aβ-disaggregation and cholinesterase activity; *Gingko biloba* (A); *Zingiber officinale* (B); *Curcuma longa* (C); *Kaempferia parviflora* (D); *Citrus hystrix* (E) and *Garnoderma lucidum* (F)

From previous reasons, although *C. inerme* has a variety of phytochemicals, there are not evaluated the bioactive compounds from this plant about antibacterial, antifungal, anti-cholinesterase and Aβ-disaggregation activities. This study then interests to evaluate the bioactive compounds related to these activities. The aspect and important of these activities are;

1.5 Anticholinesterase Activity

AChE and BChE are serine hydrolase enzyme. They have 55% of identical amino acid [46]. During neurotransmission, acetylcholine is released from the nerve into the synaptic cleft and binds to ACh receptors on the post-synaptic membrane. AChE also locates on the post-synaptic membrane and terminates the signal transmission by hydrolyzing ACh. Choline is turned to ACh by activity of choline acetyltransferase [47, 48]. The loss of AChE leads to accumulate acetylcholine in synaptic cleft. It is results with muscle paralysis, seizure and death by asphyxiation [49].

Specific substrate of AChE is different from substrate of BChE. AChE hydrolyzes acetylcholine faster and is less active on BChE. While, BChE prefers to hydrolyzes BCh and can hydrolyze ACh [50]. Moreover, the active sites of these enzymes are different specific amino acid and depend on species. The residues of mouse AChE and human BChE at active site gorge are shown in Fig. 1.9

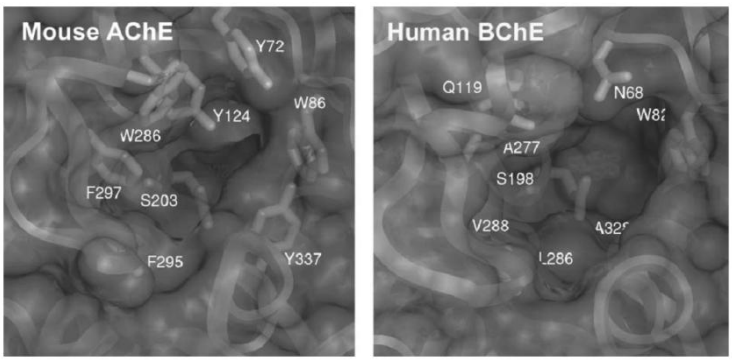

Figure 1.9 Difference of amino acid at active site gorge of mouse AChE and human BChE [51]

Moreover, volume of active site gorge of BChE is more than volume of active site gorge of AChE. The volume of catalytic gorge of BChE from *Oryzias latipes* is 630 $Å^3$ and that of *Torpedo californica* is 410 $Å^3$ [52]. Therefore, the specific substrates and specific activity of these enzymes are different.

1.6 Antimicrobial activity

Use of antimicrobial properties is known since 2000 years ago. Ancient Egyptians and ancient Greeks used specific molds and plant extracts to treat infection. Antibiotics can inhibit or kill microorganisms within the body. It is different target from antiseptics and disinfectants. Moreover, the antibiotics can be attained from natural products or synthesis products. The properties of antimicrobial agent are divided into microbicidal agents (kills the microbial growth) and biostatic agent (inhibits the microbial growth). Antimicrobial chemotherapy is treatment microbial infection while antimicrobial prophylaxis is prevention the infection. The classification of antibiotics are 2 groups [53].

1. β-Lactam

    1.1 Benzylpenicillins : e.g. penicillin G

    1.2 Phenoxypenicillins (oral penicillin) : e.g. penicillin V and propicillin

    1.3 Penicillanase assistant penicillins (anti-streptococcus penicillins) : e.g. oxacillin and dicloxacillin

    1.4 Aminobenzylpenicillins : e.g. ampicillin and amoxicillin

1.5 Ureidopenicillins (broad-spectrum penicillins) : e.g. mezlocillin and piperacillin

1.6 β-Lactam/β-lactamase inhibitors : e.g. ampicillin/ sulbactam and amoxicillin/clavulanate

1.7 Cephalosporins (first generation) : e.g. cefazolin and cefalexin

1.8 Cephalosporins (second generation) : e.g. cefuroxime and cefotiam

1.9 Cephalosporins (third and fourth generation) : e.g. cefotaxime and ceftriaxone

1.10 Monobactams : e.g. aztreonam

1.11 Carbapenems : e.g. imipenem and meropenem

1.12 β-Lactamase inhibitors : e.g. clavulanic acid and tazobactam

2. Other substances

2.1 Aminoglycosides : e.g. streptomycin and gentamicin

2.2 Tetracyclines : e.g. tetracycline and doxycycline

2.3 Quinolones :

Group I: e.g. Norfloxacin

Group II: e.g. Enoxacin, Ofloxacin and Ciprofloxacin

Group III: e.g. Levofloxacin

Group IV: e.g. Moxifloxacin

I: Indications essentially limited to UTI

II: Widely indicated

III: Improved activity against gram-positive and atypical pathogens

IV: Further enhanced activity against gram-positive and atypical pathogens, also against anaerobic bacteria

2.4 Lincosamides : e.g. clindamycin

2.5 Azol derivatives : e.g. miconazole and ketoconazole

2.6 Nitroimidazoles : e.g. metronidazole

2.7 Glycopeptide antibiotics : e.g. vancomycin and teicoplanin

2.8 Macrolides : e.g. erythromycin and spiramycin

2.9 Polyenes : e.g. amphotericin B and nystatin

2.10 Glycylcyclines : e.g. Tigecycline

2.11 Echinocandins : e.g. caspofungin and anidulafungin

2.12 Streptogramines : e.g. quinupristin/dalfopristin

2.13 Ketolides : e.g. telithromycin

2.14 Oxazolidinones : e.g. linezolid

Antibiotics have the specific molecular target. Bacteria commonly have 200 of conserved proteins. The important target pathways of antibiotcs are the ribosome (50S and 30S), cell wall synthesis and DNA gyrase or DNA topoisomerase (Fig 1.11).

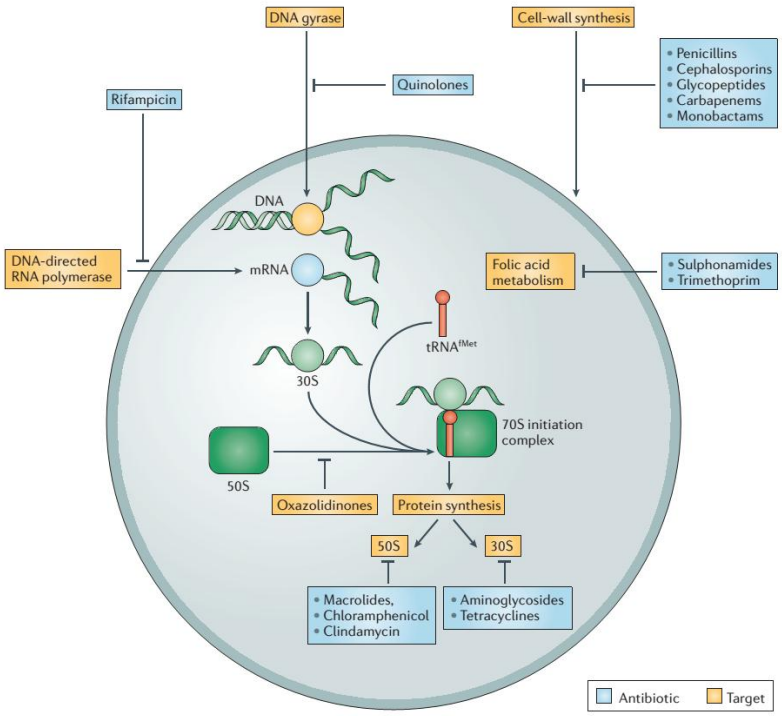

Figure 1.10 Molecular target of antibiotics [54].

Although there are number of antibiotics, the broad spectrum antibiotics are contrast and there are not innovated the more effective antibiotics. That especially suppresses bacterial resistant to antibiotics. If patients are infected with bacterial resistant to antibiotics, they may take severely for a longtime and more expensive for treatment. This is important problem of antibacterial agent in present. Then, the important or broad spectrum of antibiotics could inhibit multitarget of cell,

e.g., ciprofloxacin has DNA gyrase and DNA topoisomerase target. Ampicillin has penicillin-binding proteins target and this antibiotic responsible for peptidoglycan synthesis. Streptomycin is aminoglycoside inhibitor of protein synthesis that binds primarily to 16S ribosomal RNA, which is encoded by several operons. Structure of important antibiotics are shown in Fig. 1.12

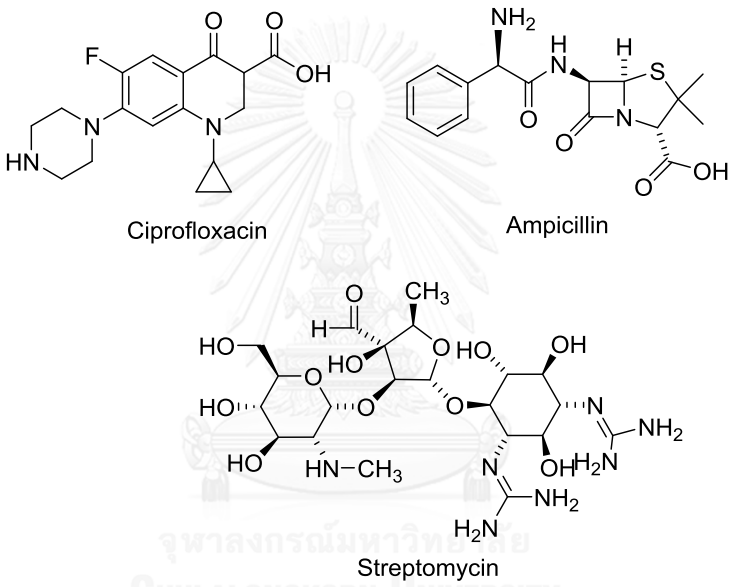

Figure 1.11 Structure of important antibiotics

1.7 Amyloid-β (Aβ)-aggregation

Accumulation of plaque in brain is one cause of Alzheimer's Disease. The plaques consist of aggregates of Aβ. The oligomerization of Aβ provides oligomers, protofibrils, fibrils and plaques as products. Small molecule of Aβ oligomer is toxicity. That can be observed in AD patients. The intermediates pathway of Aβ fibrillization is shown in Table 1.1

Table 1.1 Intermediates pathway of Aβ fibrillization [55].

Aβ species	Characteristics	References
Monomers	soluble amphipathic molecule, potential-helical, random coil or -sheet conformation	[56]
Dimers	hydrophobic core, diameter about 35 nm	[57]
Trimers	toxic oligomers	[58]
Small oligomer	heteromorphous, comsisted of 3–50 monomers, mostly transient and unstable, toxic	[59]
Annular oligomer	membranedisrupting pores or ion channels	[60]
ADDLs	nonfibrillar and neurotoxic	[61]
Protofibrils	short, flexible, rod-like structure, maximum size 8×200 nm, toxic	[62]
Fibrils	stable, filamentous Aβ aggregates consists of repeating Aβ units perpendicular to the fiber axis	[63]
Plaque	large extracellular Aβ deposits, predominantly consists of fibrils, not toxic, surrounds by dystrophic dendrites, axons, activated microglia and reactive astrocytes	[56]

The accumulation of Aβ in brain affects the neurotransmission [64, 65] and memory capacity [66]. These are observed in Alzheimer' Disease pathology.

2. Objectives

2.1 To isolate and separate the phytochemicals from roots and leaves of *C. inerme*

2.2 To elucidate the chemical structures of the isolated phytochemicals

2.3 To evaluate antibacterial, antifungal, anticholinesterase and Aβ-disaggregation activities of isolated compounds from *C. inerme*

CHAPTER II

EXPERIMENTAL

2.1 Plant preparation

The plant in this study was collected from Rayong province, Thailand in May 2012. It was identified as *C. inerme*. A voucher specimen (herbarium number 013514 (BCU)) was deposited at the Department of Botany at Chulalongkorn University.

2.2 Extraction

Air dried leaves (3.78 kg) were extracted twice with CH_2Cl_2. After evaporation the solvent, the CH_2Cl_2 extract was obtained (57.42 g). Residues were subsequently extracted twice with MeOH to yield MeOH extract (95.16 g).

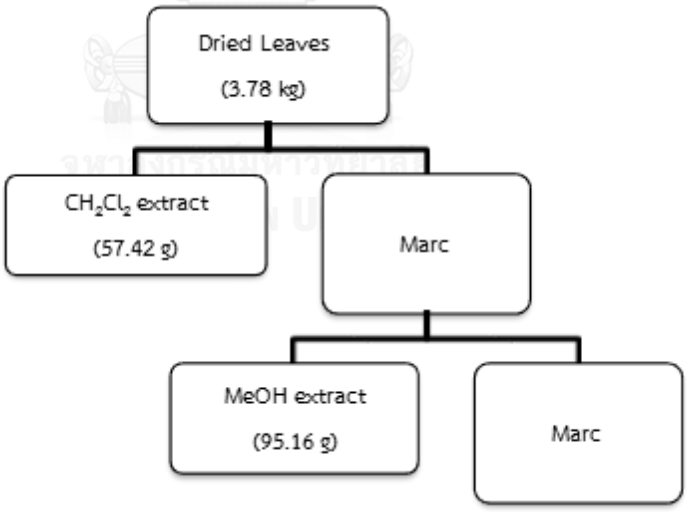

Figure 2.1 Extraction of *C. inerme* leaves.

The extraction of air dried roots (4.45 kg) was processed in the similar method as leaves extraction. The CH_2Cl_2 extract (69.88 g) and MeOH extract (446.47 g) of roots were obtained

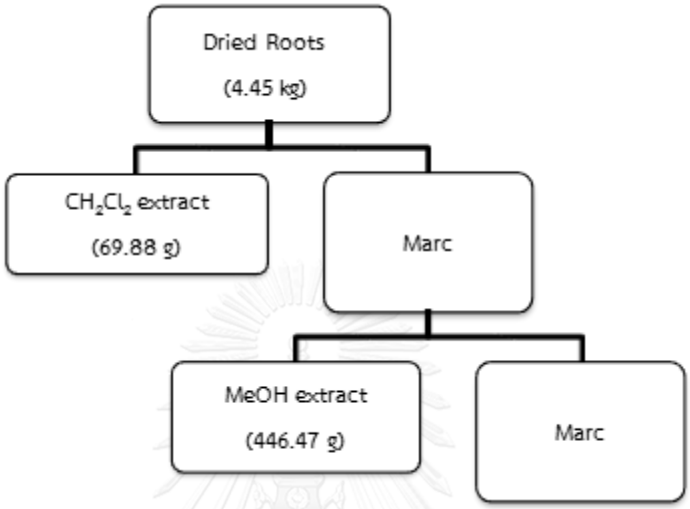

Figure 2.2 Extraction of *C. inerme* roots.

2.3 Fractionation and Isolation of CH_2Cl_2 extract of leaves

A portion of CH_2Cl_2 extract (57.42 g) was fractionated by Si-gel CC eluted with *n*-hexane:EtOAc:MeOH gradient to afford fractions C1-C7. Fraction C2 was separated by Si-gel CC eluted with *n*-hexane:EtOAc gradient to afford fractions C2.1-C2.3. Fraction C2.1 was separated by Si-gel CC eluted with *n*-hexane:EtOAc gradient to afford compound 1 (100 mg). Fraction C3 was separated by a Si-gel CC eluted with *n*-hexane:EtOAc gradient to afford fractions C3.1-C3.2. Fraction C3.1 was separated by Si-gel CC eluted with *n*-hexane:CH_2Cl_2 gradient to afford compound 2 (46.5 mg). Fraction C3.2 was separated by Sephadex LH-20 CC eluted with *n*-hexane:CH_2Cl_2:MeOH

(7:2.5:0.5) to afford fractions C3.2.1-C3.2.3. Fraction C3.2.1 was separated with Sephadex LH-20 CC eluted with *n*-hexane:CH_2Cl_2 (1:1) to afford fractions C3.2.1.1-C3.2.1.4. Fraction C3.2.1.1 was separated with Sephadex LH-20 CC eluted with *n*-hexane:CH_2Cl_2 (1:1) to afford compound 3 (25 mg) and compound 4 (7 mg). Fraction C3.2.1.2 was separated by Si-gel CC eluted with *n*-hexane:EtOAc gradient to afford compound 5 (3 mg) and compound 6 (2 mg).

Fraction C3.2.2 was separated by Sephadex LH-20 CC eluted with *n*-hexane:CH_2Cl_2 (1:1) to obtain fraction C3.2.2.1. This fraction was further separated by Si-gel CC eluted with *n*-hexane:EtOAc gradient to afford compound 7 (23 mg). Moreover, fraction C5 was separated by Si-gel CC eluted with *n*-hexane:EtOAc:MeOH gradient to afford fractions C5.1-C5.2. Fraction C5.1 was separated by Si-gel CC eluted with CH_2Cl_2:MeOH gradient to afford compound 8 (9 mg). The separation procedure of these isolated compounds were shown in Fig. 2.3

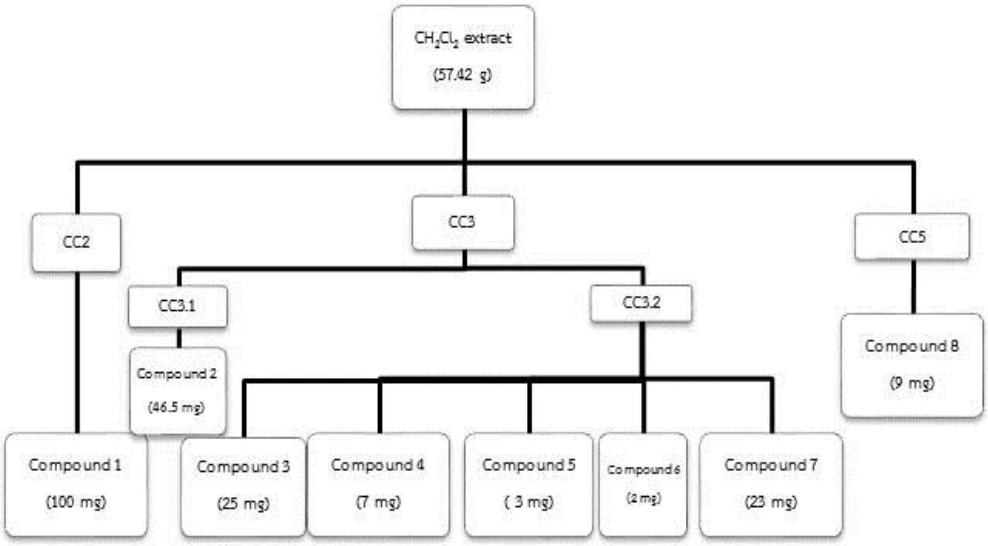

Figure 2.3 The separation procedure of CH_2Cl_2 extract of leaves

2.4 Fractionation and Isolation of CH_2Cl_2 extract of roots.

The CH_2Cl_2 extract of roots (69.88 g) was fractionated by Si-gel CC eluted with *n*-hexane:EtOAc:MeOH gradient to afford fractions R1-R9. Fraction R2 was separated by Si-gel CC eluted with *n*-hexane:EtOAc gradient to afford fractions R2.1-R2.3. Compound **9** (42 mg) and compound **10** (5 mg) was isolated from fraction R2.1. Fraction R2.2 was separated by Si-gel CC eluted with *n*-hexane:EtOAc gradient to afford fraction R2.2.1-R2.2.3. Fraction R2.2.1 was separated by Si-gel CC eluted with *n*-hexane:CH_2Cl_2 gradient to afford compound **11** (5 mg) after recrystallization with MeOH and compound **12** (5 mg) which was recrystallized using MeOH. Fraction R4 was separated by Si-gel CC eluted with *n*-hexane:EtOAc gradient to afford fractions R4.1-R4.3. Fraction R4.1 was then separated by Si-gel CC eluted with *n*-hexane:EtOAc

gradient to afford compound **13** (25 mg). Fraction R 4.2 was separated by Si-gel CC elution with *n*-hexane:EtOAc gradient to afford fraction R 4.2.1- R4.2.3 and fraction R4.2.1was further separated by Sephadex LH-20 CC eluted with CH_2Cl_2:MeOH (30:1) to afford fractions R4.2.1.1 and this fraction was separated by Sephadex LH-20 CC eluted with CH_2Cl_2:MeOH (1:1) to afford compound 14 (5 mg). Finally, fraction R4.3 was separated by Si-gel CC eluted with *n*-hexane:EtOAc gradient to afford compound 15 (10 mg). The separation procedure of these isolated compounds were shown in Fig. 2.4

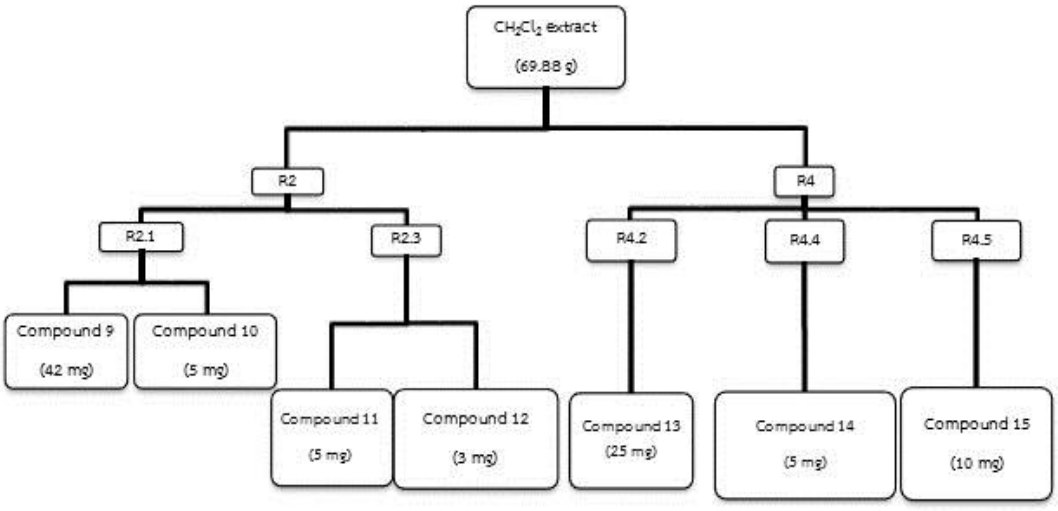

Figure 2.4 The separation procedure of CH_2Cl_2 extract of roots

All compounds were structure elucidated based on ^{1}H and ^{13}C-NMR data. In addition, compound **11-12** were analyzed their molecular mass by Mass spectroscopy (MS). These data were compared with the previous reports.

2.5 Cholinesterase inhibitory testing

The anti-cholinesterase activities towards acetylcholinesterase (AChE) and butyrylcholinesterase (BChE) were determined by modified microplate methods [67, 68]. The principle of the assay was the hydrolysis of substrates acetylthiocholine (ATCI) by AChE to generate thiocholine and acetate. BTCI was another substrate and was hydrolyzed by BChE to generate thiocholine and butyrate. Thiocholine product then reacted with 5,5′-dithiobis(2-nitrobenzoic acid) (DTNB), or Ellman's reagent, to give yellow product of 5-thio-2-nitrobenzoate. If natural product compounds or synthetic compounds have anticholinesterase activity, the reaction between substrate and enzymes were disturbed. The yellow product was changed to pale color (Fig. 2.5).

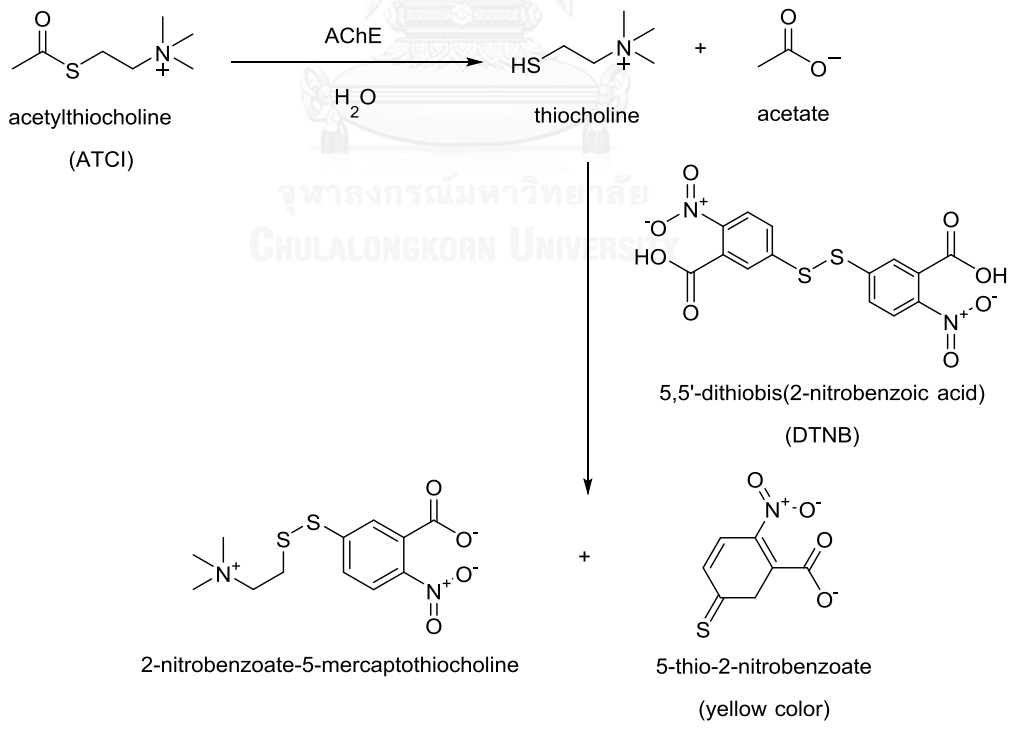

Figure 2.5 Cholinesterase catalyzed hydrolysis of acetylthiocholine

2.5.1 Chemical reagents

Acetylthiocholine iodide (ATCI), butyrylthiocholine iodide (BTCI), 5,5′-dithiobis(2-nitrobenzoic acid) (DTNB), acetylcholinesterase (AChE) from electric eel (Type-VI-Slypophilized powder, EC 3.1.1.7), butyrylcholinesterase (BChE) from equine serum (lypophilized powder, EC 3.1.1.8) and eserine as a standard compound (Sigma-Aldrich, MO, USA). Albumin from bovine serum (Fluka chemical company) and *Tris*-(hydroxymethyl)-aminomethane (*Tris*-HCl) (Merck, Darmstadt, Germany).

2.5.2 Chemical preparation [69]

Buffer A was 50 mM *Tris*-HCl (pH 8)

Buffer B was 50 mM *Tris*-HCl (pH 8) containing 0.1% BSA.

Buffer C was 50 mM *Tris*-HCl (pH 8) containing 0.1 M of NaCl and 0.02 M of $MgCl_2 \cdot 6H_2O$.

All buffers were dissolved in Milli Q water.

Enzymes at 1U/mL of concentration were dissolved in buffer B

Substrates at 1.5 mM of concentration were dissolved in Milli Q water.

Ellman's reagent (DTNB) at 3 mM of concentration was dissolved in buffer C.

2.5.3 Inhibition of cholinesterase testing

The extracts and isolated compounds from *C. inerme* were tested anti-cholinesterase activity. Concentration of the extracts were 1-10 mg/mL and

concentration of isolated compounds and eserine were 0.1-1.0 mg/mL. All samples were dissolved in MeOH. In the 96-well plate, 50 µL of buffer A, 25 µL of 1.5 mM substrate (ATCI or BTCI), 25 µL of sample, 125 µL of 3 mM DTNB, and 25 µL of 1.0 U/mL of enzyme (AChE or BChE) were added and absorbance was measured at 415 nm for 2 min at 5 sec intervals by Sunrise™ microplate reader (P-Intertrade Equipments, Australia). Each experiment was done in triplicate. The percentage of enzyme inhibition was calculated according to this equation;

$$\% \text{ inhibition} = \left(\frac{V_{blank} - V_{sample}}{V_{blank}} \right) \times 100$$

Where

V_{blank} is the velocity of reaction of blank without inhibitors

V_{sample} is the velocity of reaction of sample

If the anti-cholinesterase activity of samples showed higher than 50% inhibition at a concentration of 1 mg/mL, the IC_{50} values will be determined. The IC_{50} is the half maximum (50%) inhibitory concentration of enzymatic activity and graphically determined from a plot of percentage inhibition versus a log final concentration from ten difference concentrations using the Graph Pad Prism 5.01 software (Graph Pad Software Inc.) (Fig. 2.6)

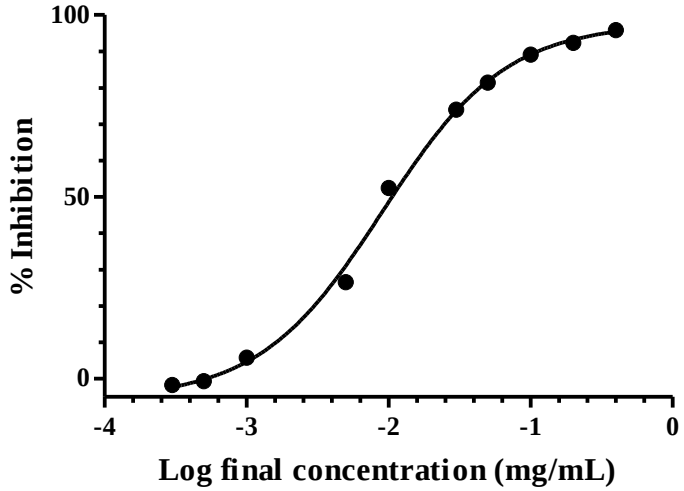

Figure 2.6 A plot of percentage inhibition versus a log final concentration

2.6 β-Amyloid disaggregation testing [70, 71]

2.6.1 Aβ42 aggregate preparation

Aβ42 (American Peptide Company) was dissolved in 100% of 1,1,1,3,3,3-hexafluoro-2-propanal (HFIP) to a concentration of 1 mg/mL, sonicated for 10 min, dried under vacuum, and stored at -20°C. The HFIP-treated Aβ42 was dissolved in 100% DMSO to 1 mg/mL and diluted to 10 mM with PBS (pH 7.4) and incubated at 37°C without shaking. Resveratrol (Sigma-Aldrich, USA) at 20 μM in 100% DMSO was a standard.

2.6.2 Thioflavin T (Th-T) fluorescence assay

Th-T dye of 16.1 mg was dissolved with 10.1 mL of MilliQ water to 100 μM and stored at 4°C before use. Th-T stock was diluted with 500 mM of glycine-NaOH buffer (pH 8.5) to 20 μM. Fluorescence was determined by 150 μl of 20 μM of Aβ42

stock was pipetted to superclear microtube. There were three of difference sample e.g. crude suspension (0.5-2 mg/mL), standard resveratrol and isolated (20 μM), Th-T dye (20 μM) and 0.2% DMSO (blank). Each sample was transferred approximately 150 μL, gentle mixed, incubated at 37°C for 28 hr and then gentle shaked for 30 min to reduce clustering fibrils. The fluorescence emission of Th-T shift when Th-T binded to Aβ-sheet aggregate. The emission was determined by 20 μL of incubated solution was added to 180 μL of 5 mM Th-T in 50 mM phosphate buffer (pH 6.5) in a well of a 96-well plate (black plate) and measured the fluorescence with excitation at 450 nm and emission at 480 nm by Cary Eclipse Fluorescence Spectrophotometer (Agilent Technology, USA). The average of three values showed the time scan after taking off the fluorescence of free Th-T. This experiments were performed in triplicate.

2.7 Antimicrobial activity assays

2.7.1 Crude extract and isolated compounds testing

Bacteria inhibitory activity was tested against gram positive bacteria (*Staphylococcus aureus* ATCC25923 and *Bacillus subtilis* ATCC6633) and gram negative bacteria (*Pseudomonas aeruginosa* ATCC27853 and *Escherichia coli* ATCC25922) by broth dilution susceptibility testing according to Clinical and Laboratory Standards Institute (2011). A single colony of bacteria was isolated by cross streaking on nutrient agar and incubation at 37°C for 24 hr. It was further cultured in Müller-Hinton broth and adjusted the turbidity with Mcfarland standard No. 0.5 (1×10^8 CFU/mL). Culture

suspension about 100 µL was mixed with the serial dilution of extract suspension in Müller-Hinton broth at concentration ranging from 50-300 µg/mL in sterile microplate. They were then incubated at 37°C for 16-18 hr. The Turbidity of bacterial growth was evaluated the minimum inhibitory concentration (MIC) comparing to clavulanic acid and tested in triplicate. Finally, isolates were tested the same method of extracts testing and varied the concentration of isolates from 5-50 µg/mL. Moreover, antifungal activity also tested similar to antifungal activity method and changed to use Sabouraud Dextrose broth (SDB) instead of Müller-Hinton broth and Amphotericin B was a positive control.

CHAPTER III
RESULTS AND DISCUSSIONS

3.1 Extraction and isolation of *C. inerme*

The CH_2Cl_2 extracts of leaves (57.42 g) and roots (69.88 g) were subjected to separate and isolate the phytochemicals. Eight compounds were obtained from leaves extract (compounds **1-8**) and seven compounds (compounds **9**-**15**) were afforded from roots extract. The chemical structures of these isolated compounds were elucidated based on the ^{1}H-NMR and ^{13}C-NMR data and were compared to those reports in the literatures.

3.2 Structural elucidation of isolated compounds from *C. inerme*

CH_2Cl_2 extracts from roots and leaves of *C. inerme* were isolated to obtain 15 compounds. These isolated compounds were classified into 4 main classes which were terpenoids (**1**, **8**-**9** and **11**-**15**), flavones (**2**-**7**) and retroester (**10**). The structure elucidation of isolated compounds were shown in details;

Compound **1** was isolated as white and amorphous powder (m.p 121-126 ^{o}C). The ^{1}H and ^{13}C NMR spectroscopic assignments of compound **1** (Table 3.1 and Appendix A1-A2) were in agreement with literature data for (3β, 22*E,* 24*S*)-stigmasta-5, 22, 25-trien-3-ol [72]. The chemical structure of compound **1** was shown in Fig 3.1.

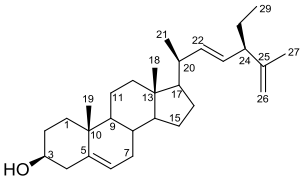

Figure 3.1 Structure of compound **1**

Table 3.1 ^{1}H and ^{13}C-NMR of compound **1** and (3β, 22*E,* 24*S*)-stigmasta-5, 22, 25 trien-3-ol [72]

No.	Compound 1 ($CDCl_3$)		(3β, 22*E,* 24*S*)-stigmasta-5,22,25-trien-3-ol ($CDCl_3$)	
	δ_C	δ_H (int., mult., *J* in Hz)	δ_C	δ_H (int., mult., *J* in Hz)
1	37.3	-	37.9	-
2	31.9	-	32.3	-
3	71.8	3.54 (1H, *m*)	71.3	3.85 (1H,*m*)
4	42.3	-	43.5	-
5	140.8	-	142.0	-
6	121.7	5.36 (1H, *d*, 4.8)	121.2	5.45 (1H, *d*, 5.2)
7	31.9	-	32.6	-
8	31.7	-	32.2	-
9	50.2	-	50.5	-
10	36.5	-	36.9	-
11	21.1	-	21.4	-
12	39.7	-	39.9	-
13	42.3	-	42.4	-
14	56.9	-	57.1	-
15	24.3	-	24.5	-
16	28.7	-	29.1	-
17	55.9	-	56.0	-
18	12.1	0.72 (3H, *brs*)	12.2	ND
19	19.4	1.03 (3H, *s*)	19.6	ND
20	40.1	-	40.5	-

ND = no data

Table 3.1 (Continue) ^{1}H and ^{13}C-NMR of compound **1** and (3β, 22*E,* 24*S*)-stigmasta-5, 22, 25-trien-3-ol [72]

No.	Compound 1 ($CDCl_3$)		(3β, 22*E,* 24*S*)-stigmasta-5,22,25-trien-3-ol ($CDCl_3$)	
	δ_C	δ_H (int., mult., *J* in Hz)	δ_C	δ_H (int., mult., *J* in Hz)
21	20.8	1.04 (3H, *s*)	21.0	ND
22	137.2	5.28 (1H, *dd*, 15.6, 8.0)	137.6	5.34 (1H, *dd*, 15.4, 7.6)
23	130.1	5.21 (1H, *dd*, 15.2, 7.2)	130.3	5.29 (1H, *dd*, 15.4, 7.7)
24	52.0	-	52.3	-
25	148.6	-	148.6	-
26	109.5	4.72 (2H, *m*)	110.2	4.89 (2H, *m*)
27	20.2	1.67 (3H, *s*)	20.3	1.73 (3H, *s*)
28	25.7	-	26.0	-
29	12.1	0.86 (3H, *t*, 7.4)	12.4	ND

ND = no data

Compound **2** was isolated as yellow needle (m.p 211-212 °C). The ^{1}H and ^{13}C NMR spectroscopic assignments of compound **2** (Table 3.2 and Appendix A3-A4) were in agreement with literature data for pectolinarigenin [73]. Moreover, the positions of substituents were confirmed by means of HMBC-, HSQC- and COSY-spectra (Appendix A5-A7). The chemical structure of compound **2** was shown in Fig 3.2.

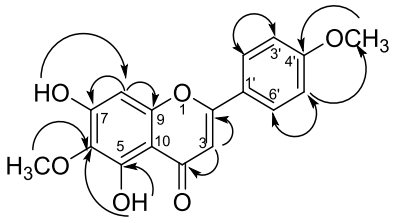

Figure 3.2 Key of HMBC correlation and COSY correlation of compound **2**

Table 3.2 ^{1}H and ^{13}C-NMR of compound **2** and pectolinarigenin [73]

No.	compound 2 (Acetone-*d6*)		Pectolinarigenin (DMSO-*d6*)	
	δ_C	δ_H (int., mult., *J* in Hz)	δ_C	δ_H (int., mult., *J* in Hz)
2	165.0	-	163.3	-
3	104.0	6.53 (1H, *s*)	103.9	6.83 (1H, *s*)
4	183.6	-	182.6	-
5	154.0	-	152.2	-
6	132.3	-	131.3	-
7	157.8	-	152.3	-
8	94.8	6.48 (1H, *s*)	94.3	6.59 (1H, *s*)
9	154.0	-	151.9	-
10	105.8	-	104.1	-
1′	124.4	-	123.7	-
2′	129.1	7.87d (1H, *d*, 8.8)	128.8	8.00 (1H, *d*, 8.9)
3′	115.4	6.96 d (1H, *d*, 8.8)	114.8	7.08 (1H, *d*, 8.9)
4′	163.0	-	160.9	-
5′	115.4	6.96 (1H, *d*, 8.8)	114.8	7.08 (1H, *d*, 8.9)
6′	129.1	7.87 (1H, *d*, 8.8)	128.8	8.00 (1H, *d*, 8.9)
6-OMe	60.7	3.72 (3H, *s*)	60.4	3.75 (3H, *s*)
4′-OMe	56.0	3.76 (3H, *s*)	55.8	3.84 (3H, *s*)
7-OH	-	9.31 (1H, *s*)	-	10.67 (1H, *s*)
5-OH	-	13.02 (1H, *s*)	-	13.01 (1H, *s*)

Compound **3** was isolated as yellow needle (m.p 184-185 °C). The ^{1}H and ^{13}C NMR spectroscopic assignments of compound **3** (Table 3.3 and Appendix A8-A9) were

in agreement with literature data for acacetin [74]. The chemical structure of compound **2** was shown in Fig 3.3.

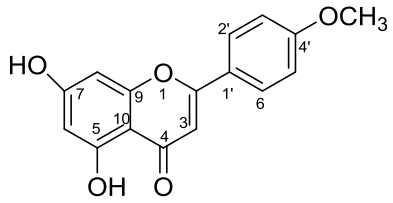

Figure 3.3 Structure of compound **3**

Table 3.3 ^{1}H and ^{13}C-NMR of compound **3** and acacetin [74]

No.	Compound 3 (Acetone-*d6*)		Acacetin (CD_3OD in $CDCl_3$)	
	δ_C	δ_H (int., mult., *J* in Hz)	δ_C	δ_H (int., mult., *J* in Hz)
2	165.1	-	164.1	-
3	104.5	6.59 (1H, *s*)	103.3	6.63 (1H, *s*)
4	183.1	-	182.3	-
5	163.7	-	161.4	-
6	99.8	6.17 (1H, *d*, 1.6)	99.1	6.21 (1H, *d*, 2.0)
7	164.8	-	163.9	-
8	94.7	6.46 (1H, *d*, 1.6)	94.1	6.46 (1H, *d*, 2.0)
9	158.9	-	157.8	-
10	104.6	-	104.4	-
1′	124.3	-	123.3	-
2′, 6′	129.1	7.94 (2H, *d*, 8.8)	127.9	7.94 (2H, *d*, 9.0)
3′,5′	115.4	7.05 (2H, *d*, 8.8)	114.3	7.08 (2H, *d*, 9.0)
4′	163.3	-	162.5	-
4′-OMe	56.0	3.93 (3H, *s*)	55.3	3.88 (3H, *s*)
7-OH		12.87 (1H, *s*)		ND

ND = no data

Compound **4** was isolated as yellow and amorphous powder (m.p 203-205 °C). The ^{1}H and ^{13}C NMR spectroscopic assignments of compound **4** (Table 3.4 and Appendix A10) were in agreement with literature data for 5,8-dihydroxy-7,4′-dimethoxyflavone [75]**.** The chemical structure of compound **4** was shown in Fig 3.4.

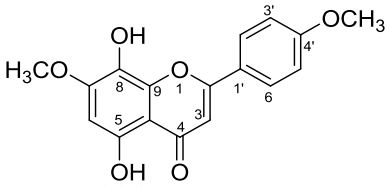

Figure 3.4 Structure of compound **4**

Table 3.4 ^{1}H-NMR of compound **4** and 5,8-dihydroxy-7,4′-dimethoxyflavone [75]

No.	Compound 4 (CD_3OD)	5,8-dihydroxy-7,4′-dimethoxyflavone (DMSO-*d6*)
	δ_H (int., mult., *J* in Hz)	δ_H (int., mult., *J* in Hz)
3	6.65 (1H, *s*)	6.88 (1H, *s*)
6	6.59 (1H, *s*)	6.56 (1H, *s*)
2′, 6′	7.95 (2H, *d*, 8.8)	8.15 (2H, *d*, 8.0)
3′,5′	7.08 (2H, *d*, 8.8)	7.13 (2H, *d*, 8.0)
7-OMe	3.89 (3H, *s*)	3.87 (3H, *s*)
4′-OMe	3.88 (3H, *s*)	3.91 (3H, *s*)
5-OH	ND	12.44 (1H, *s*)

ND = no data

Compound **5** was isolated as yellow and amorphous powder (m.p 225-230 °C). The ^{1}H and ^{13}C NMR spectroscopic assignments of compound **5** (Table 3.5 and

Appendix A11-A12) were in agreement with literature data for scutellarein-4′-methyl ether [76]. The chemical structure of compound **5** was shown in Fig 3.5.

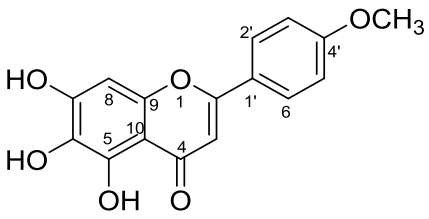

Figure 3.5 Structure of compound **5**

Table 3.5 ^{1}H and ^{13}C-NMR of compound **5** and scutellarein-4′-methyl ether [76]

No.	Compound 5 (Acetone-*d6*)		Scutellarein-4′-methyl ether (^{1}H in $CDCl_3$+CD_3OD; ^{13}C in DMSO-*d6*)	
	δ_C	δ_H (int., mult., *J* in Hz)	δ_C	δ_H (int., mult., *J* in Hz)
2	165.3	-	163.0	-
3	103.6	6.59 (1H, *s*)	102.8	6.69 (1H, *s*)
4	183.6	-	181.9	-
5	146.9	-	147.0	-
6	129.3	-	129.1	-
7	157.6	-	153.3	-
8	94.8	6.58 (1H, *s*)	93.8	6.50 (1H, *s*)
9	143.7	-	149.6	-
10	103.6	-	104.0	-
1′	123.3	-	123.0	-
2′, 6′	127.2	7.88 (2H, *d*, 8.80)	128.2	7.98 (2H, *d*, 7.97)
3′,5′	116.9	6.98 (2H, *d*, 8.80)	114.6	7.08 (2H, *d*, 7.10)
4′	162.0	-	162.2	-
4′-OMe	60.7	3.82 (3H, *s*)	55.5	3.88 (3H, *s*)

Compound **6** was isolated as yellow and amorphous powder (m.p 246-248 °C). The ^{1}H and ^{13}C NMR spectroscopic assignments of compound **6** (Table 3.6 and

Appendix A13) were in agreement with literature data for ladanein [77]. The chemical structure of compound **6** was shown in Fig 3.6.

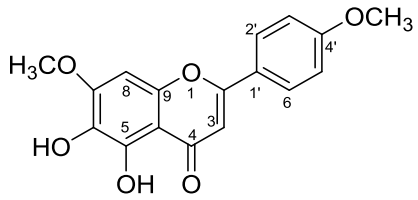

Figure 3.6 Structure of compound **6**

Table 3.6 ^{1}H-NMR of compound **6** and ladanein [77]

No.	Compound *6* (Acetone-*d6*)	Ladanein ($CDCl_3$)
	δ_H (int., mult., *J* in Hz)	δ_H (int., mult., *J* in Hz)
3	6.84 (1H, *s*)	6.70 (1H, *s*)
8	6.68 (1H, *s*)	6.88 (1H, *s*)
2′, 6′	7.90 (2H, *d*, 8.8)	8.04 (2H, *d*, 8.9)
3′, 5′	6.94 (2H, *d*, 8.8)	7.13 (2H, *d*, 8.9)
7-OMe	3.84 (3H, *s*)	3.99 (3H, *s*)
4′-OMe	3.99 (3H, *s*)	3.92 (3H, *s*)
5-OH	ND	12.65 (1H, *s*)

ND = no data

Compound **7** was isolated as yellow and amorphous powder (m.p 209-215 °C). The ^{1}H and ^{13}C NMR spectroscopic assignments of compound **7** (Table 3.7 and Appendix A14-A15) were in agreement with literature data for 5-hydroxy-4',7-dimethoxyflavone [78]. The chemical structure of compound **7** was shown in Fig 3.7.

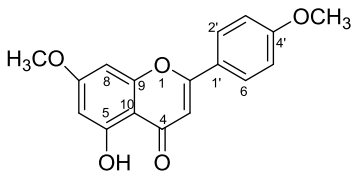

Figure 3.7 Structure of compound **7**

Table 3.7 ^{1}H and ^{13}C-NMR of compound **7** and 5-hydroxy-4',7-dimethoxyflavone [78]

No.	Compound 7 ($CDCl_3$)		5-hydroxy-4',7-dimethoxyflavone ($CDCl_3$)	
	δ_C	δ_H (int., mult., *J* in Hz)	δ_C	δ_H (int., mult., *J* in Hz)
2	164.2	-	162.6	-
3	103.8	6.59 (1H, *s*)	104.4	6.57 (1H, *s*)
4	183.0	-	182.5	-
5	155.0	-	157.7	-
6	103.8	6.61 (1H, *d, 0.24*)	98.0	6.48 (1H, *d*, 2.2)
8	93.3	6.61 (1H, *d, 0.36*)	92.6	6.36 (1H, *d*, 2.2)
9	162.7	-	162.2	-
10	105.8	-	105.6	-
1′	123.6	-	123.6	-
2′, 6′	128.1	7.84 (2H, *d*, 8.8)	128.0	7.85 (2H, *d*, 8.8)
3′,5′	114.5	7.02 (2H, *d*, 8.8)	114.5	7.02 (2H, *d*, 8.8)
4′	164.2	-	164.0	-
4′-OMe	55.5	3.89 (3H, *s*)	55.5	3.88 (3H, *s*)
7-OMe	60.9	4.04 (3H, *s*)	55.8	3.89 (3H, *s*)
5-OH	-	13.09 (1H, *brs*)	-	12.81 (1H, *brs*)

Compound **8** was isolated as white and amorphous powder (m.p 259-261 °C). The ^{1}H and ^{13}C-NMR spectroscopic assignments of compound **8** (Table 3.8 and Appendix A16-A17) were in agreement with literature data for (3β, 22*E*, 24*S*)-stigmasta-

5, 22, 25-trien-3-yl-β-D-glucopyranoside [79]. The chemical structure of compound **8** was shown in Fig 3.8.

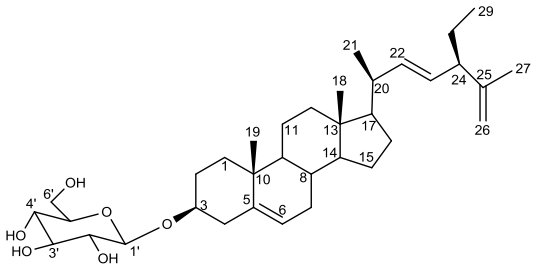

Figure 3.8 Structure of compound **8**

Table 3.8 ^{1}H and ^{13}C-NMR of compound **8** and (3β, 22*E*, 24*S*)-stigmasta-5, 22, 25-trien-3-yl-β-D-glucopyranoside [79]

No.	Compound 8 ($CDCl_3$)		(3β, 22*E*, 24*S*)-stigmasta-5,22,25-trien-3-yl-β-D-glucopyranoside (C_5D_5N)	
	δ_C	δ_H (int., mult., *J* in Hz)	δ_C	δ_H(int., mult., *J* in Hz)
1	38.7	-	38.0	-
2	29.6	-	30.7	-
3	76.3	3.51 (1H, *m*)	79.1	3.91 (1H, *m*)
4	42.2	-	40.3	-
5	140.2	-	141.4	-
6	122.1	5.29 (1H, *brd*, 4.4)	122.4	5.33 (1H)*
7	31.8	-	32.6	-
8	36.7	-	32.5	-
9	50.1	-	50.8	-
10	37.2	-	37.4	-
11	21.0	-	21.8	-
12	39.6	-	39.8	-
13	48.5	-	42.8	-

*no coupling constant data

Table 3.8 (continue) ^{1}H and ^{13}C-NMR of compound **8** and (3β, 22*E*, 24*S*)-stigmasta-5, 22, 25-trien-3-yl-β-D-glucopyranoside [79]

No.	Compound 8 ($CDCl_3$)		(3β, 22*E*, 24*S*)-stigmasta-5,22,25-trien-3-yl-β-D-glucopyranoside (C_5D_5N)	
	δ_C	δ_H (int., mult., *J* in Hz)	δ_C	δ_H(int., mult., *J* in Hz)
14	56.8	-	57.3	-
15	24.2	-	25.0	-
16	28.6	-	29.5	-
17	55.8	-	56.5	-
18	12.0	-	12.6	-
19	20.7	-	19.9	-
20	40.1	-	40.9	-
21	21.0	-	21.5	-
22	137.1	5.12 (1H, *m*)	138.1	5.28 (1H, *m*)
23	130.0	5.12 (1H, *m*)	130.8	5.28 (1H, *m*)
24	51.9	-	52.8	-
25	148.6	-	149.1	-
26	109.4	4.63 (1H, *brs*)	110.6	4.59 (1H, *brs*)
27	19.2	1.59 (3H, *s*)	20.8	1.61 (3H, *s*)
28	25.7	-	26.5	-
29	12.0	-	12.9	-
1′	101.0	4.35 (1H, *d*, 7.6)	103.0	4.26 (1H)*
2′	73.5	3.76 (1H, *m*)	75.8	4.26 (1H, *m*)
3′	79.2	3.76 (1H, *m*)	78.6	4.26 (1H, *m*)
4′	69.9	3.40 (1H, *m*)	72.2	4.26 (1H, *m*)
5′	75.6	3.33 (1H, *m*)	78.9	4.26 (1H, *m*)
6′	61.7	3.40 (2H, *m*)	63.3	4.262H, *m*)

*no coupling constant data

Compound **9** was isolated as white and amorphous powder (m.p 147-155 °C). The ^{1}H and ^{13}C-NMR spectroscopic assignments of compound **9** (Table 3.9 and

Appendix A18-A19) were in agreement with literature data for stigmasterol [80]. The chemical structure of compound **9** was shown in Fig 3.9.

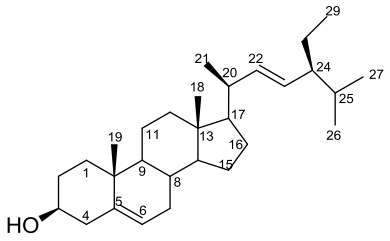

Figure 3.9 Structure of compound **9**

Table 3.9 ^{1}H and ^{13}C-NMR of compound **9** and stigmasterol [80]

No.	Compound 9 ($CDCl_3$)		Stigmasterol ($CDCl_3$)	
	δ_C	δ_H (int., mult., *J* in Hz)	δ_C	δ_H (int., mult., *J* in Hz)
1α	39.7	1.25 (1H, *m*)	37.6	1.09 (1H, *m*)
1β		1.99 (1H, *m*)		1.86 (1H, *m*)
2α	31.7	1.52 (1H, *m*)	32.0	1.52 (1H, *m*)
2β		1.83 (1H, *m*)		1.84 (1H, *m*)
3	71.8	3.52 (1H, *m*)	72.2	3.52 (1H, *m*)
4α	42.3	2.27 (1H, *m*)	42.7	2.23 (1H, *m*)
4β		2.27 (1H, *m*)		2.31 (1H, *m*
5	140.8	-	141.1	-
6	121.7	5.34 (1H, *m*)	122.1	5.35 (1H, *m*)
7α	31.9	1.60 (1H, *m*)	32.0	1.50 (1H, *m*)
7β		1.83 (1H, *m*)		1.96 (1H, *m*)
8	31.9	1.52 (1H, *m*)	32.3	1.47 (1H, *m*)

*Overlapped signal

Table 3.9 (continue) ^{1}H and ^{13}C-NMR of compound **9** and stigmasterol [80]

No.	Compound 9 ($CDCl_3$)		Stigmasterol ($CDCl_3$)	
	δ_C	δ_H (int., mult., *J* in Hz)	δ_C	δ_H (int., mult., *J* in Hz)
9	51.2	1.03 (1H, *m*)	50.5	0.93 (1H, *m*)
10	37.3	-	36.6	-
11α	21.2	1.52 (1H, *m*)	21.5	1.50 (1H, *m*)
11β		1.60 (1H, *m*)		1.50 (1H, *m*)
12α	36.5	1.25 (1H, m)	40.0	1.18 (1H, *m*)
12β		1.99 (1H, *m*)		2.00 (1H, *m*)
13	42.2	-	42.6	-
14	56.9	1.25 (1H, m)	57.2	1.04 (1H, *m*)
15α	25.4	1.03 (1H, *m*)	24.7	1.04 (1H, *m*)
15β		1.60 (1H, *m*)		1.56 (1H, *m*)
16α	29.7	1.25 (1H, m)	28.7	1.29 (1H, *m*)
16β		1.69 (1H, *m*)		1.72 (1H, *m*)
17	56.0	1.25 (1H, m)	56.3	1.15 (1H, *m*)
18	12.0	0.70 (3H, *s*)	12.3	0.70 (3H, *s*)
19	21.0	1.01 (3H, *s*)	19.4	1.01 (3H, *s*)
20	40.4	1.99 (1H, *m*)	41.0	2.06 (1H, *m*)
21*	24.4	1.01 (3H, *s*)	21.5	1.04 (3H, *s*)
22	138.3	5.15 (1H, *m*)	138.7	5.15 (1H, *dd*, 15.2, 8.6)
23	129.3	5.02 (1H, *dd*, 15.2, 8.4)	129.6	5.02 (1H, *dd*, 15.2, 8.6)
24	50.2	1.52 (1H, *m*)	51.6	1.53 (1H, *m*)
25	31.9	1.52 (1H, *m*)	32.3	1.54 (1H, *m*)
26	21.1	0.80 (3H, *m*)	21.5	0.92 (3H, *d*, 5.8)
27	19.4	0.84 (3H, *brs*)	19.2	0.81 (3H, *brs*)
28α	28.9	1.25 (1H, *m*)	25.8	1.22 (1H, *m*)
28β		1.52 (1H, *m*)		1.56 (1H, *m*)
29	12.2	0.79 (3H, *brs*)	12.4	(3H, *brs*)

*Overlapped signal

Compound **10** was isolated as white and amorphous powder (m.p 169-174 °C). The ^{1}H and ^{13}C NMR spectroscopic assignments of compound **10** (Table 3.10 and Appendix A20-21) were in agreement with literature data for *n*-hexadecyl propionate [81]. The chemical structure of compound **10** was shown in Fig 3.10.

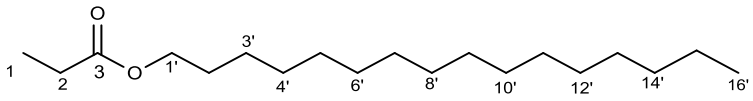

Figure 3.10 Structure of compound **10**

Table 3.10 ^{1}H and ^{13}C-NMR of compound **10** and *n*-hexadecyl propionate [81]

No.	Compound 10 ($CDCl_3$)		*n*-hexadecyl propionate ($CDCl_3$)	
	δ_C	δ_H (int., mult., *J* in Hz)	δ_C	δ_H (int., mult., *J* in Hz)
1	14.2	0.86 (3H, *t*, 3.4)	14.1	0.86 (3H, *t*, 3.0)
2	29.6	1.25 (2H, *m*)	29.3	1.21 (2H, *m*)
3	174.0	-	174.5	-
1′	64.4	4.01 (2H, *t,* 6.8)	64.5	4.06 (2H, *t*, 7.0)
2′	32.1	2.29 (2H, *m*)	32.0	2.31 (2H, *q*, 12)
3′	29.9	1.61 (2H, *m*)	29.3	1.45 (2H, *m*)
4′-15′	25.2-29.8	1.25 (2H, *m*)	29.3	1.21 (2H, *m*)
16′	9.50	0.86 (3H, *t*, 3.4)	9.18	1.12 (3H, *t*, 3.0)

Compound **11** was isolated as white and amorphous powder (m.p 214-220 °C). The ^{1}H and ^{13}C NMR spectroscopic assignments of compound **11** (Table 3.11 and Appendix A22-24) were in agreement with literature data for lupeol laurate [82].

Moreover, the number of methylene carbons at C-2 to C-11 were confirmed by its HRMS spectrum ($[M+Na]^+$ 631.51190) (Appendix 37). The chemical structure of compound **11** was shown in Fig 3.11.

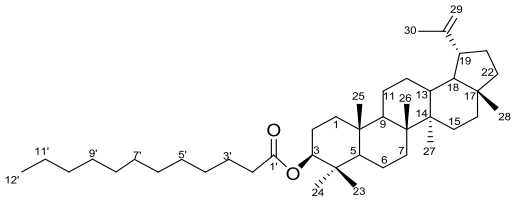

Figure 3.11 Structure of compound **11**

Table 3.11 ^{1}H and ^{13}C-NMR of compound **11** and lupeol laurate [82]

No.	Compound 11 ($CDCl_3$)		Lupeol laurate ($CDCl_3$)	
	δ_C	δ_H (int., mult., *J* in Hz)	δ_C	δ_H (int., mult., *J* in Hz)
1	39.9	-	38.3	-
2	23.6	-	23.7	-
3	80.5	4.47 (1H, *dd*, 5.6, 10.4)	80.8	4.32 (1H, *dd*, 6, 9.7)
4	38.3	-	37.8	-
5	55.3	-	55.4	-
6	18.1	-	18.2	-
7	34.1	-	34.2	-
8	42.9	-	40.8	-
9	50.2	-	50.3	-
10	37.7	-	37.0	-
11	22.5	-	21.0	-
12	25.0	-	25.1	-
13	37.9	-	38.0	-
14	42.7	-	42.8	-
15	29.7	-	27.4	-

Table 3.11 (Continue) ^{1}H and ^{13}C-NMR of compound **11** and lupeol laurate [82]

No.	Compound 11 ($CDCl_3$)		Lupeol laurate ($CDCl_3$)	
	δ_C	δ_H (int., mult., *J* in Hz)	δ_C	δ_H (int., mult., *J* in Hz)
16	34.7	-	35.6	-
17	40.7	-	43.0	-
18	48.2	-	48.3	-
19	47.8	2.36 (1H, *m*)	47.9	2.6-2.2 (1H, *m*)
20	151.0	-	150.8	-
21	27.8	-	29.8	-
22	37.0	-	40.0	-
23	29.5	0.88 (3H, *s*)	27.9	0.87 (3H, *s*)
24	17.9	1.02 (3H, *s*)	15.9	1.07 (3H, *s*)
25	16.4	0.88 (3H, *s*)	16.2	0.86 (3H, *s*)
26	16.0	0.85 (3H, *s*)	16.5	0.86 (3H, *s*)
27	14.4	0.94 (3H, *s*)	14.5	0.98 (3H, *s*)
28	15.9	0.84 (3H, *s*)	18.0	0.80 (3H, *s*)
28	15.9	0.84 (3H, *s*)	18.0	0.80 (3H, *s*)
29	109.2	4.68 (1H, *brs*) 4.57 (1H, *brs*)	109.5	4.72(1H, *brs*), 4.52(1H, *brs*)
30	20.8	1.68(3H, *brs*)	19.3	1.72(3H, *brs*)
1′	173.5	-	173.7	-
2′	35.5	2.28 (2H, *t*, 7.6)	34.8	2.32 (2H, *t*, 7.4)
3′	23.0	1.25 (2H, *brs*)	25.2	1.27(2H, *brs*)
4′-9′	27.3	1.25 (2H, *brs*)	29.7-29.2	1.27(2H, *brs*)
10′	31.8	1.25 (2H, *brs*)	31.9	1.27(2H, *brs*)
11′	19.1	1.25 (2H, *brs*)	22.7	1.27(2H, *brs*)
12′	13.9	0.87 (3H, *t*, 6.8)	15.99	0.91 (3H, *t*, 7)

Compound **12** was isolated as white and amorphous powder (m.p 79-89 °C). The ^{1}H and ^{13}C NMR spectroscopic assignments of compound **12** (Table 3.12 and Appendix A25-30) were in agreement with literature data for β-Amyrin docosanoate [83]. Moreover, the number of methylene carbons at C-2 to C-21 were confirmed by its HRMS spectrum ($[M+Na]^{+}$ 771.50034) (Appendix 38). The chemical structure of compound **12** was shown in Fig 3.12.

Figure 3.12 Structure of compound **12**

Table 3.12 ^{1}H and ^{13}C-NMR of compound **12** and β-Amyrin docosanoate [83]

No.	Compound 12 ($CDCl_3$)		β-Amyrin docosanoate ($CDCl_3$)	
	δ_C	δ_H (mult., int., J in Hz)	δ_C	δ_H (mult., int., J in Hz)
1	38.2	1.86 (2H, *m*)	38.7	1.62 (2H, *m*)
2	22.5	1.57 (2H, *m*)	22.9	1.64 (2H, *m*)
3	80.5	4.50 (1H, *m*)	80.8	4.50 (1H, *m*)
4	36.7	-	38.0	-
5	55.2	1.25 (1H, *m*)	55.5	0.87(1H, *m*)
6	16.7	1.57 (2H, *m*)	18.5	1.55 (2H, *m*)

Table 3.12 (continue) ^{1}H and ^{13}C-NMR of compound **12** and β-Amyrin docosanoate [83]

No.	Compound 12 ($CDCl_3$)		**β**-Amyrin docosanoate ($CDCl_3$)	
	δ_C	δ_H (mult., int., J in Hz)	δ_C	δ_H (mult., int., J in Hz)
7	33.2	1.57 (2H, *m*)	32.2	1.37 (2H, *m*)
8	39.7	-	40.1	-
9	47.4	1.57 (2H, *m*)	47.9	1.55 (1H, *m*)
10	34.3	-	37.0	-
11	23.6	1.96 (1H, *m*)	23.6	1.90 (1H, *m*)
12	121.5	5.18 (1H, *t*)	124.6	5.12 (1H, *t*)
13	145.1	-	139.9	-
14	41.6	-	42.3	-
15	26.0	1.96 (1H, *m*)	26.9	1.62 (2H, *m*)
16	25.8	1.57 (2H, *m*)	25.4	1.64 (2H, *m*)
17	34.6	-	34.0	-
18	47.1	1.57 (2H, *m*)	47.9	1.58 (1H, *m*)
19	37.9	1.57 (2H, *m*)	41.8	1.44 (2H, *m*)
20	32.4	-	31.5	-
21	34.7	1.25 (2H, *m*)	35.1	1.25 (2H, *m*)
22	37.6	1.57 (2H, *m*)	38.0	1.53 (2H, *m*)
23	23.4	1.25 (3H, *s*)	28.3	0.87 (3H, *s*)
24	15.4	1.25 (3H, *s*)	17.1	0.85 (3H, *s*)
25	16.6	1.25 (3H, *s*)	16.0	1.01 (3H, *s*)
26	18.1	1.25 (3H, *s*)	17.1	0.80 (3H, *s*)
27	26.8	1.25 (3H, *s*)	26.9	1.07 (3H, *s*)
28	28.2	1.25 (3H, *s*)	29.0	0.87 (3H, *s*)
29	31.8	1.25 (3H, *s*)	34.0	0.85 (3H, *s*)
30	23.5	1.25 (3H, *s*)	23.5	1.07 (3H, *s*)
1′	173.5	-	173.9	-
2′	37.0	2.25 (2H, *m*)	33.1	2.31 (2H, *m*)
3′	29.6	1.57 (2H, *m*)	26.9	1.64 (2H, *m*)
4′-19′	25.0-29.5	1.25 (2H, *m*)	29.4	1.25 (2H, *m*)
20′	30.9	1.25 (2H, *m*)	31.5	1.30 (2H, *m*)
21′	24.9	1.25 (2H, *m*)	23.9	1.30 (2H, *m*)
22′	13.9	0.83 (3H, *m*)	14.3	0.85 (3H, *m*)

Compound **13** was isolated as white and amorphous powder (m.p 219-220 °C). The ^{1}H and ^{13}C NMR spectroscopic assignments of compound **13** (Table 3.13 and Appendix A31-32) were in agreement with literature data for betulinic acid [84]. The chemical structure of compound **13** was shown in Fig 3.13.

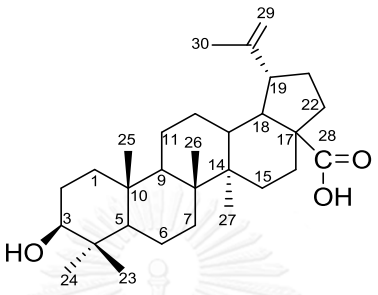

Figure 3.13 Structure of compound **13**

Table 3.13 ^{1}H and ^{13}C-NMR of compound **13** and betulinic acid [84]

No.	Compound 13 ($CDCl_3$)		Betulinic acid ($CDCl_3$)	
	δ_C	δ_H (int., mult., *J* in Hz)	δ_C	δ_H (int., mult., *J* in Hz)
1α	38.8	0.91 (1H, *m*)	39.3	0.99 (1H, *m*)
1β		1.69(1H, *m*)		1.67 (1H, *m*)
2	27.4	1.69 (2H, *m*)	28.3	1.85 (2H, *m*)
3	79.0	3.00 (1H, *m*)	78.1	3.45 (1H, *m*)
4	39.0	-	39.5	-
5	55.4	0.75 (1H, *m*)	56.0	0.82 (1H, *m*)
6α	18.3	1.69 (1H, *m*)	18.8	1.56 (1H, *m*)
6β		1.41 (1H, *m*)		1.38 (1H, *m*)
7α	34.4	1.41 (1H, *m*)	34.9	1.45 (1H, *m*)
7β		1.38 (1H, *m*)		1.38 (1H, *m*)
8	40.7	-	41.1	-
9	50.6	1.38 (1H, *m*)	51.0	1.38 (1H, *m*)
10	37.0	-	37.5	-
11α	20.9	1.38 (1H, *m*)	21.2	1.43 (1H, *m*)
11β		1.25 (1H, *m*)		1.21 (1H, *m*)
12α	25.5	1.25 (1H, *m*)	26.1	1.21 (1H, *m*)
12β		2.23 (1H, *m*)		1.94 (1H, *m*)

Table 3.13 (continue) ^{1}H and ^{13}C-NMR of compound **13** and betulinic acid [84]

No.	Compound 13 ($CDCl_3$)		Betulinic acid ($CDCl_3$)	
	δ_C	δ_H (int., mult., *J* in Hz)	δ_C	δ_H (int., mult., *J* in Hz)
13	38.4	2.23 (1H, *m*)	38.6	2.74 (1H, *m*)
14	42.5	-	42.9	
15α 15β	29.7	1.25 (1H, *m*) 2.23 (1H, *m*)	30.3	1.26 (1H, *m*) 1.88 (1H, *m*)
16α	32.2	1.69 (1H, *m*)	32.9	1.55 (1H, *m*)
17	56.3	-	56.6	-
18	49.3	1.69 (1H, *m*)	49.8	1.77 (1H, *m*)
19	46.9	3.18 (1H, *m*)	47.8	3.52 (1H, *m*)
20	150.4	-	151.3	-
21α	30.6	1.53 (1H, *m*)	31.2	1.53 (1H, *m*)
22α 22β	37.2	1.53 (1H, *m*) 1.98 (1H, *m*)	37.6	1.57 (1H, *m*) 2.25 (1H, *m*)
23	28.0	1.21 (1H, *m*)	28.7	1.22 (1H, *s*)
24	16.1	0.94 (3H, *s*)	16.3	1.00 (3H, *s*)
25	15.3	0.83 (3H, *s*)	16.4	0.83 (3H, *s*)
26	16.0	0.97 (3H, *s*)	16.4	1.06 (3H, *s*)
27	14.7	0.98 (3H, *s*)	14.9	1.07 (3H, *s*)
28	179.9	-	178.8	-
29α 29β	109.7	4.74 (1H, *s*) 4.61 (1H, *s*)	109.9	4.95 (3H, *s*) 4.77 (3H, *s*)
30	19.4	1.69 (3H, *s*)	19.5	17.9 (3H, *s*)

Compound **14** was isolated as white and amorphous powder (m.p 114-122 °C). The ^{1}H and ^{13}C NMR spectroscopic assignments of compound **14** (Table 3.14 and Appendix A33-34) were in agreement with literature data for 6,11,12,16-tetrahydroxy-5,8,11,13-abitetetraen-7-one [85]. The chemical structure of compound **14** was shown in Fig 3.14.

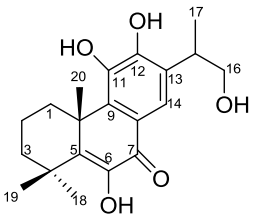

Figure 3.14 Structure of compound **14**

Table 3.14 ^{1}H and ^{13}C-NMR of compound **14** and 6,11,12,16-tetrahydroxy-5,8,11,13-abitetetraen-7-one [85]

No.	Compound 14 ($CDCl_3$)		6,11,12,16-tetrahydroxy-5,8,11,13-abitetetraen-7-one ($CDCl_3$)	
	δ_C	δ_H (int., mult., *J* in Hz)	δ_C	δ_H (int., mult., *J* in Hz)
1α	29.6	1.54 (1H, *m*)	29.4	1.64 (1H, *m*)
1β		2.91 (1H, *m*)		3.07 (1H, *m*)
2α	17.8	1.54 (1H, *m*)	17.6	1.64 (1H, *m*)
2β		1.71 (1H, *m*)		1.85 (1H, *m*)
3α	36.7	1.21 (1H, *m*)	36.4	1.41 (1H, *m*)
3β		2.75 (1H, *m*)		2.03 (1H, *m*)
4	36.6	-	36.4	-
5	143.9	-	144.1	-
6	143.0	6.76 (1H, *s*)	142.9	7.05 (1H, *s*)
7	180.2	-	180.1	-
8	121.0	-	120.6	-
9	138.3	-	138.2	-
10	41.0	-	40.9	-
11	143.0	6.02 (1H, *s*)	142.8	6.35 (1H, *s*)
12	146.9	-	146.9	-
13	129.7	-	129.6	-
14	117.9	6.92 (1H, *s*)	117.7	7.58 (1H, *s*)
15	37.9	3.48 (1H, *m*)	37.8	3.23 (1H, *m*)

*Overlapped signal

Table 3.14 (Continue) ^{1}H and ^{13}C-NMR of compound **14** and 6,11,12,16-tetrahydroxy-5,8,11,13-abitetetraen-7-one [85]

No.	Compound 14 ($CDCl_3$)		6,11,12,16-tetrahydroxy-5,8,11,13-abitetetraen-7-one ($CDCl_3$)	
	δ_C	δ_H (int., mult., *J* in Hz)	δ_C	δ_H (int., mult., *J* in Hz)
16	70.1	3.74 (2H, *dd,* 9.6, 2.4)	69.6	4.06 (2H, *dd,* 9.5,2.6)
17	15.4	1.33 (3H, *d*, 8)*	15.2	1.37 (3H, *d,* 7.4)
18	28.2	1.12 (3H, *s*)	27.9	1.44 (3H, *s*)
19	27.4	1.12 (3H, *s*)	27.9	1.44 (3H, *s*)
20	27.4	1.33 (3H, *s*)	27.2	1.65 (3H, *s*)

*Overlapped signal

Compound **15** was isolated as white and amorphous powder (m.p 258-260 °C). The ^{1}H and ^{13}C NMR spectroscopic assignments of compound **15** (Table 3.15 and Appendix A35-36) were in agreement with literature data for 3-*O*-acetyl-betulinic acid [86]. The chemical structure of compound **15** was shown in Fig 3.15.

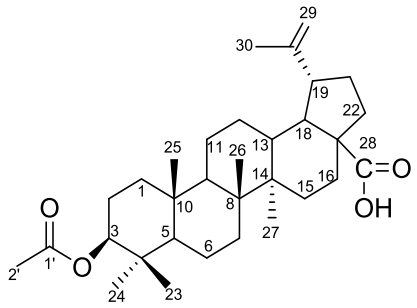

Figure 3.15 Structure of compound **15**

Table 3.15 ^{1}H-MNR of compound **15** and 3-*O*-acetyl-betulinic acid [86]

No.	Compound 15 ($CDCl_3$)	3-*O*-acetyl-betulinic acid ($CDCl_3$)
	δ_H (int., mult., *J* in Hz)	δ_H (int., mult., *J* in Hz)
1	-	-
2	-	-
3	4.60 (1H, *m*)	4.48 (1H, *dd, J*=5.5, 10.5)
4	-	-
5	-	-
6	-	-
7	-	-
8	-	-
9	-	-
10	-	-
11	-	-
12	-	-
13	-	-
14	-	-
15	-	-
16	-	-
17	-	-
18	3.18 (1H, *m*)	3.00 (1H, *m*)
19	-	-
20	-	-
21	-	-
22	-	-
23	0.82 (3H, *s*)	0.84 (3H, *s*)
24	0.93 (3H, *s*)	0.85 (3H, *s*)
25	0.96 (3H, *s*)	0.86 (3H, *s*)
26	0.97 (3H, *s*)	0.94 (3H, *s*)
27	1.37 (3H, *s*)	0.98 (3H, *s*)
28	-	-
29	4.68 (1H, *brs*) 4.73 (1H, *brs*)	4.62 (1H, *brs*) 4.75 (1H, *brs*)
30	1.68 (3H, *s*)	1.70 (3H, *s*)
2′	2.17 (3H, *s*)	2.05 (3H, *s*)

The classes of all isolated compounds from *C. inerme* were shown in figure 3.16

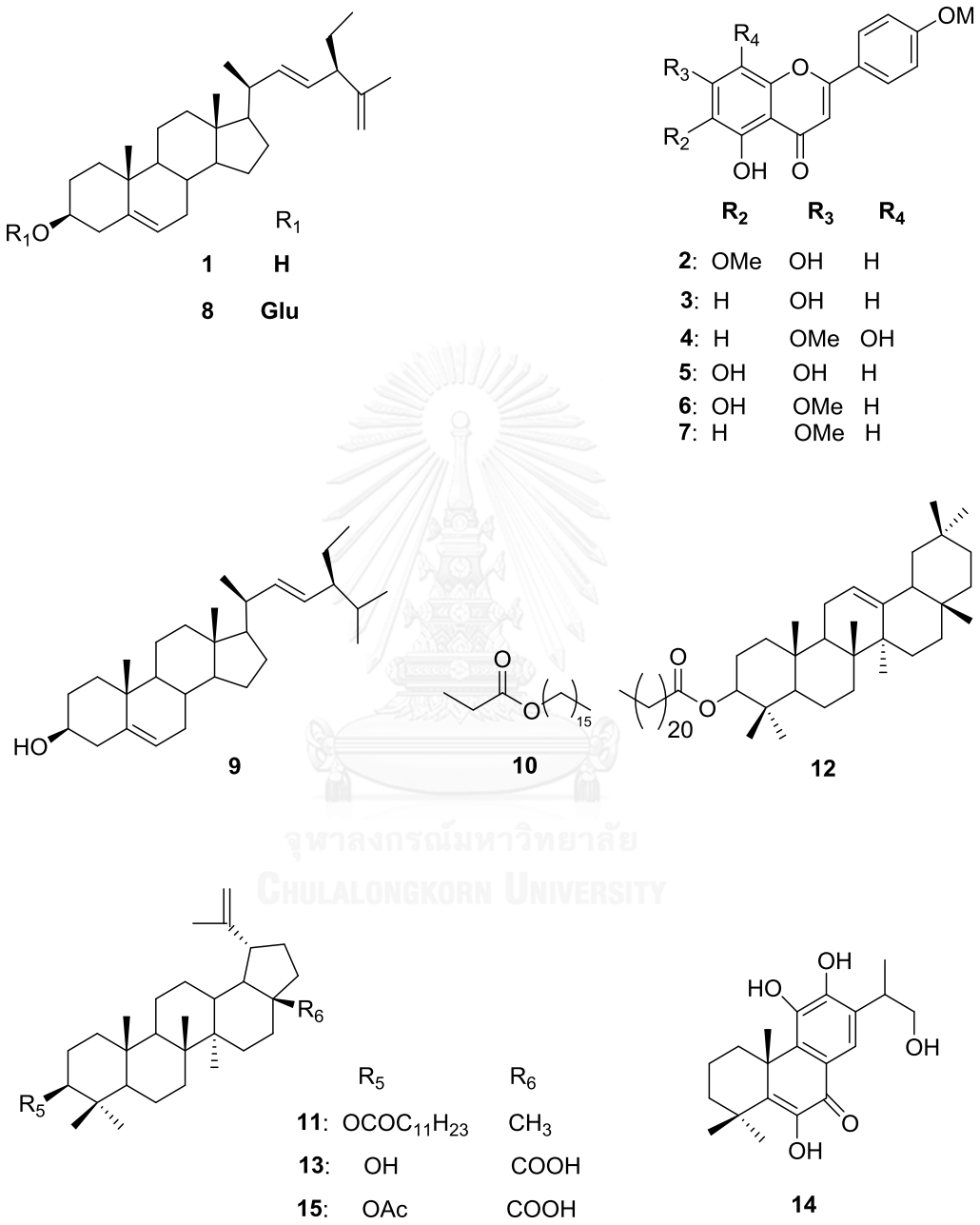

Figure 3.16 The classes of all isolated compounds from roots and leaves of

C. inerme

3.3 Antimicrobial activity

The CH_2Cl_2 and MeOH extracts of *C. inerme* were evaluated the antibacterial activity on gram positive bacteria (*S. aureus* ATCC25923 and *B. subtilis* ATCC6633) and gram negative bacteria (*P. aeruginosa* ATCC27853 and *E. coli* ATCC25922) at a range of concentration of 50-300 µg/mL (Table 3.16). All extracts showed a good potency to inhibit bacteria with the concentrations of 50 and 100 µg/mL. This result was found to agree with a previous report in which the methanolic extract of *C. inerme* inhibited these four bacteria Chahal *et al*. (2010) [12].

Table 3.16 Minimum inhibitory concentration (MIC) of extracts from *C. inerme* against *S. aureus*, *B. subtilis, P. aeruginosa* and *E. coli*

Part of Plant	Solvent	MIC (µg/mL)			
		Gram Positive Bacteria		Gram negative Bacteria	
		S. aureus	*B. subtilis*	*P. aeruginosa*	*E. coli*
Leaves	CH_2Cl_2	50	50	100	50
	MeOH	50	100	50	100
Roots	CH_2Cl_2	100	100	100	100
	MeOH	100	100	50	100

All isolated compounds except compounds **5-6**, **10**, **12** and **14** were evaluated the antimicrobial activity (Table 3.17). It was found that, compound **1** showed the highest inhibition on *S. aureus* growth with the MIC value of 20 µg/mL while compound **7** showed the highest inhibition on *P. aeruginosa* with the higher MIC value

(40 μg/mL). The best *C. candida* inhibitor was compound **4**. This study is the first report of compounds **1** and **11** activities against *S. aureus* and *P. aeruginosa*.

The glucoside moiety on compound **8** was found to significantly reduce the anti-bacterial and also anti-fungal activities (compound **1** *vs.* compound **8**). This phenomenon was previously found in the saponin skeleton reported by Avato *et al*. (2006) [87]. Flavonoids **2** and **3** exerted the inhibition on *S. aureus* and *C. albicans* which might be related to the hydroxyl groups at C-5 and C-7 of ring A [88].

Table 3.17 Minimum inhibitory concentration (MIC) of phytochemicals from *C. inerme* against *S. aureus, P. aeruginosa* and *C. albicans*

Compound	Name	MIC (μg/mL) ± SE		
		S. aureus	*P. aeruginosa*	*C. albicans*
1	(3β, 22*E*, 24*S*)-stigmasta-5,22,25-trien-3-ol	20.0±0.00	45.0±0.00	45.0±0.00
2	Pectolinarigenin	45.0±0.00	> 50.0	40.0±0.00
3	Acacetin	41.7±0.96	> 50.0	36.7±0.96
4	5,8-dihydroxy-7,4′-dimethoxyflavone	> 50.0	> 50.0	35.5±0.00
7	5-hydroxy-4′,7-dimethoxyflavone	> 50.0	40.0±0.00	38.3±0.96
8	(3β, 22*E*, 24*S*)-stigmasta-5,22,25-triene-3-yl-β-D-glucopyranoside	> 50.0	> 50.0	> 50.0
9	Stigmasterol	33.3±0.96	46.7±0.96	> 50.0
11	Lupeol laurate	> 50.0	45.0±0.00	> 50.0
13	Betulinic acid	45.0±0.00	45.0±0.00	> 50.0
15	3-*O*-acetyl-betulinic acid	40.0±0.00	> 50.0	> 50.0
Positive control	Clavulanic acid	1.35±0.0.96	2.45±0.00	-
	Amphotericin B	-	-	2.51±0.00

3.4 Anti-amyloid42 aggregation activity

All isolated compounds except compounds **4-6**, **9-10** and **14** were tested for their $A\beta_{42}$ aggregation inhibition using the thioflavin T assay [70]. The isolated compounds showed the inhibition percentages ranging from 10% to 30% at 20 μM, similar to 26.65 % of curcumin (Fig. 3.17 and Fig 3.18). Among them, flavonoids **2**-**3** and **7** showed the higher inhibition than the other two families, steroids (**1** and **8**) and triterpenoids (**11**-**13** and **15**). The highest inhibition activity of 29% at 20 μM was observed for acacetin (**3**).

This activity has never been determined from isolated compounds of *C. inerme* although it was previously reported as an active constituent in *C. inerme* for treatment of neurological disease associated with excitotoxicity [16]. The $A\beta_{42}$ aggregation inhibition of the flavonoid family are however quite common and they have been extensively used as core structures for design and synthesis of new effective inhibitors of AD drugs [89, 90].

Activity of 3-*O*-acetyl-betulinic acid (**15**) indicated similar anti-amyloid aggregation activity to curcumin and also showed markedly higher inhibition than betulinic acid (**13**). Triterpenoids are lupeol derivatives (**11**) which differ in the substituents at the positions 3 and 17, which suggest another interesting core structure for new potent $A\beta_{42}$ inhibitors for AD drugs. More extensive investigation to establish structure-activity relationships between the lupeol derivatives and $A\beta_{42}$ aggregation

inhibition activity should also be another interesting in future research topic.

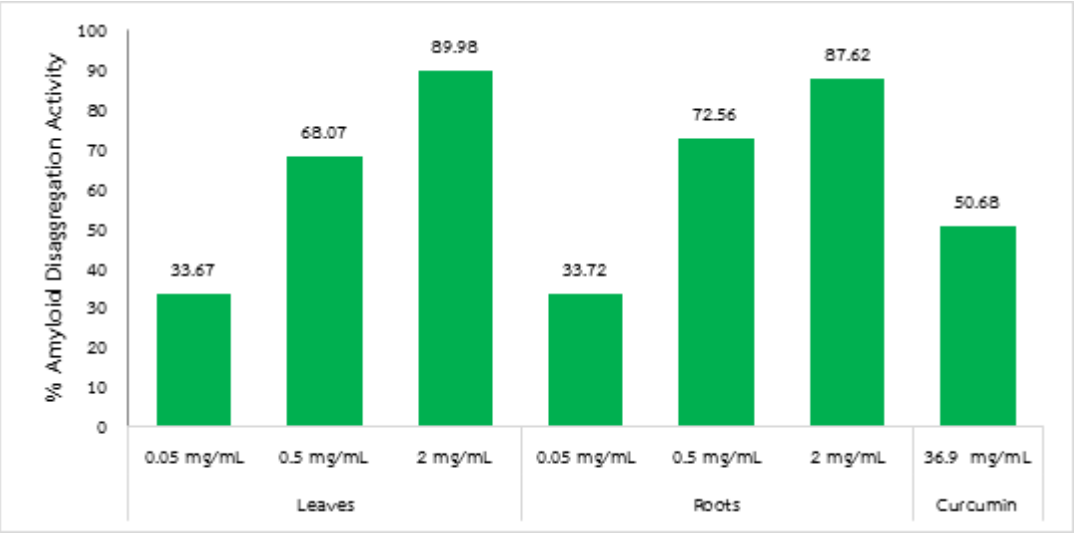

Figure 3.17 The $A\beta_{42}$ aggregation inhibitory of CH_2Cl_2 extract from leaves and roots of *C. inerme* at concentrations of 0.05, 0.5 and 2.0 mg/mL.

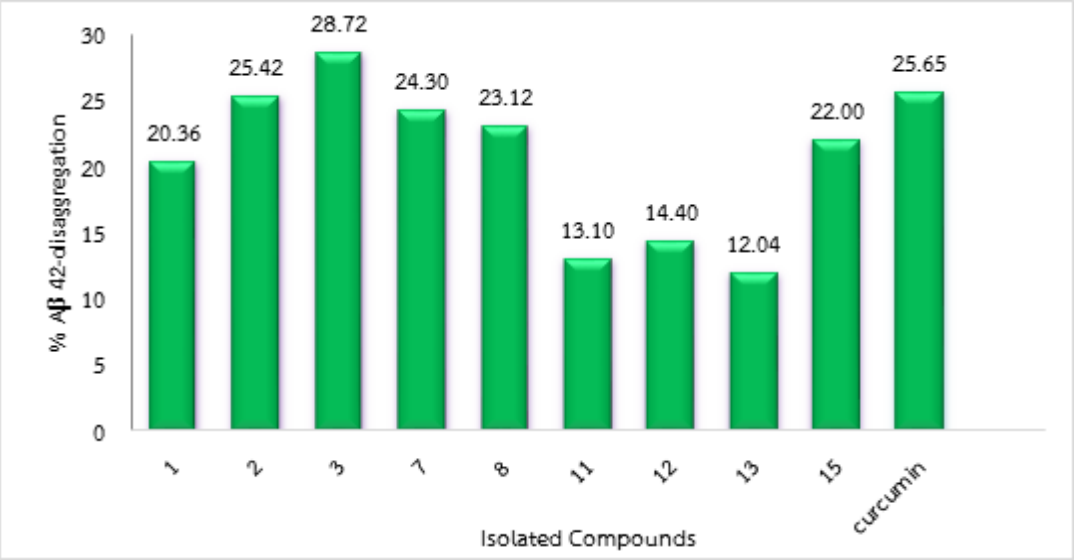

Figure 3.18 The inhibition of Aβ42 aggregation of the isolated compounds from *C. inerme* and curcumin (cur).

Moreover, mixing compounds also were evaluated the synergistics activity of Aβ42 disaggregation. (Table 3.15). It was found that mixing of isolated compounds at 20 μM of **7**, **8** and **13** with flavonoids and triterpenoids indicated different synergistic activity of Aβ42 disaggregation. Mixing with **3** showed higher activity increasing while activity at 20 μM of **3** with triterpenoids showed lower activity. Moreover, mixing of **3** and **15** showed dramatically activity reducing than mixing with **1**.

Moreover, activity of mixed compound on this activity was depended on type of compounds. It may support by specific biological activity of each natural compounds similar Conte *et al.* (2013) [41] study. Mixing of catechin and resveratrol improved protective effect cell from Aβ42 toxicity. Resveratrol showed effect depending on biphasic effect and protected cell from Aβ42 toxicity while catechin showed less protective effect than resveratrol and not showed antiproliferative effect of resveratrol.

The biological activity of mixed compound may decrease because each compound can regenerate other compounds [91]. Mixing of 17 β-extradiol and glutathione showed synergistic interaction against Aβ25-35 toxicity. There was not observed this interaction of mixing with ascorbic acid or α-tocopherol although ascorbic and α-tocopherol were high potent antioxidants. This antagonistic activity may be postulated by the regeneration ability of tocopherol radical to estrogen.

However, isolated compounds from *C. inerme* were not evaluated the protection of cell from Aβ toxicity. It should be investigated the optimum

concentration of specific substrate in the next study. It may helpful improve the effective formulation on synergistic activity for treatment the Aβ toxicity and protection cell from the Aβ toxicity in the next study.

Table 3.18 Anti- Aβ42 aggregation activity of mixed-compounds at 20 μM

Mixing Compounds	Name	% Aβ42 disaggregation ±SE
7+1	5-hydroxy-4',7-dimethoxyflavone + (3β, 22*E*, 24*S*)-stigmasta-5,22,25-trien-3-ol	24.94±0.03
7+2	5-hydroxy-4',7-dimethoxyflavone + pectolinarigenin	28.37±0.04
7+3	5-hydroxy-4',7-dimethoxyflavone + acacetin	29.33±0.06
7+8	5-hydroxy-4',7-dimethoxyflavone + (3β, 22*E*, 24*S*)-stigmasta-5,22,25-triene-3-yl-β-D-glucopyranoside	27.59±0.00
7+13	5-hydroxy-4',7-dimethoxyflavone + betulinic acid	24.74±0.07
7+15	5-hydroxy-4',7-dimethoxyflavone + 3-*O*-acetyl-betulinic acid	25.26±0.26
8+1	(3β, 22*E*, 24*S*)-stigmasta-5,22,25-triene-3-yl-β-D-glucopyranoside + (3β, 22*E*, 24*S*)-stigmasta-5,22,25-trien-3-ol	25.41±0.12
8+2	(3β, 22*E*, 24*S*)-stigmasta-5,22,25-triene-3-yl-β-D-glucopyranoside + Pectolinarigenin	27.06±0.10
8+3	(3β, 22*E*, 24*S*)-stigmasta-5,22,25-triene-3-yl-β-D-glucopyranoside + Acacetin	29.45±0.09
8+13	(3β, 22*E*, 24*S*)-stigmasta-5,22,25-triene-3-yl-β-D-glucopyranoside + Betulinic acid	24.34±0.02
8+15	(3β, 22*E*, 24*S*)-stigmasta-5,22,25-triene-3-yl-β-D-glucopyranoside + 3-*O*-acetyl-betulinic acid	25.16±0.20
-	Curcumin	25.65±0.09

Table 3.18 (continue) Anti- Aβ42 aggregation activity of mixed-compounds at 20 μM

Mixing Compounds	Name	% Aβ42 disaggregation ±SE
2+1	Pectolinarigenin + (3β, 22*E*, 24*S*)-stigmasta-5,22,25-trien-3-ol	25.36±0.12
2+3	Pectolinarigenin + acacetin	29.10±0.03
2+15	Pectolinarigenin + 3-*O*-acetyl-betulinic acid	25.42±0.30
13+1	Betulinic acid + (3β, 22*E*, 24*S*)-stigmasta-5,22,25-trien-3-ol	23.77±0.13
13+2	Betulinic acid + pectolinarigenin	25.17±0.22
13+3	Betulinic acid + acacetin	25.90±0.03
13+15	Betulinic acid + 3-*O*-acetyl-betulinic acid	23.46±0.12
3+1	Acacetin + (3β, 22*E*, 24*S*)-stigmasta-5,22,25-trien-3-ol	28.53±0.04
3+15	Acacetin + 3-*O*-acetyl-betulinic acid	25.59±0.07
-	Curcumin	25.65±0.09

3.5 Anticholinesterase activity

Isolated compounds, except **5**-**7**, **10**-**12** and **14**-**15** were determined the anti-cholinesterase activity (Table 3.16). The results were compared with Eserine. All isolated compounds showed moderate AChE inhibitior rather than BChE inhibitor. Compound **4**, a dimethoxyflavone showed higher AChE inibition (38.81 %). It may relate by the present of –OMe substitution in structure at C-5 and C-7 of ring A compound **4**.

Triterpenoid skeleton also showeded the AChE inhibition activity [92, 93]. Compound **8** slightly decreased the AChE inhibition from compound **1**, although compound **8** had a glucose moiety at C-3. This phenomenon related by the effect of

position of sugar moiety [94]. The more active compound should have the optimum length and interglycosidic linkage of sugar moiety. The active compounds should include the strong hydrogen bonding to the important amino acid residues of enzymes. Moreover, a number of hydrophobic interactions were also influence of compounds to inhibit AChE [95]. Among compounds **2**-**3** and **7**, structure relation activity were compared by the substitution of –OH. Alhough, the active flavonoids should have proton at C-3, the substitution of –OH at C-7 was also important. Then, compound **2** improved activity from compound **7** similar Katalinic *et al*. (2010) [96] study.

All isolated compounds showed BChE inhibitior property less than AChE inhibitor property. Compound **2** remained higher AChE inhibition activity (14.43%). Compound **1** can inhibit BChE less than inhibit AChE similar Ahmad *et al.* (2007) [97] study. Inhibition of these compounds on AChE and BChE were difference. It may relate by the different amino acid of active site between AChE and BChE [51].

Table 3.19 Anticholinesterase activity of isolated compounds from *C. inerme*

Compound	Name	% AChE Inibition ±SE	% BChE Inibition ±SE
		100 µg/mL	100 µg/mL
1	(3β, 22*E*, 24*S*)-stigmasta-5,22,25-trien-3-ol	30.81±8.00	9.84±0.91
2	Pectolinarigenin	38.81±7.9	14.43±5.1
3	Acacetin	36.95±3.3	0.00±4.40
7	5-hydroxy-4',7-dimethoxyflavone	39.80±0.54	0.00±0.23
8	(3β, 22*E*, 24*S*)-stigmasta-5,22,25-triene-3-yl-β-D-glucopyranoside	28.23±8.3	0.00±1.2
9	Stigmasterol	29.50±0.98	0.00±0.65
13	Betulinic acid	35.60±0.87	7.20±0.84
Positive Control	Eserine	99.90±0.05	99.60±0.08

CHAPTER IV
CONCLUSION

The separation of CH_2Cl_2 extracts from roots and leaves of *C. inerme* can afford 8 isolated compounds from leaves, (3β, 22*E,* 24*S*)-stigmasta-5,22,25-trien-3-ol (**1**), pectolinarigenin (**2**), acacetin (**3**), 5,8-dihydroxy-7,4′-dimethoxyflavone (**4**), scutellarein-4′-methyl ether (**5**), ladanein (**6**), 5-hydroxy-4′,7-dimethoxyflavone (**7**) and (3β, 22*E*, 24*S*)-stigmasterol-5,22,25-triene-3-yl-glucopyranoside (**8**) including 7 isolated compounds from roots, stigmasterol (**9**), *n*-hexadecyl propionate (**10**), lupeol laurate (**11**), β-amyrin decosanoate (**12**), betulinic acid (**13**), 6,11,12,16-tetrahydroxy-5,8,11,13-abitetetraen-7-one (**14**) and 3-*O*-acetyl-betulinic acid (**15**).

Isolated compounds were selected to evaluate their optimum biological activity (antimicrobial activity, anti-cholinesterase activity and anti-Aβ digaggregation activity). Selected compounds except **5**, **6**, **10**, **12** and **14** were evaluated the antimicrobial activity on *S. aureus*, *P. aeruginosa* and *C. albicans* according to Clinical and laboratory standard (2011). It was found that selected compounds showed active against *S. aureus*, *P. aeruginosa* and *C. albicans* at concentration ranging from 5-50 μg/mL and this study was the first reported the antibacterial activity of (3β, 22*E,* 24*S*)-stigmasta-5,22,25-trien-3-ol (**1**) and luepol laurate (**11**) on *S. aureus* and *P. aeruginosa*. (3β, 22*E,* 24*S*)-stigmasta-5,22,25-trien-3-ol (**1**) showed more active against *S. aureus* growth, 5-hydroxy-4′,7-dimethoxyflavone (**7**) showed more active against *P. aeruginosa*

growth and acacetin (**3**) indicated more active against *C. albicans*. Although, selected compounds showed active in this range, the efficient constitutents should be investigated from another part of *C. inerme.*

Isolated compounds, except **4**-**6**, **9**-**10** and **14**, were evaluated the inhibition of Aβ aggregation according to Feng *et al.* (2009) and Jan *et al*. (2010) testing. Their activity at 20 μM were distinguished level of inhibition by the influence of skeleton and substituents. Among them, acacetin (**3**) (28.72%) showed more active against Aβ aggregation and showed more active than activity of positive control (Curcumin) (25.65%). Moreover, the synergistic activity of mixed compound with flavonoids were improved. Mixing with acacetin (**3**) tended to increase the Aβ disaggregation contrast to mixing with triterpenoid skeleton species. The activity of Aβ aggregation should be improved by optimum the concentration of mixed compounds.

Furthermore, the anticholinesterase activity of isolated compounds were determined according to Ellman *et al.* (1961) and Ingkaninan *et al.* (2003). It was found that, selected compounds, except **5**-**7**, **10**-**12** and **14**-**15** showed moderate activity. (5-hydroxy-4′,7-dimethoxyflavone (**7**) showed more active on AChE activity and pectolinarigenin (**2**) showed more active on BChE activity. This study had observed the specific substrate of isolated compounds from *C. inerme* to AChE. These isolated compounds showed less specific substrate to BChE. It may responsible by the difference of aspects of active site gorge between AChE and BChE.

In conclusion, *C. inerme* is possible to be a source of bioactive compounds because acacetin showed higher activity than curcumin at the same concentration (20 μM) against Aβ-aggregation activity. Although, there were not distinct the bioactive compounds on antimicrobial and anticholinesterase activity from *C. inerme*. The optimum biological activity of specific compound will be improved by optimum the substrate and its concentration.

In future work may separate MeOH extract, change solvent of extraction including synthesize the bioactive compounds. It may has a benefit for the development of high effective constituents. This thesis has provided some information of biological activity. It may encourage to increase the useful of *C. inerme* for pharmacology benefit in the near future.

REFERENCES

[1] Biesalski, H.K., Dragsted, L.O., Elmadfa, I., Schrenk, D., Walter, P., and Weber, P. Bioactive compounds: definition and assessment of activity. Nutrition 25(11-12) (2009): 1202-1205.

[2] Tiangburanatham, W. (ed.). Dictionary of thai medicinal plants. Bangkok, Thailand : Prachumtong printing, 1996.

[3] Masuda, T., Yonemori, S., Oyama, Y., Takeda, Y., Tanaka, T., Andoh, T. Evaluation of the antioxidant activity of environmental plants: Activity of the leaf extracts from seashore plants. Journal of Agricultural and Food Chemistry 47(4) (1999): 1749-1754.

[4] Gurudeeban, S., Satyavani, K., Shanmugapriya, R., Ramanathan, T., Umamaheswari, G., and Muthazagan, K. Antioxidant and radical scavenging effect of *Clerodendrum inerme* (L.). Global Journal of Pharmacology 4(2) (2010): 91-94.

[5] Khan, S.A., Rasool, N., Riaz, M., Nadeem, R., Rashid, U., Rizwan, K., Zubair, M., Bukhari, I. H., Gulzar, T. Evaluation of antioxidant and cytotoxicity studies of *Clerodendrum inerme*. Asian Journal of Chemistry 25(13) (2013): 7457-7462.

[6] Gopal, N. and Sengottuvelu, S. Hepatoprotective activity of *Clerodendrum inerme* against CCL4 induced hepatic injury in rats. Fitoterapia 79(1) (2008): 24-26.

[7] Guessan, K.N., Zirihi, G.N., and Mea, A. Hypotensive effect of aqueous extract of *Clerodendrum inerme* leaves on the arterial pressure of rabbits International journal of pharmaceutical and biomedical research 1(2) (2010): 73-77.

[8] Upmanyu, G., Tanu, M., Gupta, M., Gupta, A.K., Sushma, A., and Dhakar, R.C. Acute toxicity and diuretic studies of leaves of *Clerodendrum inerme.* Journal of Pharmacy Research 4 (2011).

[9] Tiralongo, E., Uddin, S.J., and Grice, I.D. Cytotoxic effects of Bangladeshi medicinal plant extracts. Evidence-based Complementary and Alternative Medicine 2011 (2011).

[10] Waghmare, M.B., Waghmare, R.M., and Kamble, S.S. Bioefficacy of plant extracts on growth of *Botrytis cinerea* causing leaf blight of rose. The Bioscan 6(4) (2001): 643-645.

[11] Anitha, R. and Kannan, P. Antifungal activity of *Clerodendrum inerme* (L). and *Clerodendrum phlomidis* (L). Turkish Journal of Biology 30(3) (2006): 139-142.

[12] Chahal, J.K., Sarin, R., and Malwal, M. Efficacy of *Clerodendrum inerme* L. (garden quinine) against some human pathogenic strains. International Journal of Pharma and Bio Sciences 1(4) (2010).

[13] Murthy, Y.L.N., Nageswar, P.E., Viswanath, I.V.K., and Lakshmi, B.S. Phytochemical analysis and screening for antimicrobial activity of *Clerodendrum inerme* L. Gaertn : a mangrove plant. Journal of Phamacy and Chemistry 3(2) (2009): 51-56.

[14] Yankanchi, S.R. and Gadache, A.H. Grain protectant efficacy of certain plant extracts against rice weevil, *Sitophilus oryzae* L. (Coleoptera: Curculionidae). Journal of Biopesticides 3(2) (2010): 511-513.

[15] Kovendan, K. and Murugan, K. Effect of medicinal plants on the mosquito vectors from the different agroclimatic regions of Tamil Nadu, India. Advances in Environmental Biology 5(2 SPEC. ISSUE) (2011): 335-344.

[16] Lin, T.Y., Huang, W.J., Wu, C.C., Lu, C.W., and Wang, S.J. Acacetin inhibits glutamate release and prevents kainic acid-induced neurotoxicity in rats. PLoS ONE 9(2) (2014).

[17] Florence, A.R., Joselin, J., and Jeeva, S. Intra-specific variation of bioactive principles in select members of the genus *Clerodendrum* L. Journal of Chemical and Pharmaceutical Research 4(11) (2012): 4908-4914.

[18] Prince, M., Albanese, E., Guerchet, M., and Prina, M. World alzheimer report 2014, dementia and risk reduction, an analysis of protective and modifiable factors. 2014.

[19] Puzzo, D., Privitera, L., Leznik, E., Fà, M., Staniszewski, A., and Palmeri, A. Picomolar amyloid-β positively modulates synaptic plasticity and memory in hippocampus. Journal of Neuroscience 28(53) (2008): 14537-14545.

[20] Russell, C.L., Semerdjieva, S., Empson, R.M., Austen, B.M., Beesley, P.W., and Alifragis, P. Amyloid-β acts as a regulator of neurotransmitter release disrupting the interaction between synaptophysin and VAMP2. PLoS ONE 7(8) (2012).

[21] Kar, S., Slowikowski, S.P.M., Westaway, D., and Mount, H.T.J. Interactions between β-amyloid and central cholinergic neurons: Implications for Alzheimer's disease. Journal of Psychiatry and Neuroscience 29(6) (2004): 427-441.

[22] Masters, C.L., Simms, G., and Weinman, N.A. Amyloid plaque core protein in Alzheimer Disease and down syndrome. Proceedings of the National Academy of Sciences of the United States of America 82(12) (1985): 4245-4249.

[23] Wong, C.W., Quaranta, V., and Glenner, G.G. Neuritic plaques and cerebrovascular amyloid in Alzheimer disease are antigenically related. Proceedings of the National Academy of Sciences of the United States of America 82(24) (1985): 8729-8732.

[24] Selkoe, D.J. Alzheimer's disease: Genes, proteins, and therapy. Physiological Reviews 81(2) (2001): 741-766.

[25] Younkin, S.G. The role of Aβ42 in Alzheimer's disease. Journal of Physiology Paris 92(3-4) (1998): 289-292.

[26] Durkin, J.T., Murthy, S., Husten, E.J., Trusko, S.P., Savage, M.J., and Rotella, D.P. Rank-order of potencies for inhibition of the secretion of Aβ40 and Aβ42 suggests that

both are generated by a single γ-secretase. Journal of Biological Chemistry 274(29) (1999): 20499-20504.

[27] Nelson, R., Sawaya, M.R., Balbirnie, M., Madsen, A.O., Riekel, C., and Grothe, R. Structure of the cross-β spine of amyloid-like fibrils. Nature 435(7043) (2005): 773-778.

[28] Wetzel, R. Kinetics and thermodynamics of amyloid fibril assembly. Accounts of Chemical Research 39(9) (2006): 671-679.

[29] DaSilva, K.A., Shaw, J.E., and McLaurin, J. Amyloid-β fibrillogenesis: Structural insight and therapeutic intervention. Experimental Neurology 223(2) (2010): 311-321.

[30] Meyer-Luehmann, M., Spires-Jones, T.L., Prada, C., Garcia-Alloza, M., and De Calignon, A. Rapid appearance and local toxicity of amyloid-β plaques in a mouse model of Alzheimer's disease. Nature 451(7179) (2008): 720-724.

[31] Fiala, J.C., Spacek, J., and Harris, K.M. Dendritic spine pathology: Cause or consequence of neurological disorders? Brain Research Reviews 39(1) (2002): 29-54.

[32] Sawasdee, P., Sabphon, C., Sitthiwongwanit, D., and Kokpol, U. Anticholinesterase activity of 7-methoxyflavones isolated from *Kaempferia parviflora.* Phytotherapy Research 23(12) (2009): 1792-1794.

[33] Naveed, M.A., Riaz, N., Saleem, M., Jabeen, B., Ashraf, M., and Ismail, T. Longipetalosides A-C, new steroidal saponins from *Tribulus longipetalus.* Steroids 83 (2014): 45-51.

[34] Jung, M. and Park, M. Acetylcholinesterase inhibition by flavonoids from *Agrimonia pilosa.* Molecules 12(9) (2007): 2130-2139.

[35] Kim, S.Y., Park, J.Y., Park, P.S., Bang, S.H., Lee, K.M., and Lee, Y.R. Flavonoid glycosides as acetylcholinesterase inhibitors from the whole plants of *Persicaria thunbergii.* Natural Product Sciences 20(3) (2014): 191-195.

[36] Lai, C.S.W., Yu, M.S., Yuen, W.H., So, K.F., Zee, S.Y., and Chang, R.C.C. Antagonizing β-amyloid peptide neurotoxicity of the anti-aging fungus *Ganoderma lucidum.* Brain Research 1190(1) (2008): 215-224.

[37] Chaiyana, W., Saeio, K., Hennink, W.E., and Okonogi, S. Characterization of potent anticholinesterase plant oil based microemulsion. International Journal of Pharmaceutics 401(1-2) (2010): 32-40.

[38] Kim, D.S.H.L., Kim, J.Y., and Han, Y.S. Alzheimer's disease drug discovery from herbs: Neuroprotectivity from β-amyloid (1-42) insult. Journal of Alternative and Complementary Medicine 13(3) (2007): 333-340.

[39] Shi, C., Zhao, L., Zhu, B., Li, Q., Yew, D.T., and Yao, Z. Protective effects of *Ginkgo biloba* extract (EGb761) and its constituents quercetin and ginkgolide B against β-amyloid peptide-induced toxicity in SH-SY5Y cells. Chemico-Biological Interactions 181(1) (2009): 115-123.

[40] Wang, D., Liu, L., Zhu, X., Wu, W., and Wang, Y. Hesperidin alleviates cognitive impairment, mitochondrial dysfunction and oxidative stress in a mouse model of Alzheimer's Disease. Cellular and Molecular Neurobiology 34(8) (2014): 1209-1221.

[41] Conte, A., Pellegrini, S., and Tagliazucchi, D. Synergistic protection of PC12 cells from β-amyloid toxicity by resveratrol and catechin. Brain Research Bulletin 62(1) (2003): 29-38.

[42] Liu, R., Zhang, T.T., Zhou, D., Bai, X.Y., Zhou, W.L., and Huang, C. Quercetin protects against the Aβ25-35-induced amnesic injury: Involvement of inactivation of RAGE-mediated pathway and conservation of the NVU. Neuropharmacology 67 (2013): 419-431.

[43] Jiménez-Aliaga, K., Bermejo-Bescós, P., Benedí, J., and Martín-Aragón, S. Quercetin and rutin exhibit antiamyloidogenic and fibril-disaggregating effects *in vitro* and potent antioxidant activity in APPswe cells. Life Sciences 89(25-26) (2011): 939-945.

[44] Xie, H., Wang, J.R., Yau, L.F., Liu, Y., Liu, L., and Han, Q.B. Quantitative analysis of the flavonoid glycosides and terpene trilactones in the extract of *ginkgo biloba* and evaluation of their inhibitory activity towards fibril formation of β-amyloid peptide. Molecules 19(4) (2014): 4466-4478.

[45] Thapa, A., Vernon, B.C., De La Peña, K., Soliz, G., Moreno, H.A., and López, G.P. Membrane-mediated neuroprotection by curcumin from amyloid-β-peptide- induced toxicity. Langmuir 29(37) (2013): 11713-11723.

[46] Cygler, M., Schrag, J.D., Sussman, J.L., Harel, M., Silman, I., and Gentry, M.K. Relationship between sequence conservation and three-dimensional structure in a large family of esterases, lipases, and related proteins. Protein Science 2(3) (1993): 366-382.

[47] Whittaker, V.P. The contribution of drugs and toxins to understanding of cholinergic function. Trends in Pharmacological Sciences 11(1) (1990): 8-13.

[48] Pohanka, M. Alpha7 nicotinic acetylcholine receptor is a target in pharmacology and toxicology. International Journal of Molecular Sciences 13(2) (2012): 2219-2238.

[49] Raveh, L., Grunwald, J., Marcus, D., Papier, Y., Cohen, E., and Ashani, Y. Human butyrylcholinesterase as a general prophylactic antidote for nerve agent toxicity. *In vitro* and *in vivo* quantitative characterization. Biochemical Pharmacology 45(12) (1993): 2465-2474.

[50] Ekholm, M. Predicting relative binding free energies of substrates and inhibitors of acetylcholin- and butyrylcholinesterases. Journal of Molecular Structure: THEOCHEM 572 (2001): 25-34.

[51] Kovarik, Z., Bosak, A., Šinko, G., and Latas, T. Exploring the active sites of cholinesterases by inhibition with bambuterol and haloxon. Croatica Chemica Acta 76(1) (2003): 63-67.

[52] Pezzementi, L., Nachon, F., and Chatonnet, A. Evolution of acetylcholinesterase and butyrylcholinesterase in the vertebrates: An atypical butyrylcholinesterase from the medaka oryzias latipes. PLoS ONE 6(2) (2011).

[53] Frank, U. and Tacconelli, E. The daschner guide to in-hospital antibiotic therapy : European standard. Heidelberg, Germany : Springer-Verlag GmbH, 2013.

[54] Lewis, K. Platforms for antibiotic discovery. Nature Reviews Drug Discovery 12(5) (2013): 371-387.

[55] Finder, V.H. and Glockshuber, R. Amyloid-β aggregation. Neurodegenerative Diseases 4(1) (2007): 13-27.

[56] Selkoe, D.J. Cell biology of protein misfolding: The examples of Alzheimer's and Parkinson's diseases. Nature Cell Biology 6(11) (2004): 1054-1061.

[57] Walsh, D.M., Tseng, B.P., Rydel, R.E., Podlisny, M.B., and Selkoe, D.J. The oligomerization of amyloid β-protein begins intracellularly in cells derived from human brain. Biochemistry 39(35) (2000): 10831-10839.

[58] LeVine Iii, H. Alzheimer's β-peptide oligomer formation at physiologic concentrations. Analytical Biochemistry 335(1) (2004): 81-90.

[59] Walsh, D.M., Klyubin, I., Fadeeva, J.V., Cullen, W.K., Anwyl, R., and Wolfe, M.S. Naturally secreted oligomers of amyloid β protein potently inhibit hippocampal long-term potentiation *in vivo*. Nature 416(6880) (2002): 535-539.

[60] Quist, A., Doudevski, I., Lin, H., Azimova, R., Ng, D., and Frangione, B. Amyloid ion channels: A common structural link for protein-misfolding disease. Proceedings of the National Academy of Sciences of the United States of America 102(30) (2005): 10427-10432.

[61] Klein, W.L., Stine Jr, W.B., and Teplow, D.B. Small assemblies of unmodified amyloid β-protein are the proximate neurotoxin in Alzheimer's disease. Neurobiology of Aging 25(5) (2004): 569-580.

[62] Arimon, M., Díez-Pérez, I., Kogan, M.J., Durany, N., Giralt, E., and Sanz, F. Fine structure study of Aβ1-42 fibrillogenesis with atomic force microscopy. FASEB Journal 19(10) (2005): 1344-1346.

[63] Ross, C.A. and Poirier, M.A. Opinion: what is the role of protein aggregation in neurodegeneration. Natural Reviews Molecular Cell Biology 6 (2005): 891-898.

[64] Hu, L., Wong, T.P., Côté, S.L., Bell, K.F.S., and Cuello, A.C. The impact of Aβ-plaques on cortical cholinergic and non-cholinergic presynaptic boutons in alzheimer's disease-like transgenic mice. Neuroscience 121(2) (2003): 421-432.

[65] Govoni, S., Mura, E., Preda, S., Racchi, M., Lanni, C., and Grilli, M. Dangerous liaisons between beta-amyloid and cholinergic neurotransmission. Current Pharmaceutical Design 20(15) (2014): 2525-2538.

[66] Savonenko, A., Xu, G.M., Melnikova, T., Morton, J.L., Gonzales, V., and Wong, M.P.F. Episodic-like memory deficits in the APPswe/PS1dE9 mouse model of Alzheimer's disease: Relationships to β-amyloid deposition and neurotransmitter abnormalities. Neurobiology of Disease 18(3) (2005): 602-617.

[67] Ellman, G.L., Courtney, K.D., Andres Jr, V., and Featherstone, R.M. A new and rapid colorimetric determination of acetylcholinesterase activity. Biochemical Pharmacology 7(2) (1961): 88-95.

[68] Ingkaninan, K., Temkitthawon, P., Chuenchom, K., Yuyaem, T., and Thongnoi, W. Screening for acetylcholinesterase inhibitory activity in plants used in Thai traditional rejuvenating and neurotonic remedies. Journal of Ethnopharmacology 89(2-3) (2003): 261-264.

[69] Rhee, I.K., Van De Meent, M., Ingkaninan, K., and Verpoorte, R. Screening for acetylcholinesterase inhibitors from Amaryllidaceae using silica gel thin-layer chromatography in combination with bioactivity staining. Journal of Chromatography A 915(1-2) (2001): 217-223.

[70] Feng, Y., Wang, X.P., Yang, S.G., Wang, Y.J., Zhang, X., and Du, X.T. Resveratrol inhibits beta-amyloid oligomeric cytotoxicity but does not prevent oligomer formation. NeuroToxicology 30(6) (2009): 986-995.

[71] Jan, A., Hartley, D.M., and Lashuel, H.A. Preparation and characterization of toxic Abeta aggregates for structural and functional studies in Alzheimer's disease research. Nature protocols 5(6) (2010): 1186-1209.

[72] Leitão, S.G., Kaplan, M.A.C., Monache, F.D., Akihisa, T., and Tamura, T. Sterols and sterol glucosides from two Aegiphila species. Phytochemistry 31(8) (1992): 2813-2817.

[73] Segueni, N., Zellagui, A., Moussaoui, F., Lahouel, M., and Rhouati, S. Flavonoids from *Algerian propolis.* Arabian Journal of Chemistry (2013). http://dx.doi.org/10.1016/j.arabjc.2011.05.013

[74] Gomes, R.A., Ramirez, R.R.A., Da S. Maclel, J.K., De Fátima Agra, M., De Souza, M.D.F.V., and Falcão-Silva, V.S. Phenolic compounds from *Sidastrum micranthum* (A. St.-Hil.) Fryxell and evaluation of acacetin and 7,4'-di-*O*-methylisoscutellarein as motulator of bacterial drug resistence. Quimica Nova 34(8) (2011): 1385-1388.

[75] Ramesh, P. and Yuvarajan, C.R. A new flavone methyl ether from *Helicteres isora.* Journal of Natural Products 58(8) (1995): 1242-1243.

[76] Sabina, H. and Aliya, R. Seaweed as a new source of flavone, Scutellarein 4'-methyl ether. Pakistan Journal of Botany 41(4) (2009): 1927-1930.

[77] Pukalskas, A., Venskutonis, P.R., Salido, S., Waard, P.D., and Van Beek, T.A. Isolation, identification and activity of natural antioxidants from horehound (*Marrubium vulgare* L.) cultivated in Lithuania. Food Chemistry 130(3) (2012): 695-701.

[78] Saraswathy, A., Vidhya, B., and Amala, K. Apigenin-4′, 7-dimethyl ether from *Aquilaria agallocha* Roxb. Indian Drugs 49(10) (2012): 30-32.

[79] Chaves, M.H., Roque, N.F., and Costa Ayres, M.C. Steroids and flavonoids of *Porcelia macrocarpa.* Journal of the Brazilian Chemical Society 15(4) (2004): 608-613.

[80] Koay, Y.C., Wong, K.C., Osman, H., Eldeen, I.M.S., and Asmawi, M.Z. Chemical constituents and biological activities of *Strobilanthes crispus* L. Records of Natural Products 7(1) (2013): 59-64.

[81] Vandevoorde, S., Tsuboi, K., Ueda, N., Jonsson, K.O., Fowler, C.J., and Lambert, D.M. Esters, retroesters, and a retroamide of palmitic acid: Pool for the first selective inhibitors of N-palmitoylethanolamine-selective acid amidase. Journal of Medicinal Chemistry 46(21) (2003): 4373-4376.

[82] Sobrinho, D.C., Haupli, M.B., Appolinario, E.V., Kollenz, C.L.M., De Carvalho, M.G., and BrazFilho, R. Triterpenoid isolate from *Parahancornia amapa*. Journal of the Brazilian Chemical Society 2 (1991): 15-20.

[83] Maurya, R., Srivastava, A., Shah, P., Siddiqi, M.I., Rajendran, S.M., and Puri, A. β-Amyrin acetate and β-amyrin palmitate as antidyslipidemic agents from *Wrightia tomentosa* leaves. Phytomedicine 19(8-9) (2012): 682-685.

[84] Peng, C., Bodenhausen, G., Qiu, S., Fong, H.H.S., Farnsworth, N.R., and Yuan, S. Computer-assisted structure elucidation: Application of CISOC-SES to the resonance assignment and structure generation of betulinic acid. Magnetic Resonance in Chemistry 36(4) (1998): 267-278.

[85] Han, L., Huang, X., Dahse, H.M., Moellmann, U., Grabley, S., and Lin, W. New abietane diterpenoids from the mangrove *Avicennia marina*. Planta Medica 74(4) (2008): 432-437.

[86] Ahmad, F.B.H., Moghaddam, M.G., Basri, M., and Abdul Rahman, M.B. Anticancer activity of 3-*O*-acylated betulinic acid derivatives obtained by enzymatic synthesis. Bioscience, Biotechnology and Biochemistry 74(5) (2010): 1025-1029.

[87] Avato, P., Bucci, R., Tava, A., Vitali, C., Rosato, A., and Bialy, Z. Antimicrobial activity of saponins from *Medicago* sp.: Structure-activity relationship. Phytotherapy Research 20(6) (2006): 454-457.

[88] Wu, T., He, M., Zang, X., Zhou, Y., Qiu, T., and Pan, S. A structure-activity relationship study of flavonoids as inhibitors of *E. coli* by membrane interaction effect. Biochimica et Biophysica Acta - Biomembranes 1828(11) (2013): 2751-2756.

[89] Li, S.Y., Wang, X.B., Xie, S.S., Jiang, N., Wang, K.D.G., and Yao, H.Q. Multifunctional tacrine-flavonoid hybrids with cholinergic, β-amyloid-reducing, and metal chelating properties for the treatment of Alzheimer's disease. European Journal of Medicinal Chemistry 69 (2013): 632-646.

[90] Singh, S.K., Gaur, R., Kumar, A., Fatima, R., Mishra, L., and Srikrishna, S. The Flavonoid derivative 2-(4′-benzyloxyphenyl)-3-hydroxy-chromen-4-one protects against Aβ42-induced neurodegeneration in Transgenic Drosophila: Insights from in silico and *in vivo* studies. Neurotoxicity Research 26(4) (2014): 331-350.

[91] Gridley, K.E., Green, P.S., and Simpkins, J.W. A novel, synergistic interaction between 17 β-estradiol and glutathione in the protection of neurons against β-amyloid 25-35-induced toxicity *in vitro.* Molecular Pharmacology 54(5) (1998): 874-880.

[92] Nguyen, V.T., To, D.C., Tran, M.H., Oh, S.H., Kim, J.A., and Ali, M.Y. Isolation of cholinesterase and β-secretase 1 inhibiting compounds from *Lycopodiella cernua.* Bioorganic and Medicinal Chemistry (2015) : 10.1016/j.bmc.2015.04.080

[93] Liu, B., Yang, L., Xu, Y.K., Liao, S.G., Luo, H.R., and Na, Z. Two new triterpenoids from *Gelsemium elegans* and *Aglaia odorata.* Natural Product Communications 8(10) (2013): 1373-1376.

[94] Fan, P., Hay, A.E., Marston, A., and Hostettmann, K. Acetylcholinesterase-inhibitory activity of linarin from *Buddleja davidii*, structure-activity relationships of related flavonoids, and chemical investigation of *Buddleja nitida.* Pharmaceutical Biology 46(9) (2008): 596-601.

[95] Khan, M.T.H., Orhan, I., Şenol, F.S., Kartal, M., Şener, B., and Dvorská, M. Cholinesterase inhibitory activities of some flavonoid derivatives and chosen xanthone and their molecular docking studies. Chemico-Biological Interactions 181(3) (2009): 383-389.

[96] Katalinić, M., Rusak, G., Domaćinović Barović, J., Šinko, G., Jelić, D., and Antolović, R. Structural aspects of flavonoids as inhibitors of human butyrylcholinesterase. European Journal of Medicinal Chemistry 45(1) (2010): 186-192.

[97] Ahmad, Z., Mehmood, S., Ifzal, R., Malik, A., Afza, N., and Ashraf, M. A new ursane-type triterpenoid from *Salvia santolinifolia.* Turkish Journal of Chemistry 31(4) (2007): 495-501.

APPENDIX

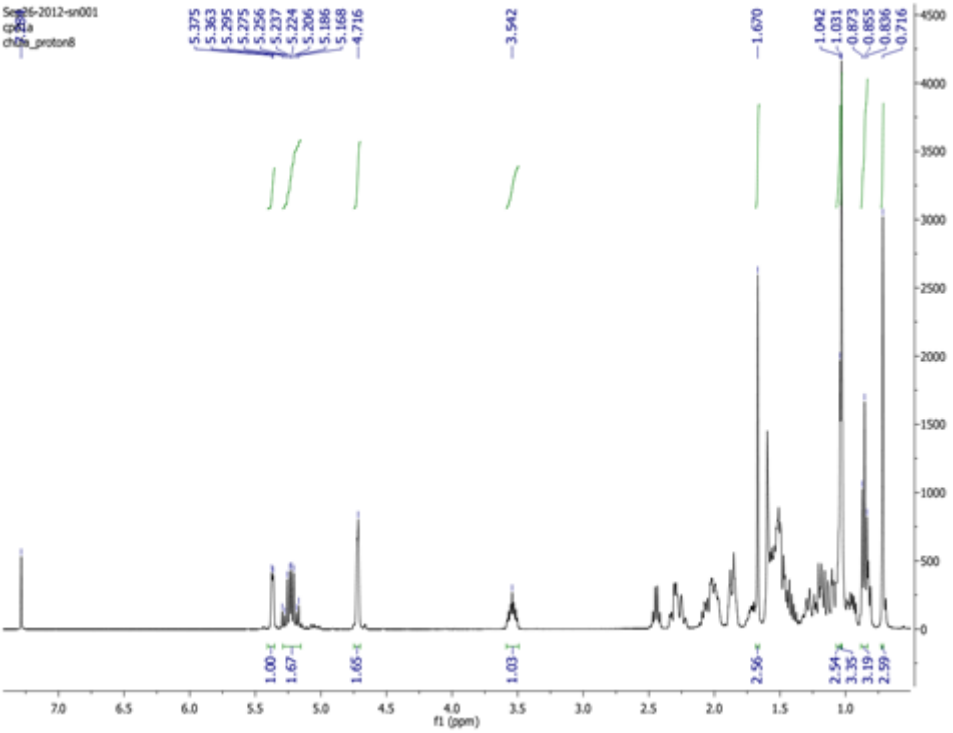

Figure A-1 ^{1}H-NMR spectrum ($CDCl_3$) of **1**

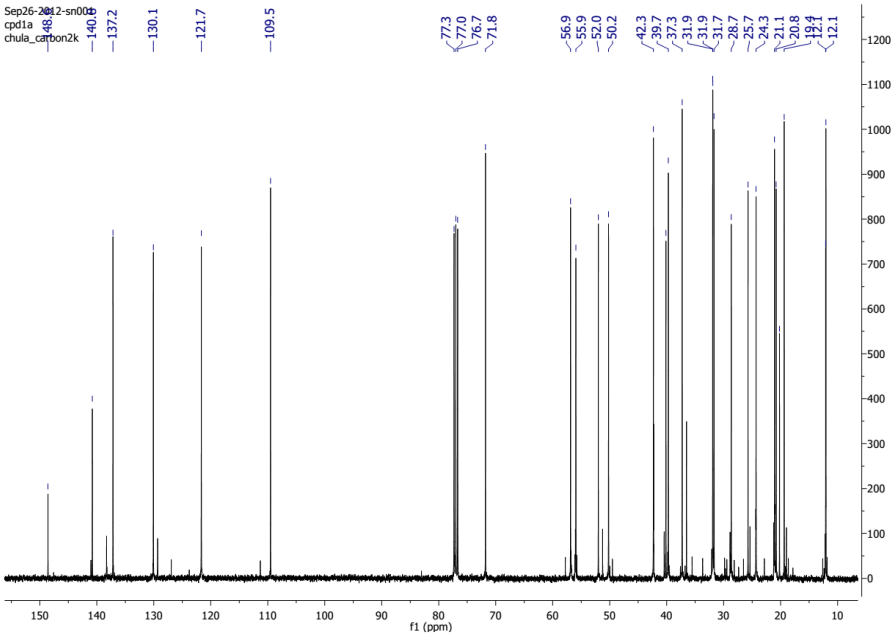

Figure A-2 ^{13}C-NMR spectrum ($CDCl_3$) of **1**

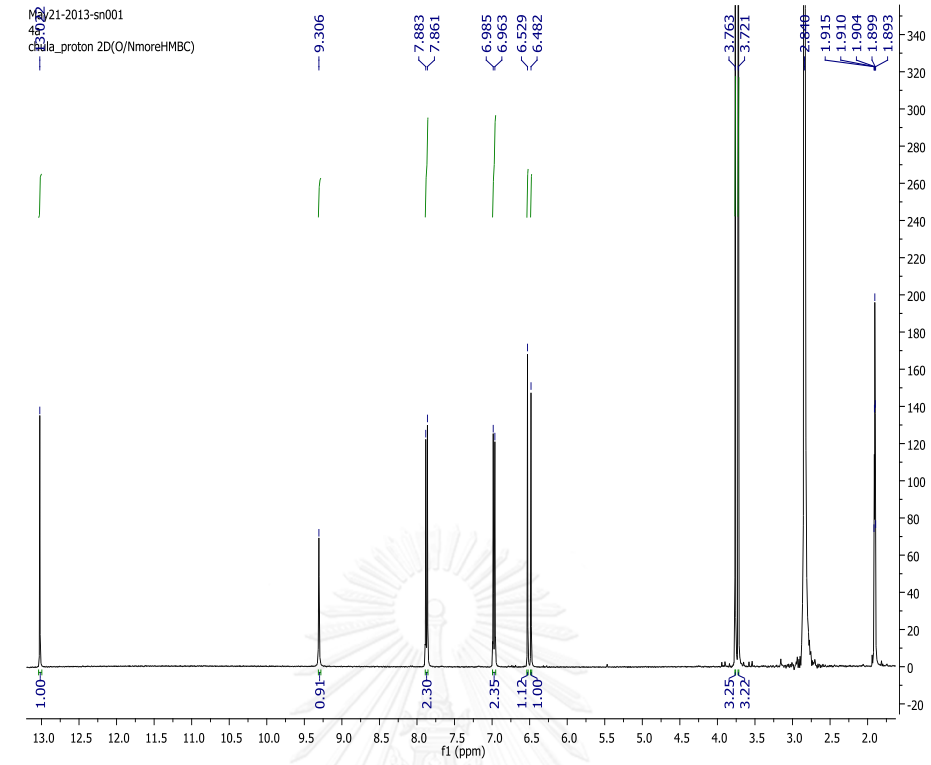

Figure A-3 ^{1}H-NMR spectrum (acetone-*d6*) of **2**

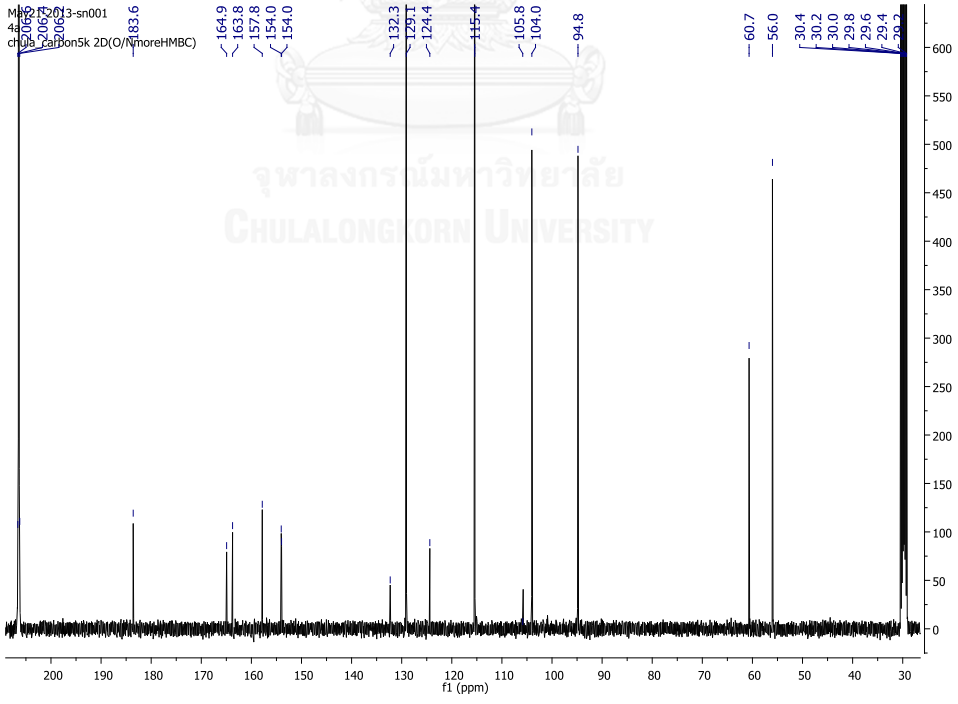

Figure A-4 ^{13}C-NMR spectrum (acetone-*d6*) of **2**

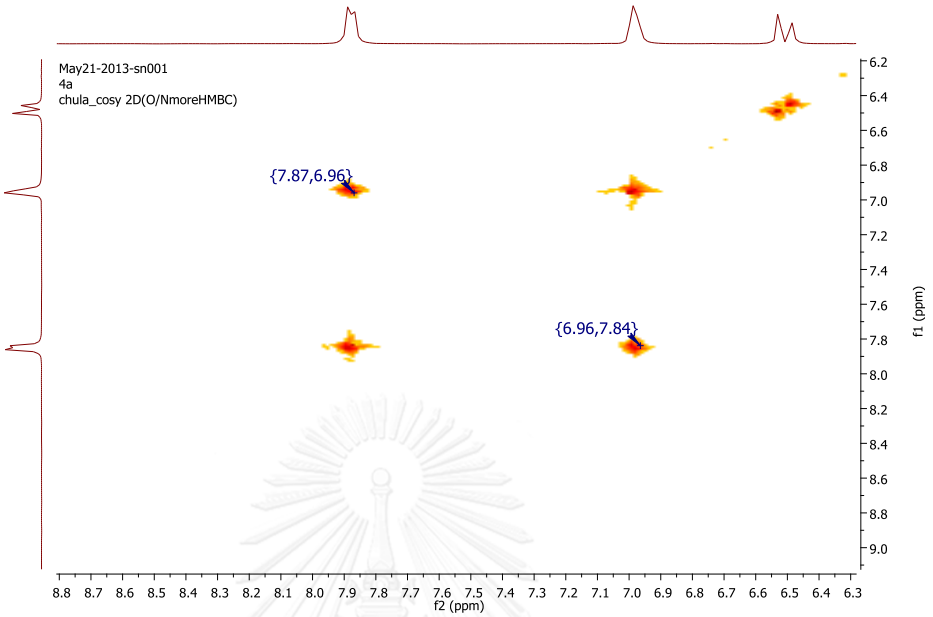

Figure A-5 COSY-NMR spectrum (acetone-*d6*) of **2**

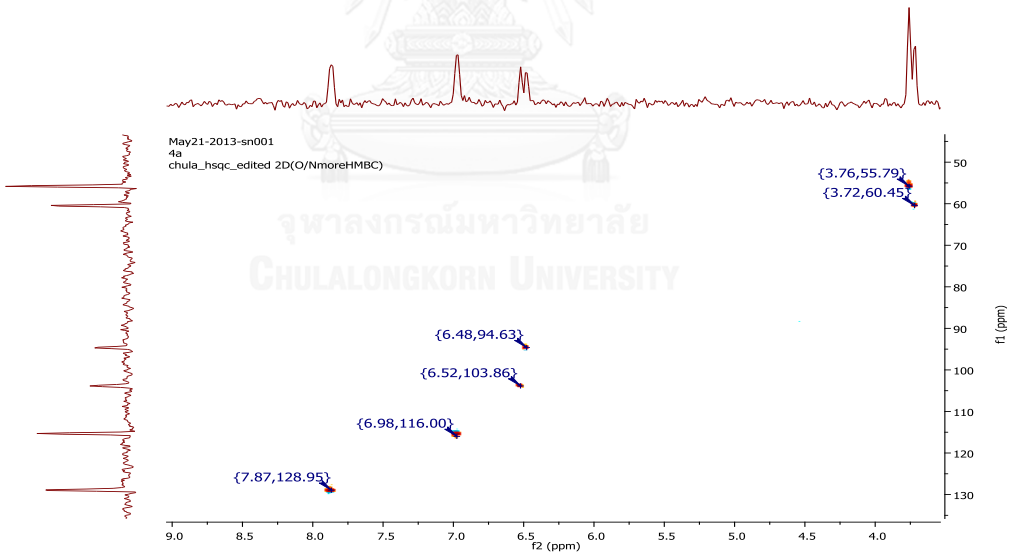

Figure A-6 HSQC-NMR spectrum (acetone-*d6*) of **2**

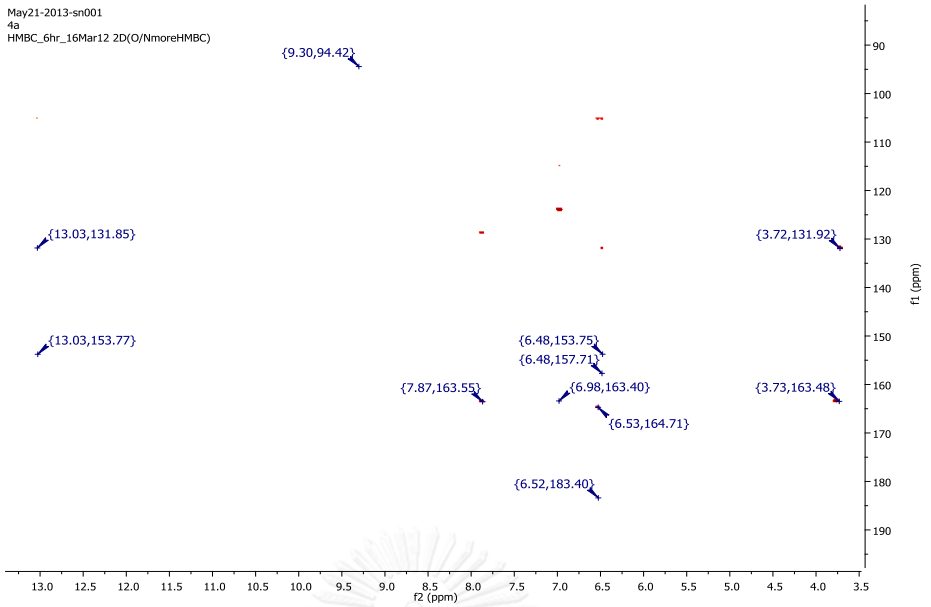

Figure A-7 HMBC-NMR spectrum (acetone-*d6*) of **2**

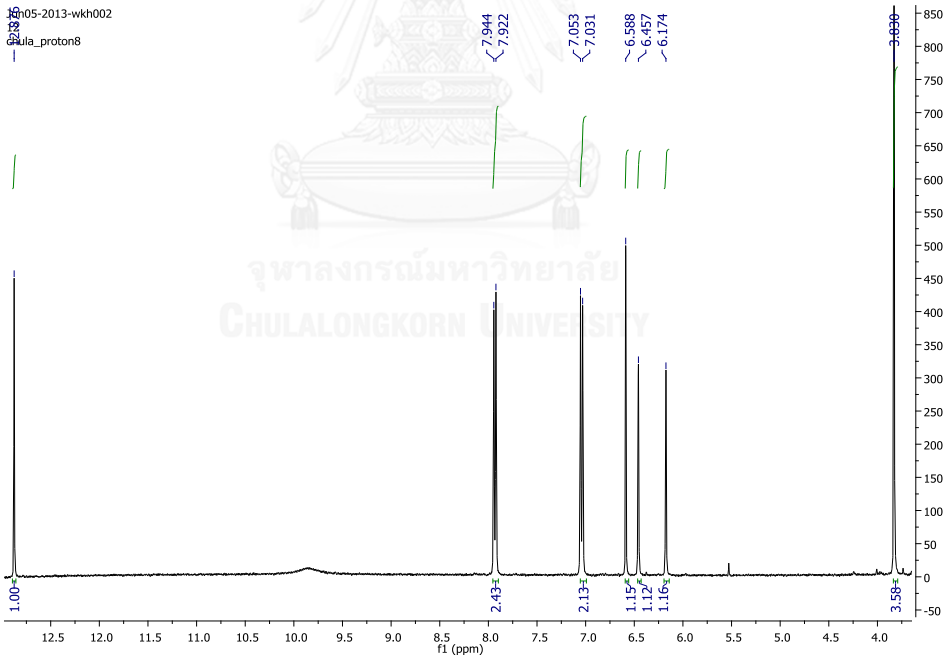

Figure A-8 ^{1}H-NMR spectrum (acetone-*d6*) of **3**

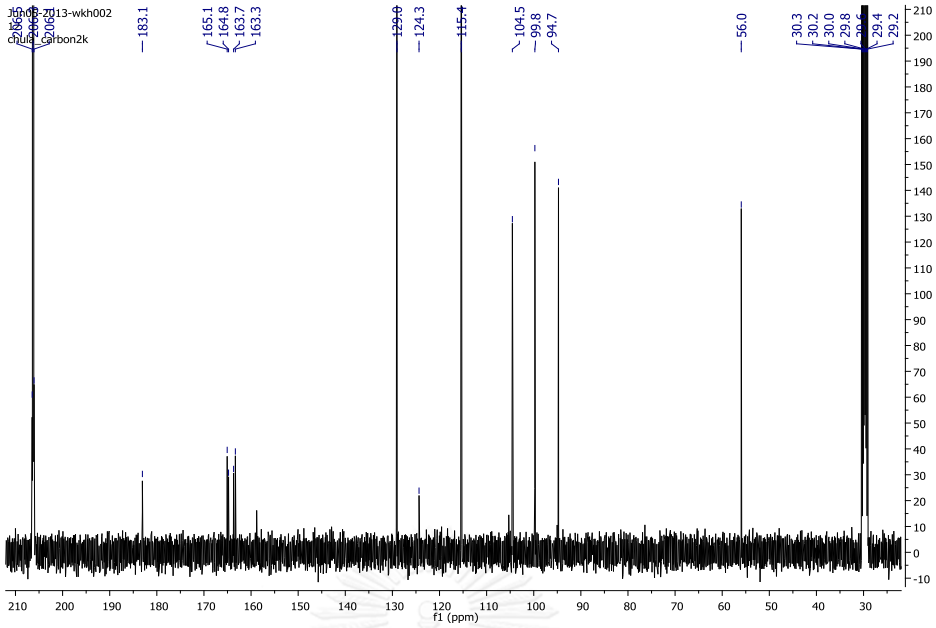

Figure A-9 ^{13}C-NMR spectrum (acetone-*d6*) of **3**

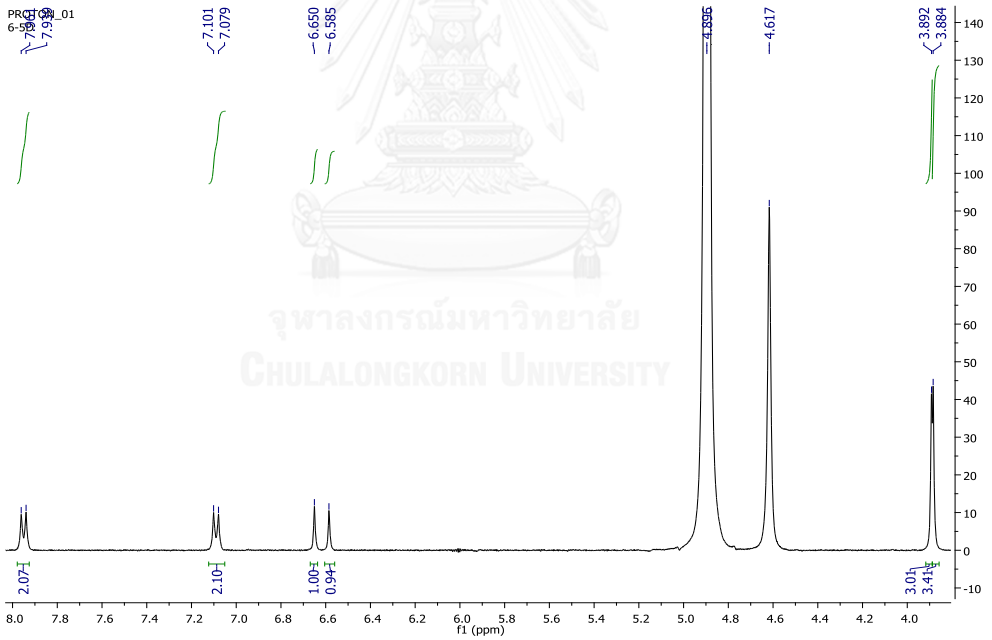

Figure A-10 ^{1}H-NMR spectrum (CD_3OD) of **4**

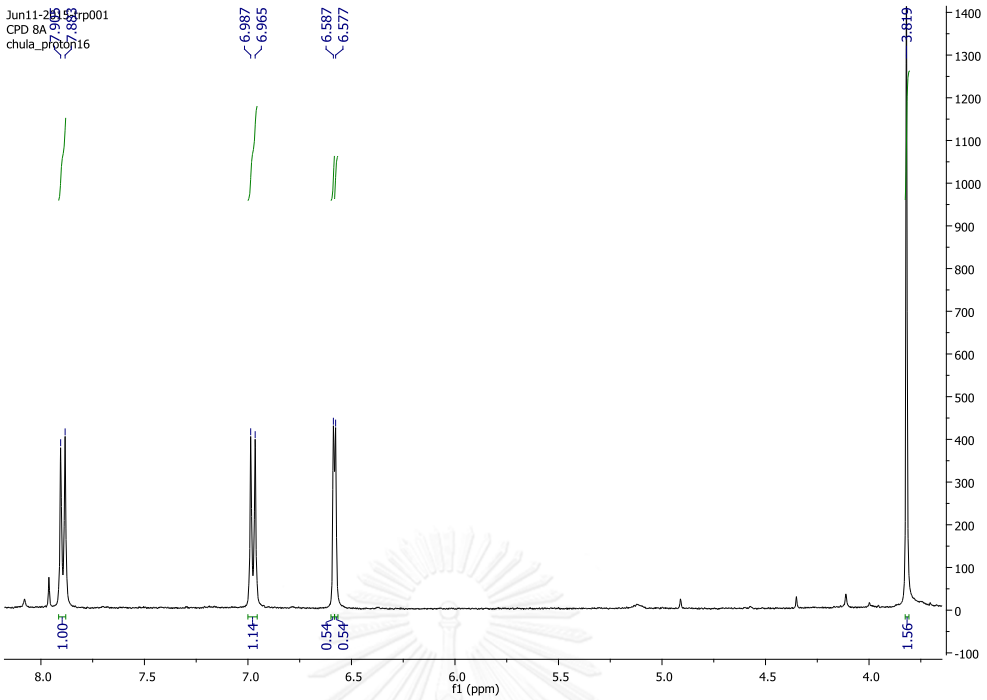

Figure A-11 ^{1}H-NMR spectrum (acetone-*d6*) of **5**

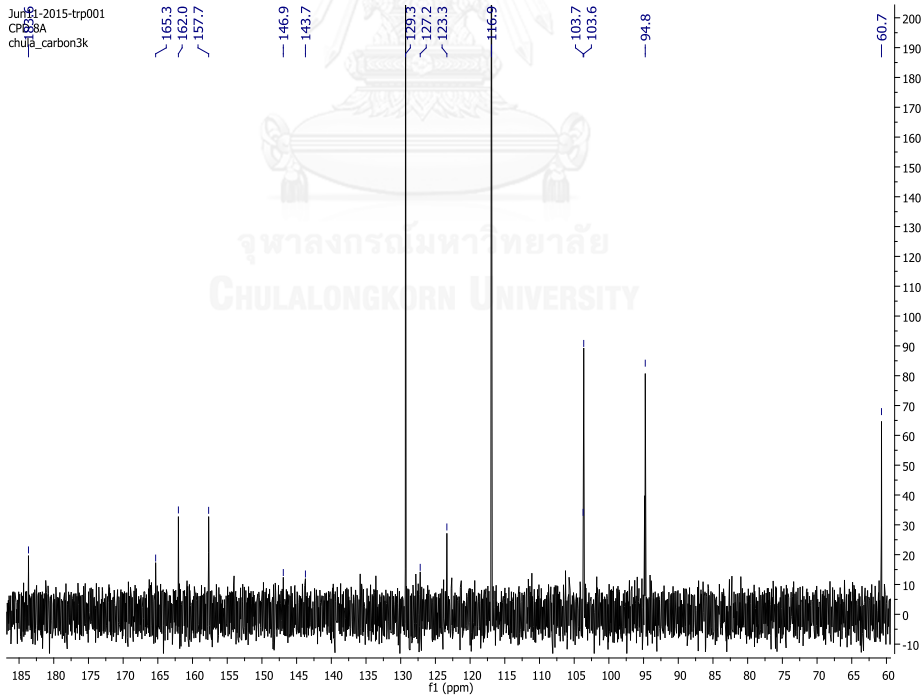

Figure A-12 ^{13}C-NMR spectrum (acetone-*d6*) of **5**

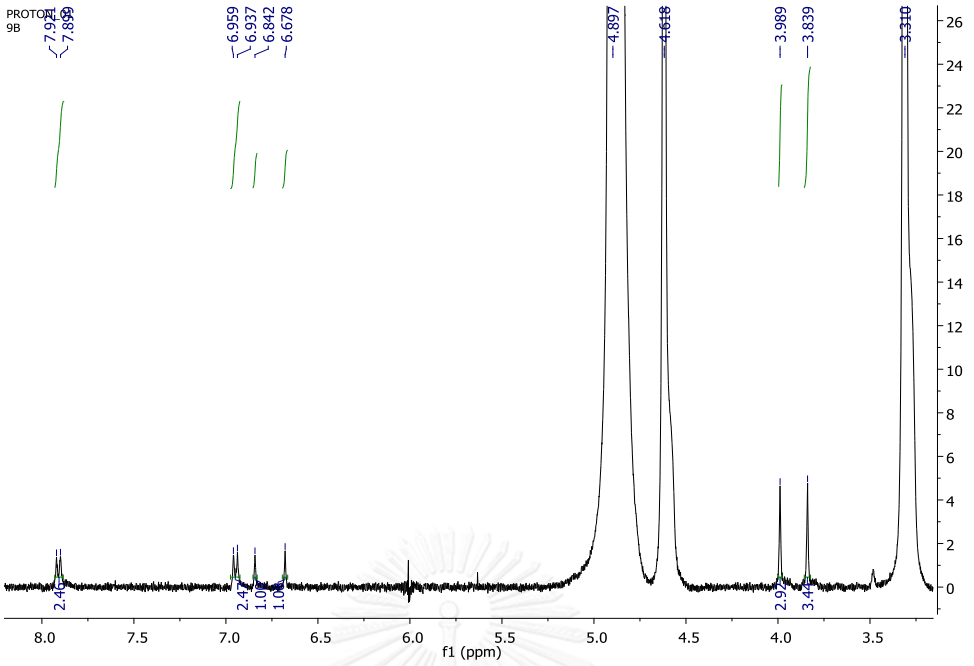

Figure A-13 ^{1}H-NMR spectrum (acetone-*d6*) of **6**

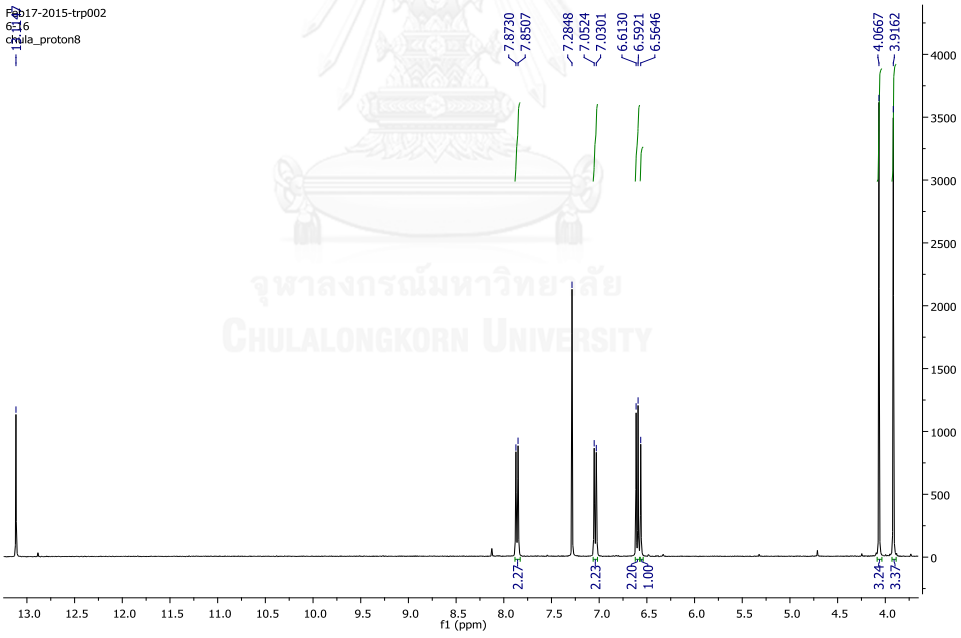

Figure A-14^{1}H-NMR spectrum ($CDCl_3$) of **7**

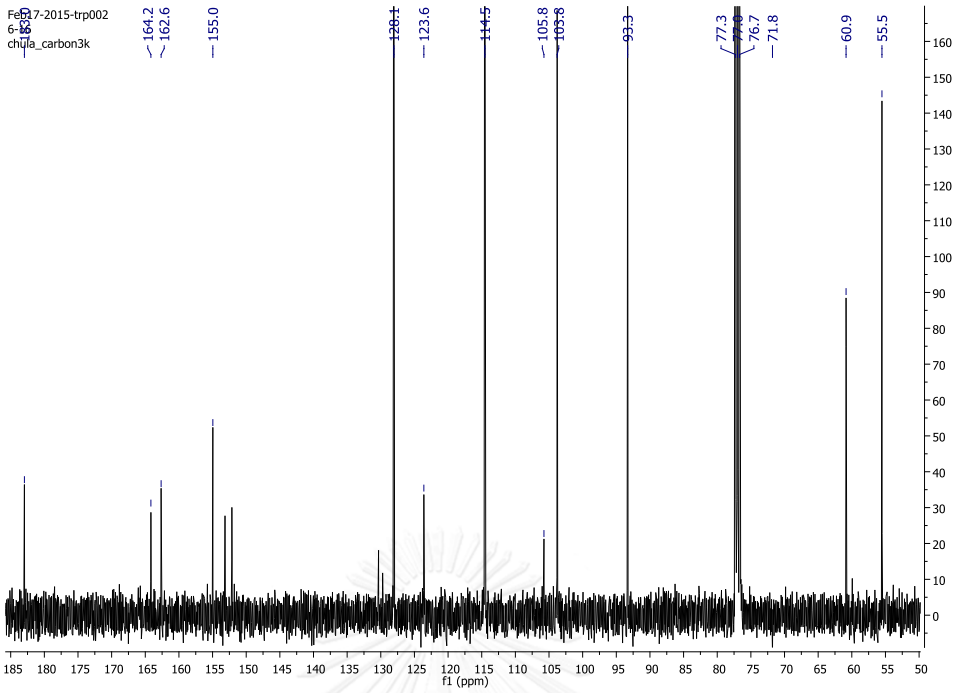

Figure A-15 ^{13}C-NMR spectrum ($CDCl_3$) of **7**

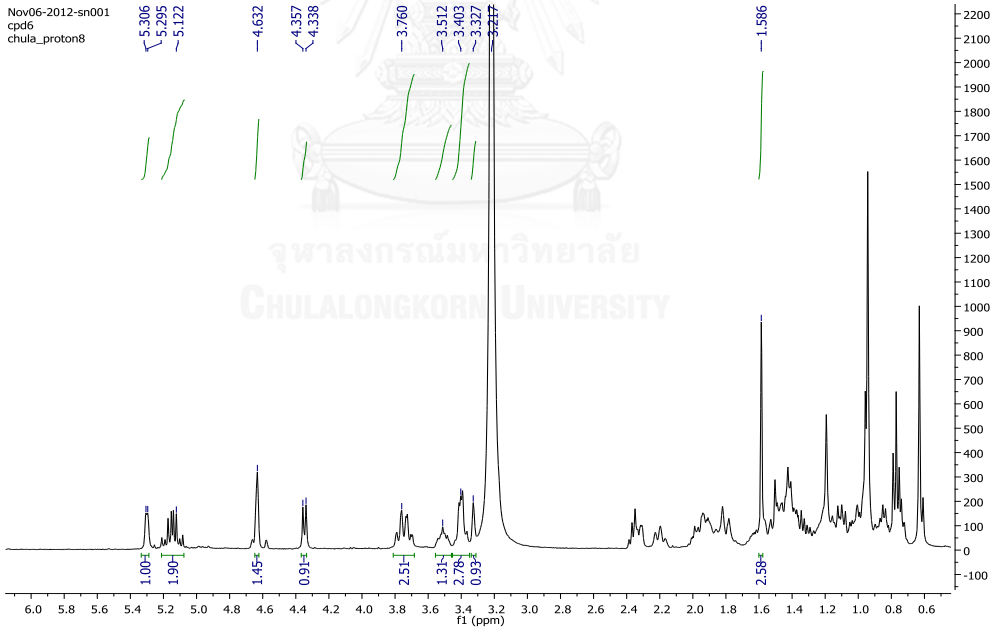

Figure A-16 ^{1}H-NMR spectrum ($CDCl_3$) of **8**

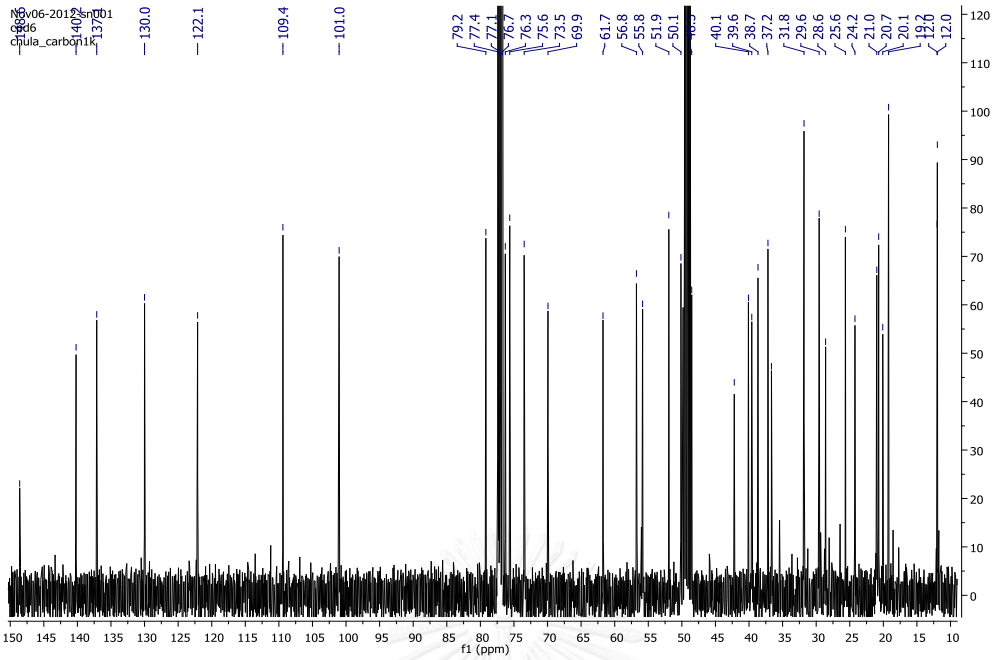

Figure A-17 ^{13}C-NMR spectrum ($CDCl_3$) of **8**

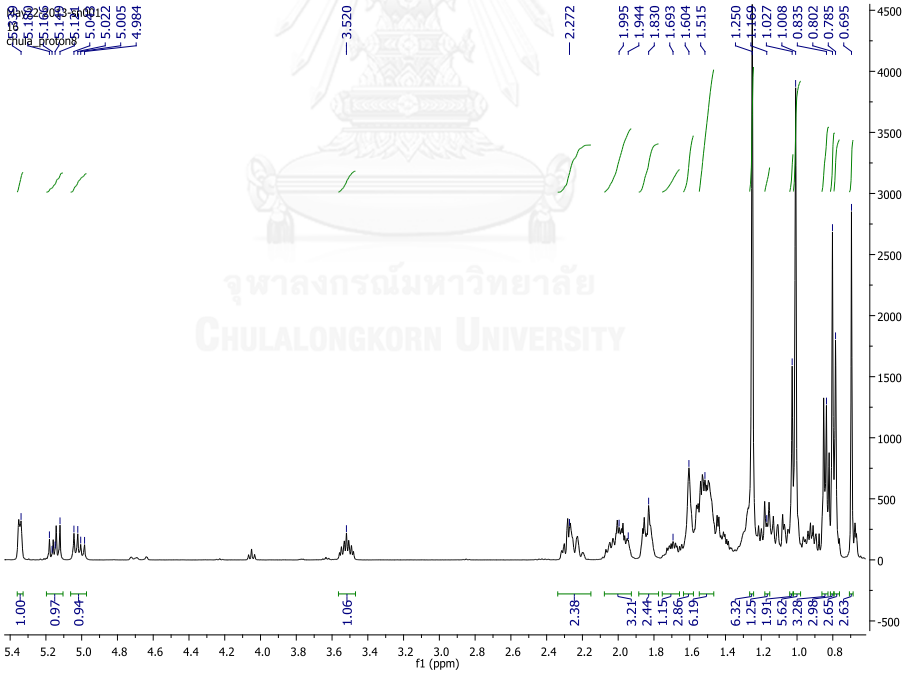

Figure A-18 ^{1}H-NMR spectrum ($CDCl_3$) of **9**

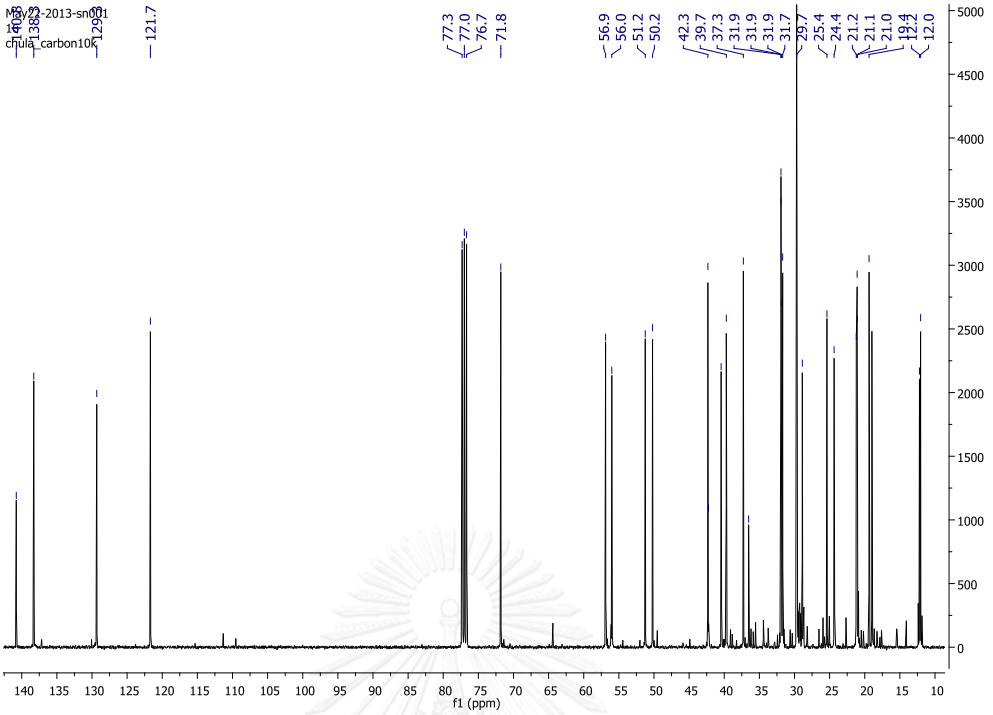

Figure A-19 ^{13}C-NMR spectrum ($CDCl_3$) of **9**

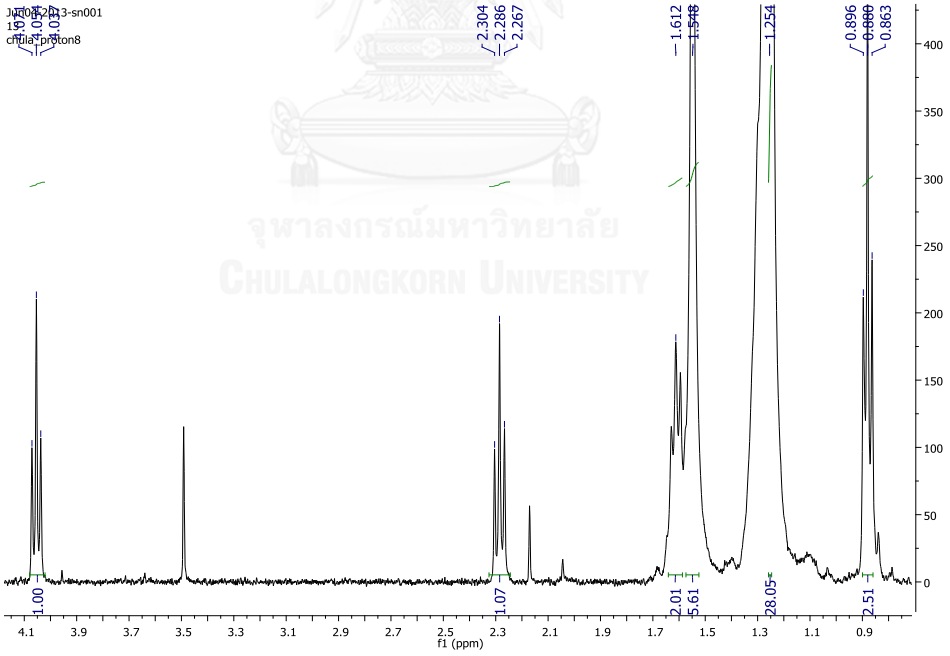

Figure A-20 ^{1}H-NMR spectrum ($CDCl_3$) of **10**

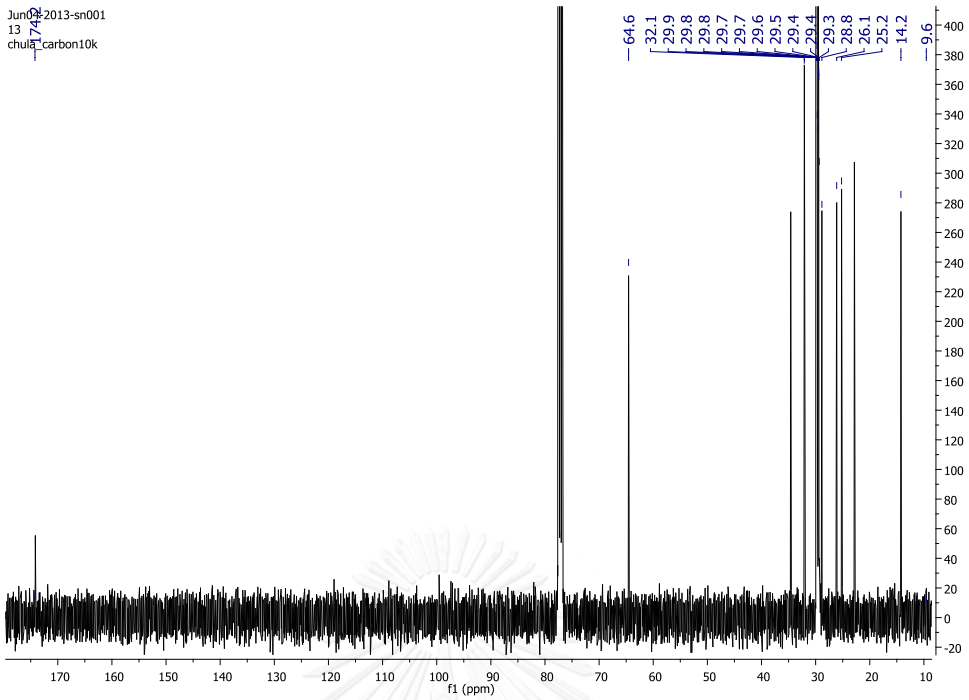

Figure A-21 ^{13}C-NMR spectrum ($CDCl_3$) of **10**

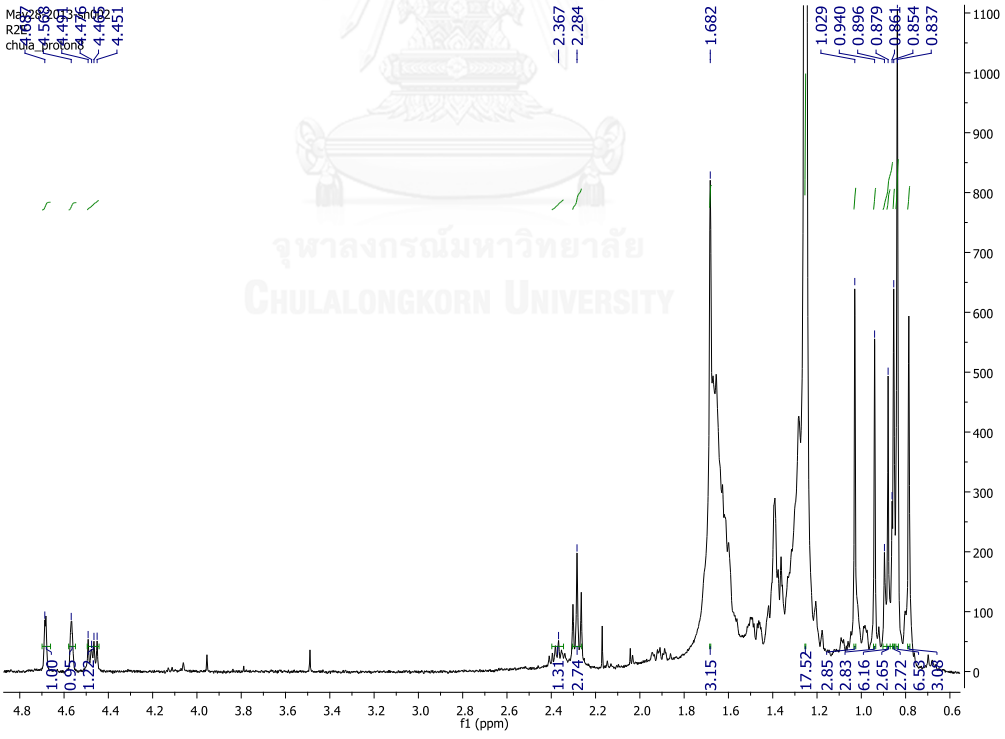

Figure A-22 ^{1}H-NMR spectrum ($CDCl_3$) of **11**

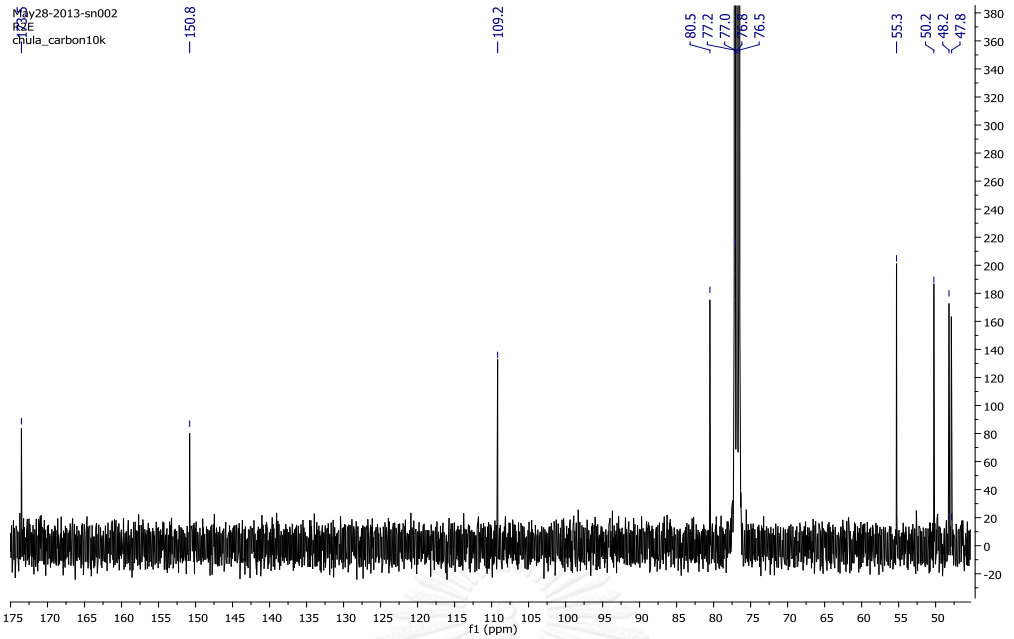

Figure A-23 ^{13}C-NMR spectrum ($CDCl_3$) of **11**

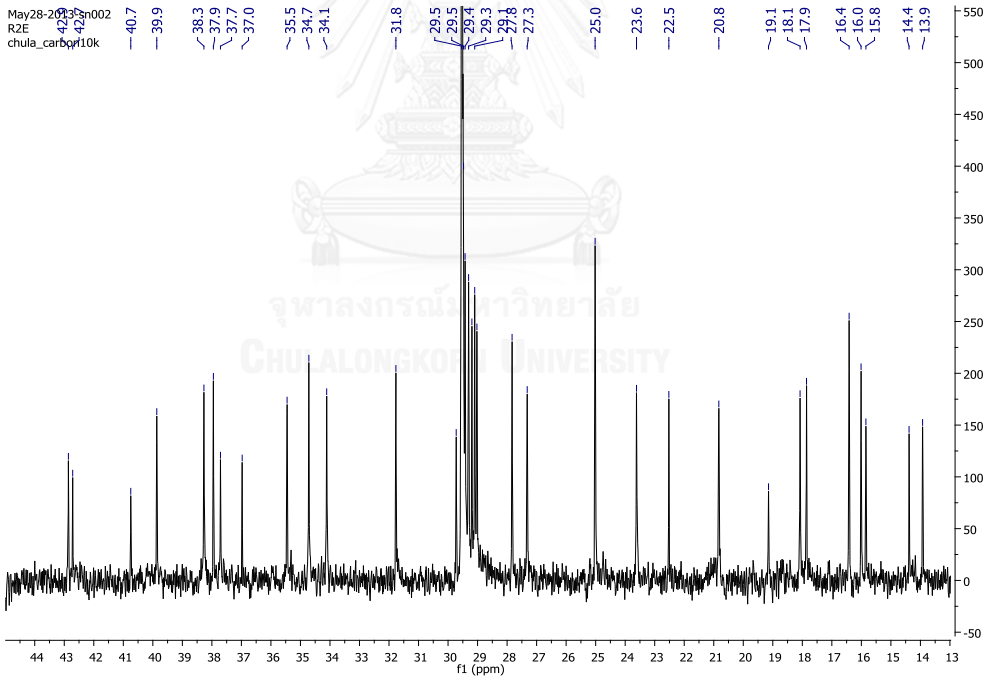

Figure A-24 The expansion of ^{13}C-NMR spectrum ($CDCl_3$) of **11**

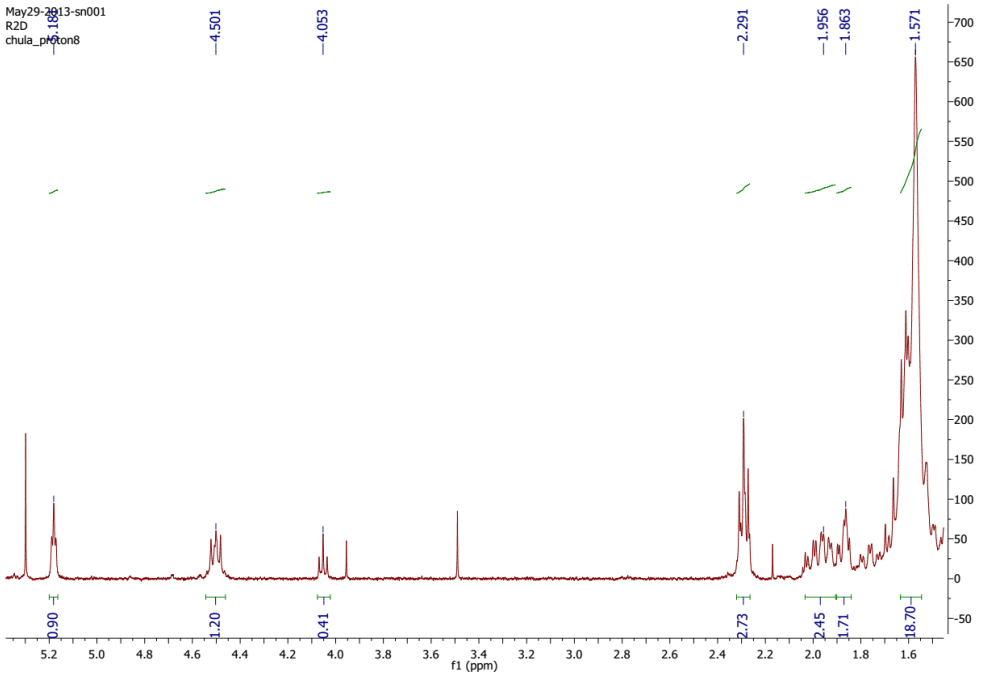

Figure A-25 ^{1}H-NMR spectrum ($CDCl_3$) of **12**

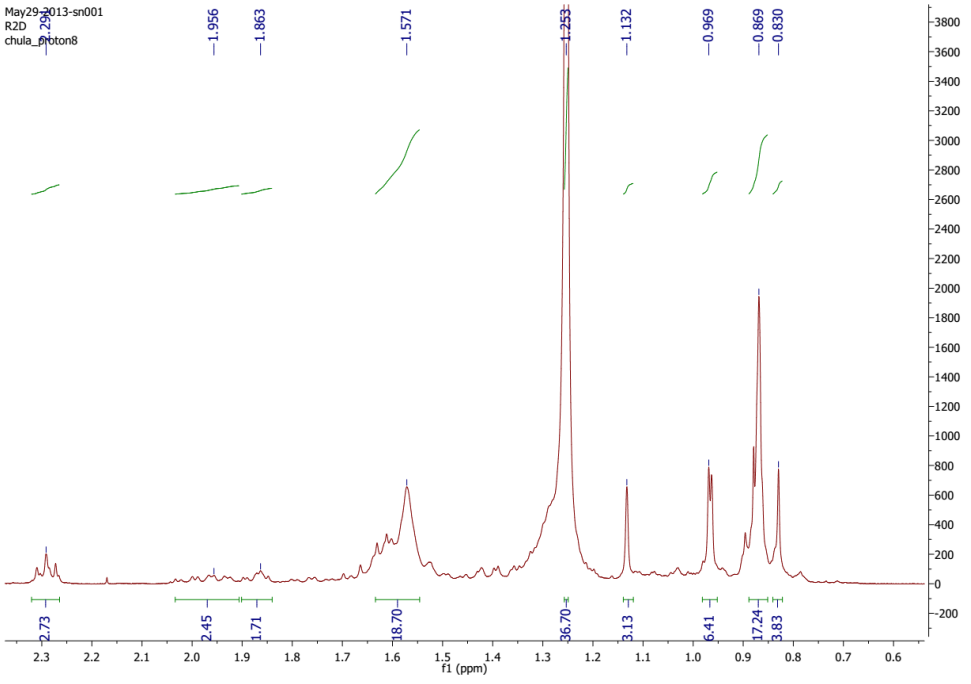

Figure A-26 The expansion of ^{1}H-NMR spectrum ($CDCl_3$) of **12**

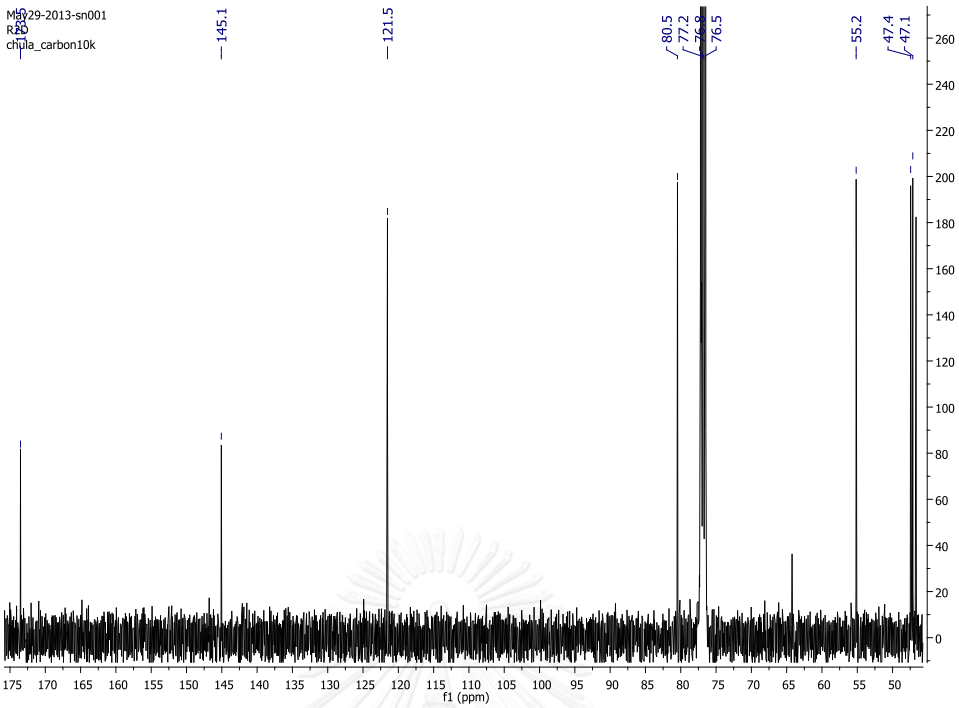

Figure A-27 ^{13}C-NMR spectrum ($CDCl_3$) of **12**

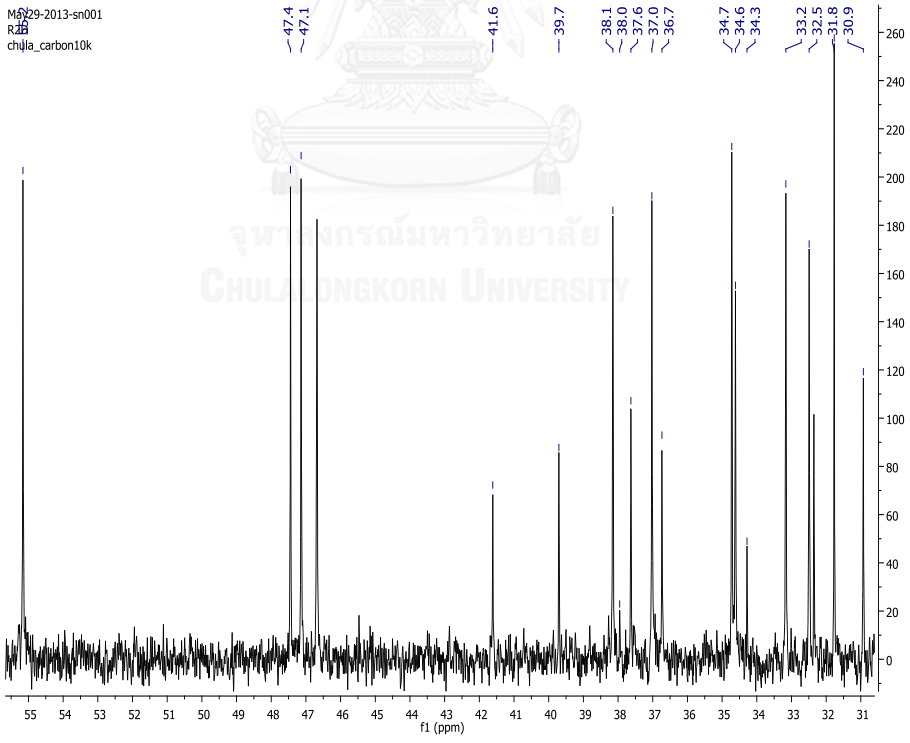

Figure A-28 The expansion of ^{13}C-NMR spectrum ($CDCl_3$) of **12**

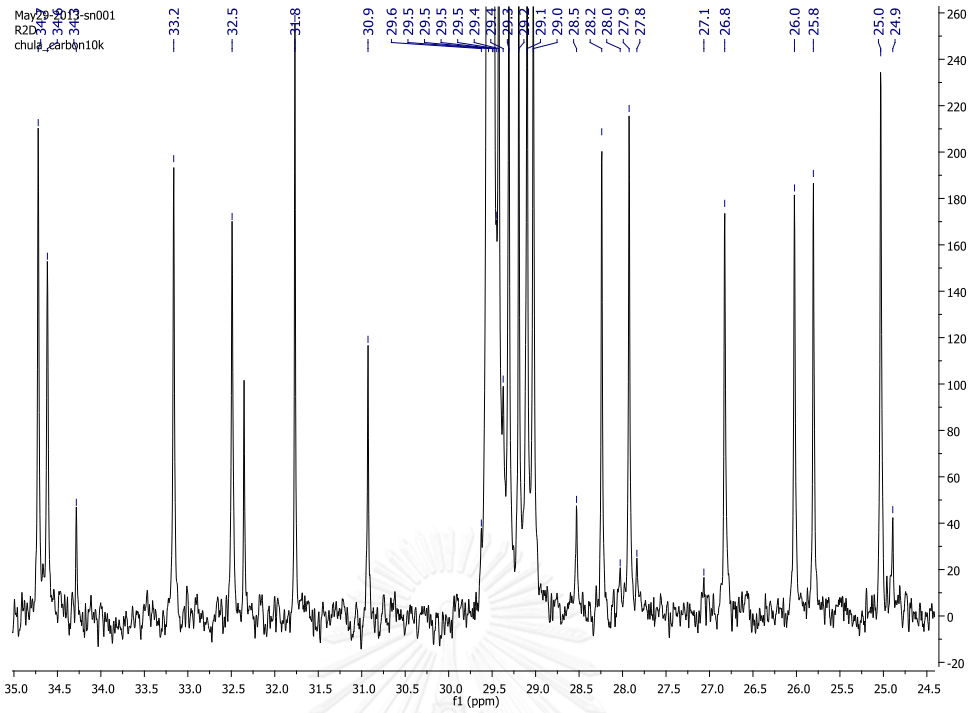

Figure A-29 The expansion of ^{13}C-NMR spectrum ($CDCl_3$) of **12**

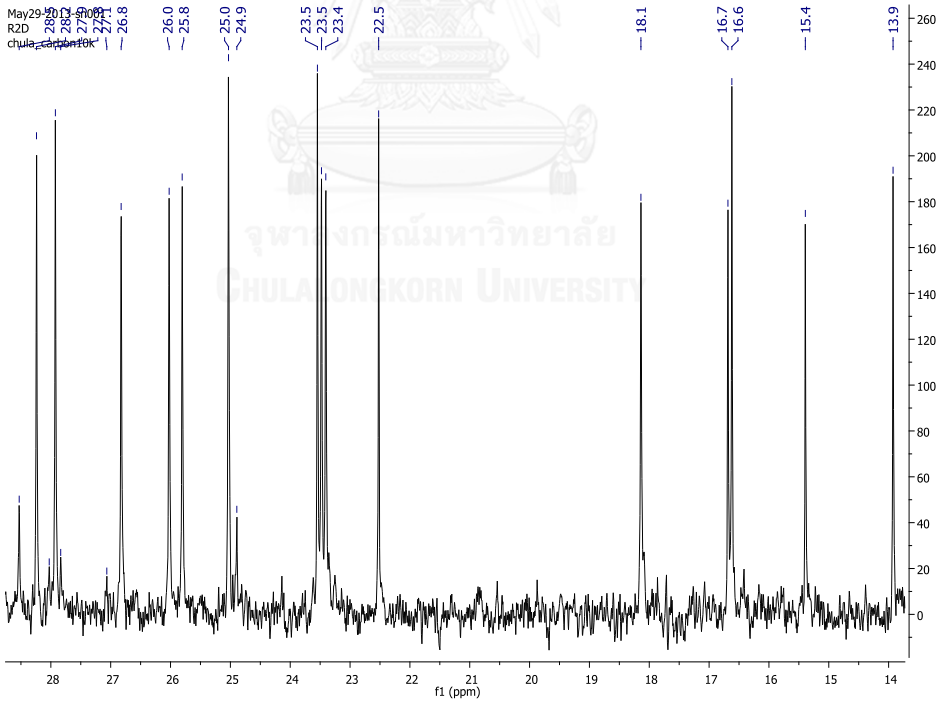

Figure A-30 The expansion of ^{13}C-NMR spectrum ($CDCl_3$) of **12**

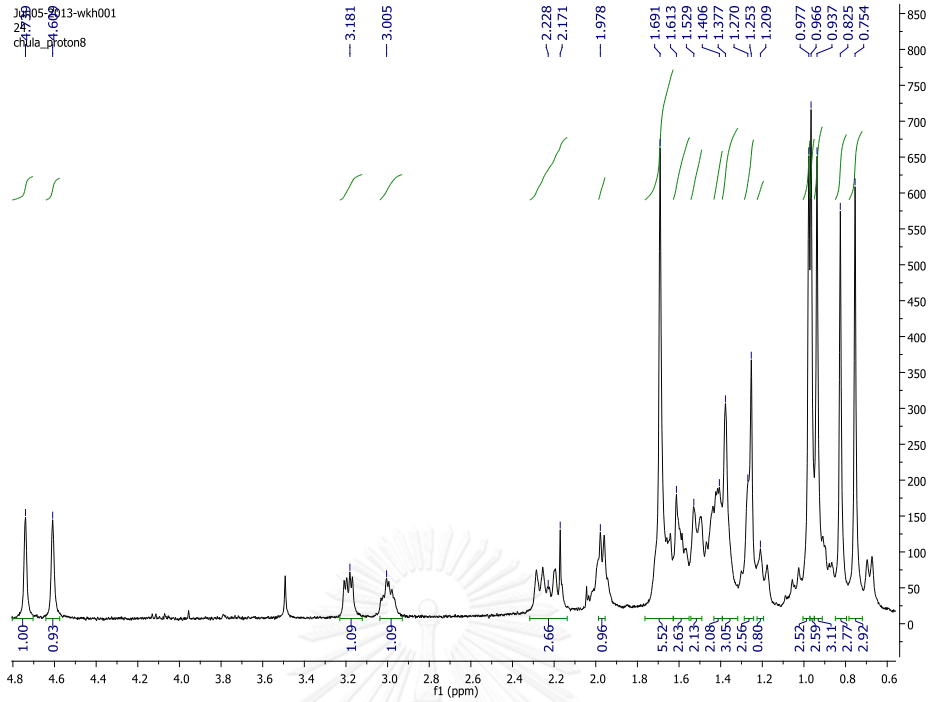

Figure A-31 ^{1}H-NMR spectrum ($CDCl_3$) of **13**

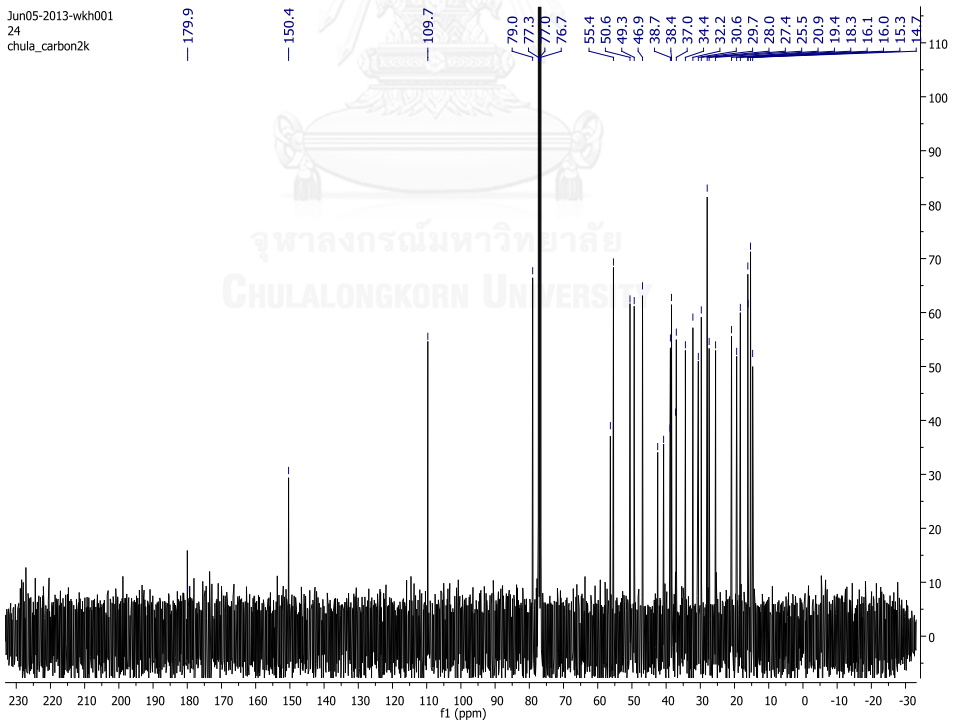

Figure A-32^{13}C-NMR spectrum ($CDCl_3$) of **13**

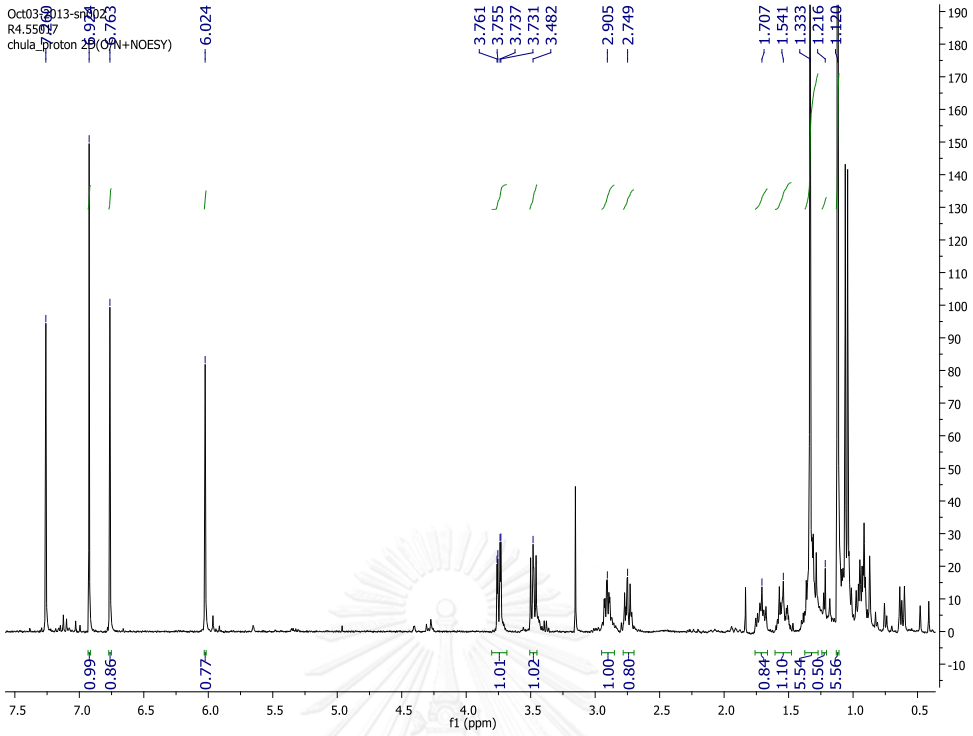

Figure A-33 ^{1}H-NMR spectrum ($CDCl_3$) of **14**

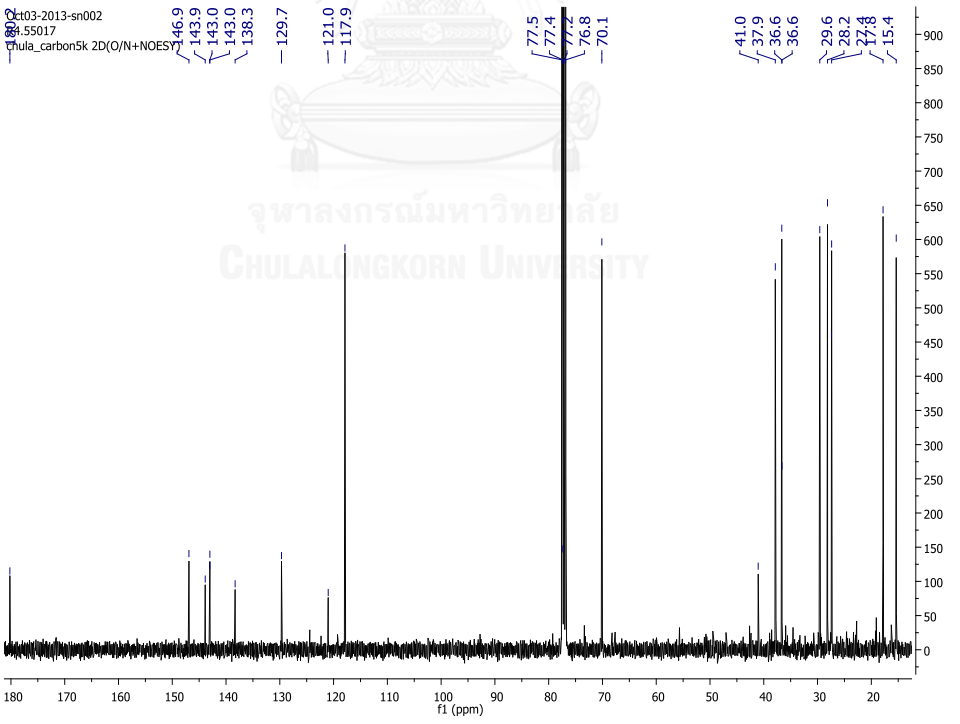

Figure A-34 ^{13}C-NMR spectrum ($CDCl_3$) of **14**

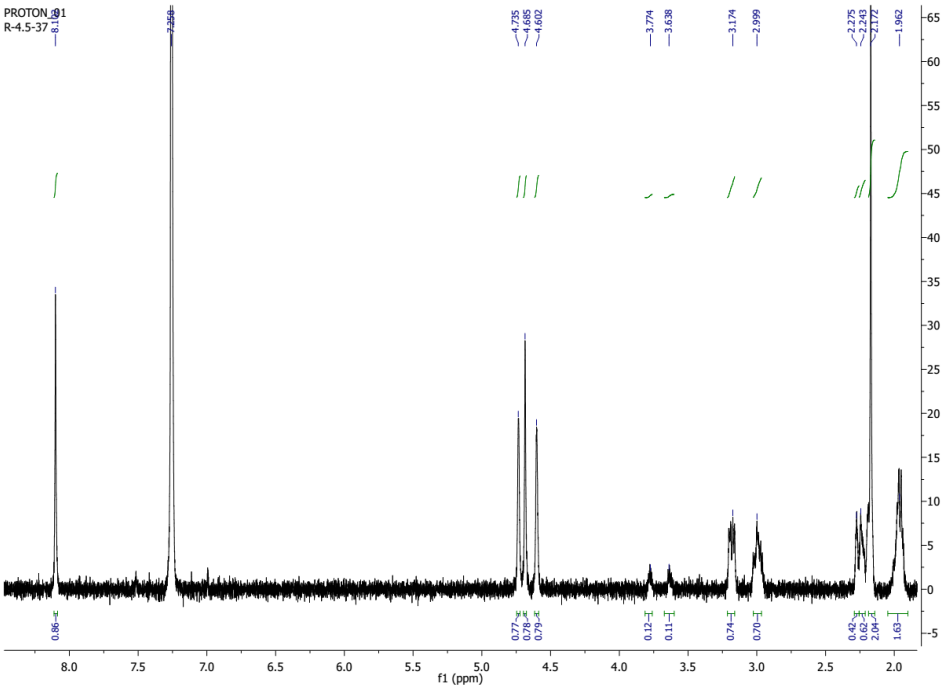

Figure A-35 ^{1}H-NMR spectrum ($CDCl_3$) of **15**

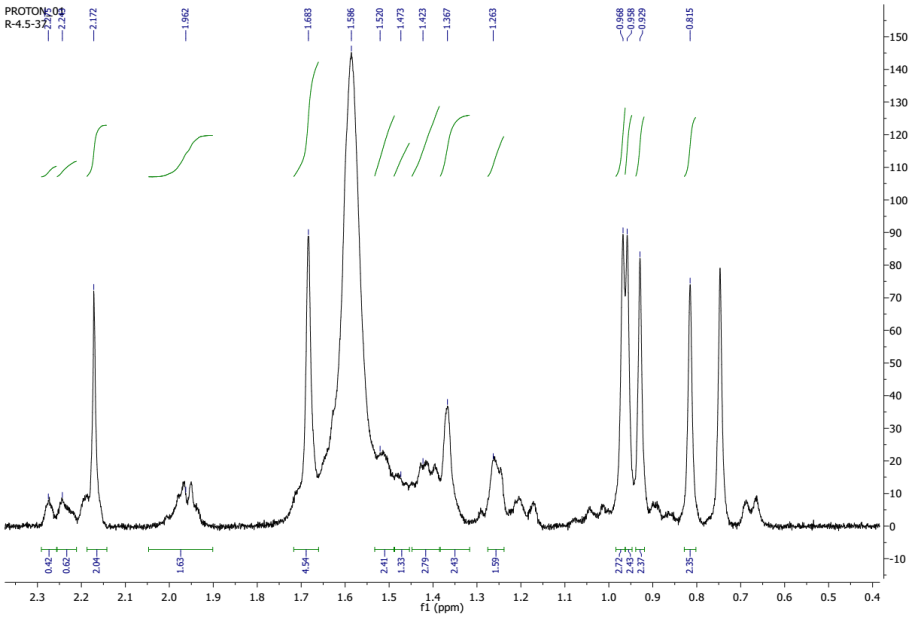

Figure A-36 The expansion of ^{1}H-NMR spectrum ($CDCl_3$) of **15**

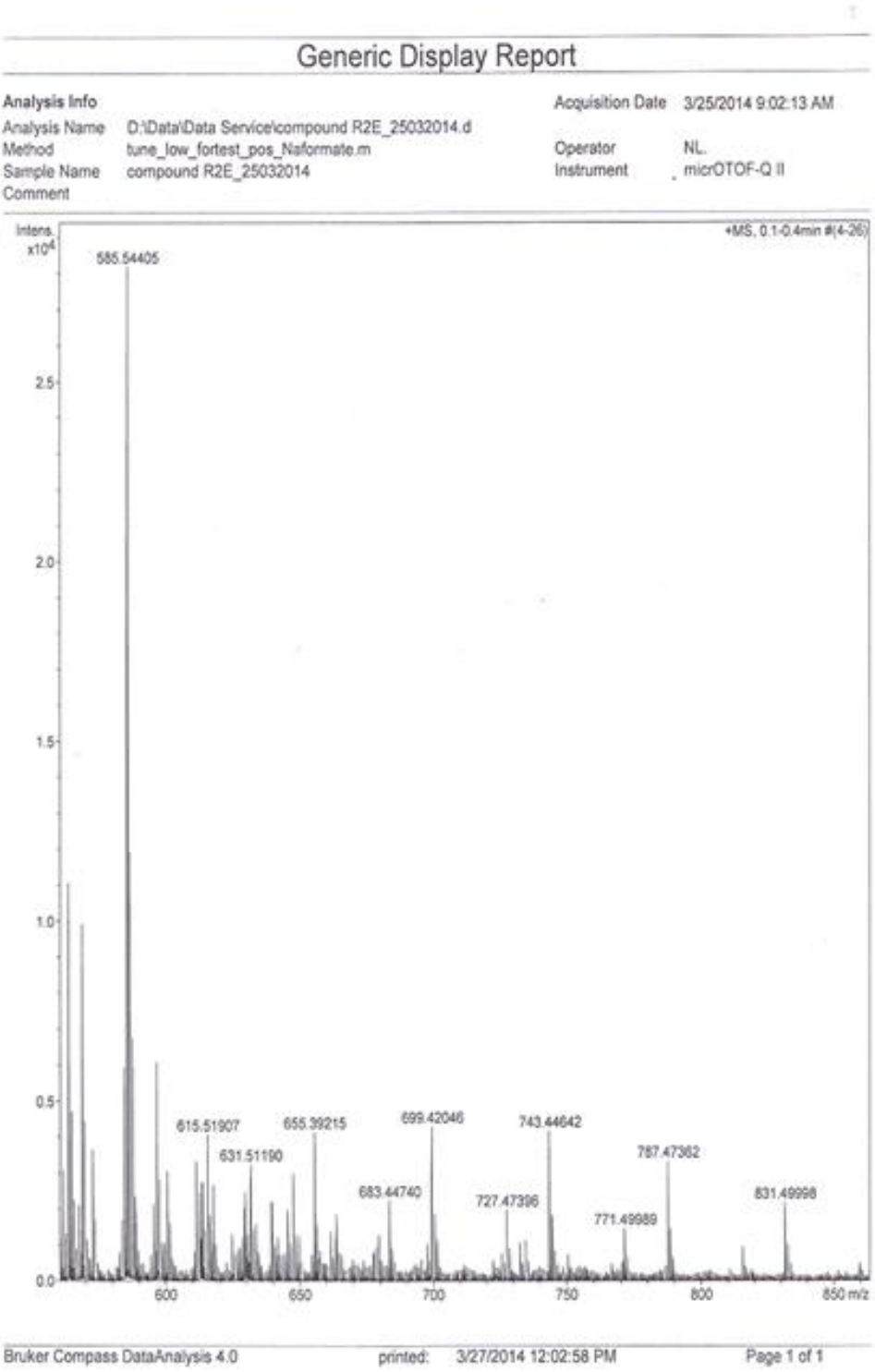

Figure A-37 HRESIMS specrtum ($CDCl_3$) of **11**

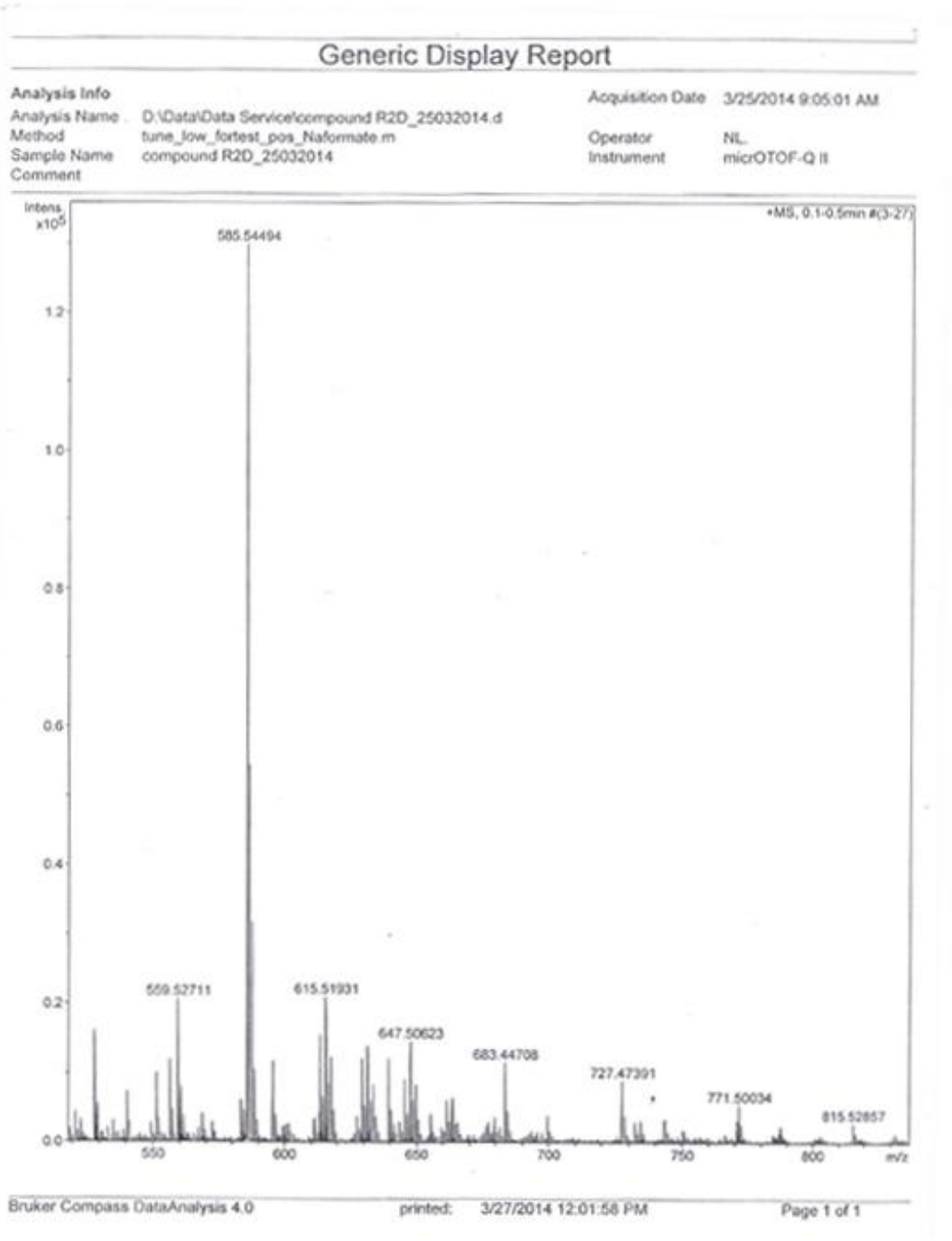

Figure A-38 HRESIMS spectrum ($CDCl_3$) of **12**

VITA

Miss Sirikorn Kor-arnan was born on 18th April, 1973 in Surin, Thailand. She obtained a Bachelor Degree of Science in Biotechnology from Faculty of Science, King Mongkut's Institute of Technology Ladkrabang (KMITL), in 1996 and graduated with Master Degree of Engineering (Chemistry), Kasetsart University in 2001. During study the Doctoral degree in Program in Biotechnology, she receive a financial support from National Science and Technology Development Agency (NSTDA).

She has been a lecturer in Department of Biology at King Mongkut's Institute of Technology Ladkrabang (KMITL) at Ladkrabang campus, Bangkok, Thailand 10520